Contributions to Mineralogy and Petrology

An insight into the first stages of the Ferrar magmatism: ultramafic cumulates from Harrow Peaks, northern Victoria Land, Antarctica.

--Manuscript Draft--

Manuscript Number:	CTMP-D-18-00104R1
Full Title:	An insight into the first stages of the Ferrar magmatism: ultramafic cumulates from Harrow Peaks, northern Victoria Land, Antarctica.
Article Type:	Original Paper
Keywords:	ultramafic xenoliths; high-Mg magmatic olivines; orthopyroxenite; Karoo-Ferrar Large Igneous Province.
Corresponding Author:	Costanza Bonadiman Universita degli Studi di Ferrara Ferrara, ITALY
Corresponding Author Secondary Information:	
Corresponding Author's Institution:	Universita degli Studi di Ferrara
Corresponding Author's Secondary Institution:	
First Author:	Beatrice Pelorosso, Ph.D.
First Author Secondary Information:	
Order of Authors:	Beatrice Pelorosso, Ph.D.
	Costanza Bonadiman
	Theodoros Ntaflos
	Michel Grégoire
	Silvia Gentili
	Alberto Zanetti
	Massimo Coltorti
Order of Authors Secondary Information:	
Funding Information:	Ministero dell'Istruzione, dell'Università e della Ricerca (MIUR-2015 20158A9CBM Grant) — Dr. Beatrice Pelorosso
Abstract:	A group of ultramafic xenoliths hosted in Cenozoic hypabyssal rocks from Harrow Peaks (northern Victoria Land, Antarctica) show textural and geochemical features far removed from anything previously observed in mantle xenoliths of this region and elsewhere in Antarctica. They consist of spinel bearing lherzolites and harzburgites, characterised by a predominant equigranular texture with orthopyroxene modal contents remarkably higher in lherzolites (18 - 26 volume. %) with respect to the harzburgite (13 vol. %), one orthopyroxenite and three composite xenoliths. The latter are formed by an olivine–dominant assemblage (olivine > 70 %) crosscut by large monomineralic (amphibole or clinopyroxene) or bimineralic (amphibole+clinopyroxene) veins. No significant correlation was observed between the lithology and the Fo content (90.21-82.81) of olivine, suggesting that these rocks could be derived from a cumulus process. The presence of the orthopyroxenite suggests that the inferred melt/s from which they stemmed, was close (or even above) to silica saturation. Based on major and trace element mineral/melt and mineral/mineral equilibrium modelling, these rocks were formed by progressive extraction of olivine from a high magnesium (Mg=72) - high temperature (~1300 °C) melt following a very short fractionation line. Thermo-barometric results indicate the stationing of Harrow Peaks cumulates in the P field of

	1.3 ± 0.2 (dunites) – 0.5 ± 0.2 (orthopyroxenite) GPa. These values well match the crust/mantle boundary (Moho) of the region. The combined geochemical and petrological data suggest that Harrow Peaks melts could be related to the initial stage of the Jurassic Ferrar magmatism, whose deep cumulates were subsequently affected by the Cenozoic alkaline metasomatism, widely detected in the northern Victoria Land lithosphere and responsible for the formation of the late amphibole /amphibole+clinopyroxene veins.
Response to Reviewers:	REPLIES TO THE REFEREES AND EDITOR - MS CTMP-D-18-00104 •In the present text, the authors report their replies (with the color code as reported below) to the comments and remarks (in black) of the Referees. •In the revised manuscript, (Pelorosso et al.2019_rev) any changes or new statements were marked with the same Referees' color code. •A clean version (black typing) of the revised manuscript (Pelorosso et al.2019_rev1) is also provided. General comments of the authors. First of all, we would like to thank the Referees and Editor, whose precious suggestions remarkably enhanced the manuscript. In the revised version, we modified the tables, both in the text and as supplementary material, adding the analytical information requested by Reviewer #1. We also simplified and clarified the original text. Finally, the abstract was totally rewritten. We are at your disposal for any further suggestions/ modifications that you believe are needed. (see also Attached file Authors'Reply to Rev_Ed) For the authors, Costanza Bonadiman ---------- Please, find the changes in the manuscript and replies to the reviewers marked by different colors: Blue, for Reviewer #1 (Rev1) Red, for Reviewer #3 (Rev3) COMMENTS FOR THE AUTHOR: AE's comments: Please pay particular attention to Reviewer #1's comments, in particular reporting errors in the data, and the plotting of all the data vs only some of the data. Reviewer #1: May 17th, 2018 This paper presents in situ major and trace element data on a suit of xenoliths from Harrow Peaks (northern Victoria Land, Antarctica). Based on major element composition of the olivine, the authors demonstrate the magmatic origin of these xenoliths as well as the secondary origin of the cpx and amphibole in these xenoliths. They also suggest a cogenetic origin from a single parental melt with high Mg# and close to silica saturation. This paper has geodynamical implications for the initiation and evolution of the Ferrar magmatism, considered as a major magmatic event of West Antarctic Rift system. I think this paper has the ingredients for publications in CMP, but I have a number of comments for the authors to consider for the revision of their paper. 1) Abstract. The abstract does not catch the main conclusions of this paper and could be much shorter (less focused on sample description, more focused on geodynamical implications Authors' reply: We rewrote the abstract and highlighted the relevance of the results. 2) Tables: Quality of the data cannot be assessed as errors on analyses are not reported in Tables (the limit of detection is not sufficient). Add the standard variation (or the internal errors when only one analysis or when the internal error is bigger than the

standard variation).
Authors' reply: We modified the tables according to this suggestion. Table 2_rev (olivine major composition) reports averaged olivine compositions and the relative standard deviation for each sample.
The entire mineral data set is, in turn, provided as supplementary tables (Tables S1-S5).

Moreover, descriptions of Tables S1 to S5 are unclear. They are way more points plotted in Fig.5 than reported in Tables S1-S5 and I don't understand why.
For instance, I can count at least 10 data points for the sample HP121 only on Fig. 5a while only 3 olivine analyses are reported in table S1 for this samples: 2 core and 1 rim, so they cannot be average compositions (otherwise I would have expect 1 core and 1 rim
Authors' reply: thank you for noticing this! The problem arose because our choice was not properly explained in the table caption notes of the original submission. The tables showed representative analyses for each sample (e.g. max, min and medium of each plotted element pairs) but in the corresponding diagrams all the data set was plotted. The revised Tables S1- S5_rev now include all the analyses plotted in the diagrams; moreover, to facilitate the reader, we inserted in the text Table 2_rev with the averaged values of olivine, for each sample (see also authors reply above).

Line 167, the range of Ni content in olivine from all samples is reported as 0.26 to 0.47. On figure 5a, the 0.47 correspond to HP121, however, this analysis is not in Table S1. …)
So how have the analyses present in Table S1 been selected? Same comments can be done for other minerals…
Authors' reply: Yes, you are right, we modified accordingly. See also the above replies. Now the tables, both in the text and as supplementary material, provide the entire chemical dataset used for supporting the HP genetic model.

Please clarify this. I suggest to do the same than for trace elements (L220-221): add a table in the main manuscript with average composition (with 2SD) and # of analyses per sample for ol, opx,cpx, spinel and hydrous phase and give all the individual analyses in supplementary tables.
Authors' reply: We followed the suggestion: the insertion of a new table in the text and the entire data set in the supplementary material provide the whole analytical frame to support the proposed HP genetic model.

Finally, why glass major element compositions are not reported in a Table?
Authors' reply: Thank you for noticing. Unintentionally, this table disappeared during the original submission process! Table S6 (_rev) is now re-introduced.

3) Parental melt compositions:
First, the authors need to give much more details on the calculation of the melt (for instance, how the P2O5 content has been determined?? - Table 3; why choosing 1wt% water? What would be the effect of more/less water?).
Authors' reply: We agree with this comment: in the original version, the modelling information was too "condensed". In the revised version of the manuscript the paragraph that explains the model and relative parameters is now implemented with additional information (lines 335-337, 345-348).
Regarding P2O5 (Table 4 of the original submission): we erroneously included P in the table, since we copied the oxide list of the preset spreadsheet: the output of the calculation is given as wt.% of melt major oxides including P. Since we used olivine to infer the initial melt (melt1), we could not properly determine P contents. The values reported in Table 4 were the content of the real melt used for comparison.
In the revised version, we recalculated all the hypothetical melt compositions based on olivine oxides. In addition, thanks to the Rev1 comments (and suggestions), calculations now include Ni contents. Ni is a clue element to disclose the origin of the HP ultramafic fragments. This is now discussed in the revised text (lines 335-337, 455-467, Table 5_rev)

Second and more importantly, the author suggest that the xenolith suite is cogenetic based mostly on major element compositions of olivine. While I agree with the

demonstration showing that they are not melting residue and consequently have a magmatic origin, I am not completely convinced by the cogenitic origin of these cumulats. In fact, (1) the global trend Fo-NiO in Fig.5a seems to be "too straight" to represent a fractional crystallization trend and looks more like what I would expect of a mixing trend… I suggest the author to do the calculations to check this. (2) Even if the trend can be reproduced by fractional crystallization, there is a very large scatter in NiO content for a given Fo content that cannot be explain by fractional crystallization.
Authors' reply: We thank Rev1 for this interesting comment. It is an hypothesis that we initially took into account, but we later discarded, after processing the olivine chemical data set. It was found that within the uncertainty of the data, diffusion rates of Fe-Mg and Ni are very similar to each other at all crystallising conditions, but Ni is more sensitive to the difference between mantle and segregation depth (Petry et al., 2004; Gordeychik et al., 2018).
We present here a plot, showing Fo vs NiO averaged olivine composition of each sample under investigation. This diagram was not inserted in the revised manuscript, because it has the same meaning as Fig.4a, however here it helps the authors to explain their reply to this comment.
Despite the limited number of samples, the positive correlation between Fo and NiO averaged for each sample is clear, with the highest values corresponding to the most primitive (HP121), and the lowest to the most evolved (oxpte HP163) olivines of the hypothetical melts from which they crystallised, as we modelled (melt1-----melt 3). The samples in between, more "scattered", should represent separates of "intermediate" melts of a system that evolves, if our model is correct, from high Mg# (picrites?) to high Mg# melt (basalts).
As stated above, to reinforce our modelling Ni contents were included in the calculations.
The same trend has been observed, and explained as a fractionation trend in i.e. olivine in Deccan trap (Krisnhamarphy et al., 2000 JP) and Haleakela submarine volcano, Hawaii (Ren et al., 2004).
However, it is important to consider that these ultramafic rocks represent cumulates, thus they are affected by variable degrees of subsolidus effect.

(3) trace elements are not discussed in this statement. If the orthopyroxenite was the result of a more evolved liquid crystallization, I would expect the opx to show more enriched trace element composition. This systematic is not obvious in Fig. 8.

Authors' reply: we agree! However, orthopyroxene that compete with olivine to accomodate REE abundances, partition low to very low REE contents, and the large uncertainties in their measurements do not allow the identification of a clear fractionation trend from the multi-element diagram, in particular in such a short line of fractionation as we modelled (melts from mg# 72 to mg# 60). If we consider Yb (or Y) and Zr (or Ti), the most robust geochemical fingerprints in orthopyroxene, this relationship emerges.
In the revised manuscript we discussed this statement (lines 412-422).

Third, the origin of the high Mg parental melt close to silica saturation is stated as "associated with an anomalous high temperature (excess Tex) melting of the Phanerozoic mantle (picrites) or the Archean cratons (komatiites)." Another potential explanation would be the contribution of a High-Mg pyroxenite. This would also potentially explain the very high Ni content of the olivine (up to 0.47%!). I think that this hypothesis is worth to be discussed (or at least mentioned and maybe dismissed if the authors have good reasons to do so.) see more comments on this below
Authors' reply: Yes, we thank the Rev 1 for these considerations. In the revised version the discussion is now enriched with this suggestion (lines 455-467)

4) Length of the manuscript: Unnecessary long sentences are sometime used in the

manuscript. This does not help the reader to assimilate the information. See editorial comments (LOM). The description of the results are also sometime mixed with part of the interpretation (mention of the residual peridotite, mantle array,…) that can confuse the reading.
Yes, we are aware of this, but in some cases the description of the results becomes an interpretation (e.g the Osma diagram). It is difficult to separate the two things. However, in the revised manuscript we avoided this mixing whenever possible.

Comments link to the text:
L 25-26: "and analysed for in situ geochemical purpose." This sentence is weird
Authors' reply: the abstract was re-written (line 159)

L 26: why "<10 cm" here and "2 to 5 cm" on page 5?
Authors' reply: Thank you for noticing. The information was harmonised as "<10 cm "(line 86)

L40 & 322: "potential temperature of crystallization" confusing because of the expression "potential mantle temperature" I suggest to replace "potential" by "estimated" or to simply remove it.
Authors' reply: we agree. In the revised manuscript we simply referred to "temperature", throughout the text.
L.77-79: need references
Authors' reply: done

L 91-92: not clear: in addition to the eight samples? Does it mean that the selected samples do not show evidence for host-basalt contamination?
Authors' reply: You are right. The sentence is confusing and we removed it. Host basalt infiltration is now mentioned ad hoc in the mineral chemistry description.

L93: "composite xenoliths": add the definition of a composite xenolith here
Authors' reply: Added (lines 93-94)

L93-94: "Hydrous phases (mainly amphibole) occur in all samples": but amph (or phlogopite) is only reported in 5 samples in Table 1.
Authors' reply: Thank you for noticing! We visually observed traces of amphiboles in all samples, but only in five samples were amphibole crystals large enough to be analysed. In the revised manuscript, we modified Table 1 (Table 1_rev) accordingly.

L104-105: it is not clear on Fig. 3b that what is outlined is a vein. Also, the text on this figure is very small and I don't think it will be visible once placed into the article. Maybe Fig.3 could go in the supplementary material.
Authors' reply: Thank you for the suggestion, we moved this figure to the supplementary material.

L107-108: What is the point of spending so much time doing point-counting (knowing that studies show that above 300-400 points, the statistical difference is small), confirming the results with color analyses to demonstrate that this matrix is a harzburgite if it's to call it dunite based on "textural similarities and high olivine modal contents". Why not continue to call it harzburgite?
Authors' reply: the nomenclature of these samples was a problem since the first petrographic observation. If we named the samples with the proper name derived by the modal classification diagram, as Rev1 suggests, the risk of making the reader confused about the composite samples is high. HP121 and HP124 are formally harzburgite and lherzolite, respectively, but they are far from being harburgite or lherzolite in the proper meaning. Both rocks are dunites with rare orthopyroxenes and clinopyroxenes, crosscut by amphibole or clinopyroxene vein.
In the revised version, we simplified as much as possible the petrographic description, but we think that it is important to address these samples as dunites, for the reasons clarified in the text (lines: 102-104) and reported in Table 1_rev.

L166 & Table S1: add Fo content in Table S1
Authors' reply: done

L167: "from 86.60 to 90.45" this degree of precision is probably unrealistic but because errors (and Fo) are not reported in Table S1, I can't tell. Same comment line 170 and in the abstract
L167: highest value reported in Table S1 for NiO is 0.42% - see comment #2 on supplementary tables
Authors' reply: See replies of the general comment point 2.

Section 4.1: I'm surprised that the author do not comment the fact, that despite a relatively small compositional range for the entire xenolith suite, there is a very limited overlapping between the different samples. This is particularly striking for the spinel on Fig. 5c.
Authors' reply: At magmatic conditions, the spinel mg-number is a function of the melt mg-number and Al2O3, whereas at near- and postmagmatic conditions it is controlled by the rate of cooling and re-equilibration with the silicates. At this stage, the variability of the spinel is reasonable.
Notwithstanding, we agree with Rev1 that mineral chemistry discussion could be improved. In the revised version of the manuscript, we discussed the Fig.4_rev that now includes lines of hypothetical melting trend for olivine (lines 285-294, 455-467) (Kamenesky et al., 2001 JP; A-Rim An, 2017 Lithos).

L 186-188: Should be in the discussion and requires more information.
Authors' reply: We removed it from this section and inserted it in the initial part of the new "Discussion" section, See also reply above.

L189-190: the "evident" disequilibrium requires more justification and reference to a figure.
Authors' reply: Thank you for the suggestion, we rephrased (lines: 192-193) and clarified these statements adding orthopyroxene-clinopyroxene Fe/Mg equilibrium values

L195: "have TiO2 and Al2O3 contents that reflect a host basalt low-pressure perturbation (Figs.7 a, b)." I do not understand what that means
Authors' reply: Yes, it was not clear, we meant that the high TiO2 and low Al2O3 observed in a few grains in individual samples, is a local effect of low-pressure host basalt infiltration. In line 195 with what we stated above, we modified this section following the Rev1's comments.

L195-197: I don't think this is relevant for the discussion
Authors' reply: we removed this sentence

Table 2: Add the internal error (when only one analysis) or the standard deviation (when multiple analyses and if bigger than the internal error) in the Table
Authors' reply: done. See also replies to general comments point. 2) of Rev1.

L 284-285: I don't see a melting "trend" on Fig. 5a in residual peridotites (green field) but I do see a trend in the samples described here that could be interpreted as a mixing trend (or maybe as a fractional crystallization trend).
Authors' reply: As stated above, Fig. 4_ rev shows theoretical fractional (and melting) trends.
The idea of mixing is intriguing. However, if Rev1 thought of mixing of the sources, it is difficult to identify it (taking into account the cumulitic nature of these rocks).

Authors should try to calculate a fractional crystallization trend and see if it can explain the Fo-NiO variation? (see e.g., Shorttle et al, 2014; Sobolev et al, 2005). If these samples have a magmatic origin as claimed by the author, that could reveal some scatter in the primitive melt composition and also reveal a certain heterogeneity of the source (i.e, variable contribution of a pyroxenite component (Sobolev et al., 2005) or variable pressure of melting (Matzen et al, 2014)).
Authors' reply: see comment above.

L287-290: Not clear and several typos. Change "there is not an observed correlation between spinel and olivine as expected in a potential residual trend, with the sole

exception of the composite xenolith HP21, where spinel Fo and Cr# values of the dunitic matrix intercept the mantle array curve," by "the Olivine Fo - Spinel Cr# relationship cannot be reproduced by melting, with the exception of the composite xenolith HP121, where spinel and olivine compositions intercept the mantle array curve".
Authors' reply: thank you for rephrasing.

L300: ΔQFM = - 2.78 seems particularly low!
Authors' reply: in this section we wanted to emphasise that amphibole and dunite matrices are not genetically related. This value, reported by literature, was determined on the "peridotite" assemblage, and testifies to the complete disequilibrium of the system.

L331-333: The composition of melt1 reported in table 4 contains a lot of different oxides, including MnO, P2O5, TiO2, etc not present in Putirka' equation (21). Please add details on how these calculations were performed.
Authors' reply: Thank you for noticing this. As mentioned above, we re-calculated the hypothetical melts, removing P2O5 (erroneously reported), but including NiO.
The revised manuscript now includes a detailed explanation of the calculations, supported by the new Table 5 (Table 5_rev)

L 334-335: same comment: please give details of the calculations.
Authors' reply: see above.

L339-340: if the olivines are cogenetic, you should be able to reproduce the Fo-NiO variation by fractional crystallization - see my comment on line 284-285. Note that IF the authors do find a crystallization trend that can broadly reproduce the NiO-Fo variation, fractional crystallization will never explain the scatter of NiO content for a given Fo content. Looking at the sample HP121 only, NiO varies from 0.32 to 0.47 (fig 5a) for a relatively constant Fo content (around 90). This covers almost all the range observed in magmatic olivine of Mauna Loa and has been interpreted as a variable high contribution (50-80%) of a pyroxenitic component to the magma (Sobolev et al., 2005). I think this is worth to be explored or at least slightly discussed in this paper.
L361-363: "parental liquid had high MgO contents (Mg# 72) and was close to silica saturation. Such melts are associated with an anomalous high temperature (excess Tex) melting of the Phanerozoic mantle (picrites) or the Archean cratons (komatiites)." Or with the contribution of a high-Mg pyroxenite! Again Sobolev et al. (2007) generate melts with mg# as high as 77 by melting of a high-mg pyroxenites.
Authors' reply: Part of this interesting discussion is now included in the revised manuscript (lines: 455-467).

Figure 2: 'dunitic" not only, the matrix of HP121 is a harzburgite. Note that the symbols look a bit offset. For instance HP121 seems to plot in the lherzolite field while the middle of the symbol should normally be exactly on the harz-lherz limit (ie, when modal proportions of ol, opx and disseminated cpx are normalized to 100%, cpx mode is 5%). same observation with HP143, the normalized ol mode is 90.1% while the middle of the symbol seems to be below the 90% line.
Authors' reply: the symbol's size is now enlarged

Figure 3. Need to stay big so we can see the details mentioned in the text. So I suggest to put this figure in the supplement
Authors' reply: Done, see also reply to Rev1 general comments, point 4.
Figures 5 &6: remove "Dunitic"
Authors' reply: done

Editorial comment:
Name of the samples are not the same in the entire manuscript: e.g, HP121 vs HP21. Make sure to check and uniform this, including in the Supplementary Tables

L109: LOM suggestion: "Regardless of the lithology, most of the samples are tabular to equigranular"
Authors' reply: done. We re-phrased accordingly line 104.

L113-114: " small irregular spinel is scattered within the olivine grains." I guess they are plural
Authors' reply: yes plural. Correct. We always use the singular form for minerals, also in the plural meaning (i.e. the case mentioned here)

L117: "small irregular spinels within the olivine grains": "within" (ie, inclusion) or "between"?
Authors' reply: corrected: Inclusion (line 112)

L120-121: it's either: "it's absent in most of the..." or "it's completely absent in other xenolith suits"
Authors' reply: corrected

L158-160 : LOM suggestion : Change it for: "Major element data on olivine, pyroxenes, spinel and amphibole are provided in the Supplementary material (Tables S1 to S5). and place this sentence below the title 4.1 Note that the Table numbers are wrong.
Authors' reply: correction accepted (158-160)

Amphibole is in Table S5, not S4.
Authors' reply: corrected

L173-174: "showing an apparent equilibrium with the coexisting olivine in all the investigated samples, and remarkable differences from those of the residual peridotites." At this point in the manuscript, I don't know on what is based this affirmation and I have no idea where the term "residual peridotites" comes from in this article and which samples the authors are talking about
Authors' reply: we modified the text and removed this sentence.
Figure 9 - L 754: typo
Authors' reply: Ok

Table2:
- n. is number of average analyses: I do not understand, do you mean: n. is number of analyses?
Authors' reply: yes it is. In Table 2_rev, we added an explicative note

- Remove the footnote Ol:olivine as there is no analyses of olivine in this table
Tables S1 to S5: The row "phase" can be removed.
Authors' reply: corrected.

References cited in this review
A.K. Matzen, M.B. Baker, J.R. Beckett, E.M. Stolper. The temperature and pressure dependence of nickel partitioning between olivine and silicate melt J. Petrol., 54 (2013), pp. 2521-2545
Sobolev AV, Hofmann AW, Kuzmin DV, Yaxley GM, Arndt NT, Chung, SL, Danyushevsky LV, Elliott T, Frey FA, Garcia MO, Gurenko AA, Kamenetsky VS, Kerr AC, Krivolutskaya NA, Matvienkov VV, Nikogosian IK, Rocholl A, Sigurdsson IA, Sushchevskaya NM, Teklay M (2007) The amount of recycled crust in sources of mantle-derived melts. Science 316:412-417. doi:10.5800/gt-2012-3-1-0059
Sobolev, A.V., Hofmann, A.W., Sobolev, S.V., Nikogosian, I.K., 2005. An olivine-free mantle source of Hawaiian shield basalts. Nature 434, 590-597
Shorttle, O., Maclennan, J., Lambart, S. (2014) Quantifying lithological variability in the mantle. Earth and Planetary Science Letters 39

Reviewer #3: This is an interesting study on mantle xenoliths from Harrow Peaks in Antarctica. I think the data are convincing and are of high quality, and the interpretation and conclusions consistent. My major comment about the manuscript is that it suffers from significant problems in grammar. I started making notes in the pdf, but stopped about half way through. The authors need to make sure that they revise the writing significantly before submitting a final version for publication. Other than that, the authors should be congratulated on a study well done.

	Authors' reply: we would thank for the appreciation of our work. The revised manuscript has been checked by mother tongue- reviewer for English language.

An insight into the first stages of the Ferrar magmatism: ultramafic cumulates from Harrow Peaks, northern Victoria Land, Antarctica.

Beatrice Pelorosso [a], Costanza Bonadiman[a*],
Theodoros Ntaflos[b], Michel Gregoire[c], Silvia Gentili[d], Alberto Zanetti[e], Massimo Coltorti[a]

a Dipartimento di Fisica e Scienze della Terra, Università di Ferrara, Italy
b Department of Lithospheric Research, University of Vienna, Austria
c GET, Université de Toulouse, CNRS, CNES, IRD, UPS, (Toulouse), France
d Dipartimento di Fisica e Geologia, Università di Perugia, Piazza dell'Università 1, 06123 Perugia, Italy
e CNR-IGG, Sezione di Pavia, via Ferrata 1, I-27100 Pavia, Italy

*corresponding author : costanza.bonadiman@unife.it ; bdc@unife.it

Key words: ultramafic xenoliths; high-Mg magmatic olivines; orthopyroxenite; Karoo-Ferrar large igneous province.

Abstract

A group of ultramafic xenoliths hosted in Cenozoic hypabyssal rocks from Harrow Peaks (northern Victoria Land, Antarctica) show textural and geochemical features far removed from anything previously observed in mantle xenoliths of this region and elsewhere in Antarctica. They consist of spinel bearing lherzolites and harzburgites, characterised by a predominant equigranular texture with orthopyroxene modal contents remarkably higher in lherzolites (18 - 26 volume. %) with respect to the harzburgite (13 vol. %), one orthopyroxenite and three composite xenoliths. The latter are formed by an olivine–dominant assemblage (olivine > 70 %) crosscut by large monomineralic (amphibole or clinopyroxene) or bimineralic (amphibole+clinopyroxene) veins.

No significant correlation was observed between the lithology and the Fo content (90.21-82.81) of olivine, suggesting that these rocks could be derived from a cumulus process.

The presence of the orthopyroxenite suggests that the inferred melt/s from which they stemmed, was close (or even above) to silica saturation. Based on major and trace element mineral/melt and

mineral/mineral equilibrium modelling, these rocks were formed by progressive extraction of olivine from a high magnesium (Mg=72) - high temperature (~1300 °C) melt following a very short fractionation line. Thermo-barometric results indicate the stationing of Harrow Peaks cumulates in the P field of 1.3 ± 0.2 (dunites) – 0.5 ± 0.2 (orthopyroxenite) GPa. These values well match the crust/mantle boundary (Moho) of the region. The combined geochemical and petrological data suggest that Harrow Peaks melts could be related to the initial stage of the Jurassic Ferrar magmatism, whose deep cumulates were subsequently affected by the Cenozoic alkaline metasomatism, widely detected in the northern Victoria Land lithosphere and responsible for the formation of the late amphibole /amphibole+clinopyroxene veins.

1. Introduction

The West Antarctic Rift system (WARS) is one of the largest continental rift areas in the world and is comparable to the East African Rift in scale (Martin et al., 2015; Le Masurier and Thomson 1990). Since the Cenozoic it was affected by alkaline magmatism represented by the Mc. Murdo volcanic and Meander intrusive rocks (Kyle 1980). The most primitive volcanic products from Victoria Land contain mafic and ultramafic xenoliths in a large spectrum of lithologies that testify for a complex mantle/crust evolution of the Subcontinental Lithospheric Mantle (SCLM). Evidence of mantle partial melting and enrichment events (due to both alkaline metasomatism and refertilisation by tholeiitic melts) as well as crystallization of alkaline melts at the Moho depth have been widely documented (Gamble et al., 1988; Beccaluva et al., 1991; Cooper et al., 2007; Martin et al., 2015; Pelorosso et al., 2016). Geochemical and isotopic data trace back the refertilisation process of SCLM in the northern Victoria Land to before the Cenozoic began (Melchiorre et al., 2011; Pelorosso et al., 2016), suggesting a possible connection with the most important magmatic activity in Antarctica, which occurred before the Cenozoic: the Jurassic magmatism, part of the Karoo-Ferrar Large Igneous Province. The Jurassic magmatism produced outcrops that stretch over 3500

km from the Theron Mountains of Antarctica to southeast Australia (Elliot & Fleming 2004), including several volcanic bodies such as mafic sills, flood basalts (i.e. Kirkpatrick basalt, Vestfjella ferropicrites), phreatomagmatic volcanic rocks, layered mafic intrusions (i.e. Ferrar dolerite sill) and mafic dykes (Kyle et al., 1989; Fleming 1995; Elliot et al., 1999; Storey et al., 2013; Heinonen and Luttinen, 2010; Bedard et al., 2007). At Harrow Peaks (74.0 2785°S 164.47466°E, Fig. 1), where the alkaline Cenozoic magmatism is dominant as well as in many other northern Victoria Land magmatic localities, lavas brought to the surface ultramafic xenoliths.

The samples available for this study were collected during the XX Italian Expedition organised by PNRA (Programma Nazionale Ricerche in Antartide) in the 2004/05 Austral summer. They are mainly (amphibole bearing) spinel peridotites, but composite xenoliths are also abundant. The Harrow Peaks samples include dunites and one orthopyroxenite, which are rarely observed or absent in the xenolith populations sampled in the region and carried by the same magmatic system (Perinelli et al., 2011; 2018; Coltorti 2004; Martin 2015 and reference therein).

A few of these xenoliths were studied by Gentili et al. (2015) to evaluate the role of amphibole formation in the modification of the original redox condition of this mantle domain. The quoted authors revealed extremely high redox conditions (Δlog QFM fO_2 = ~ +5, +7) for the amphibole formation, in clear disequilibrium with the peridotite matrix.

In this paper, we present new petrological and geochemical data of this unique group of ultramafic xenoliths, which provide evidence for a magmatic origin. Moreover, they show to what extent these rocks also experienced metasomatic event(s) that are attributable to large scale processes that occurred in Victoria Land SCLM.

2. Sample description and Petrography

The ultramafic xenoliths found in the Harrow Peaks lavas are rather small (< 10 cm) and sub-rounded in shape.

The mineral modal proportion was determined by point counting, averaging two runs with more than 2,000 points for each thin section (2.5 x 4.0 cm), Table 1. Based on the classification diagram for mafic and ultramafic rocks (Fig. 2; Streickeisen, 1974), the Harrow Peaks xenoliths consist of spinel-bearing lherzolites (HP151, HP164 and HP166), one harzburgite (HP144) and one orthopyroxenite (HP163).

Three out of the eight samples selected for this study are composite xenoliths formed by an olivine –dominant assemblage (olivine > 70 %) crosscut by large monomineralic or bimineralic veins. They combine various lithologies that make it difficult to apply the standard nomenclature for ultramafic rocks. Two composite samples are made up of a dunite matrix crossed by clinopyroxene (HP143, Fig. 1S) and clinopyroxene + amphibole + rare phlogopite (HP124, Fig.1S) veins. HP121 is also composite, with a harzburgite matrix (containing up to 6% and 4% of modal orthopyroxene and clinopyroxene, respectively) crosscut by a large amphibole vein (Fig. 1S). Considering the uncertainties of the modal content, we cannot attribute to this sample an unequivocal classification term (Fig. 2; Table1), therefore we equate the HP121 sample with the rest of the composite dunites. Hydrous phases (mainly amphibole) occur in all samples, showing significant different grain sizes and modal contents from sample to sample.

Regardless of the lithology, most of the samples are tabular to equigranular (Mercier & Nicolas 1975) with equidimensional, polygonal in shape olivine (1 mm) delimited by boundaries often converging at 120° (i.e. Figs. 3a, b). The modal content of the orthopyroxene is higher in lherzolites (18 - 26 volume. %) with respect to the harzburgite (13 vol. %). The clinopyroxene in lherzolites/harzburgite are small and interstitial (Fig. 3e); small irregular spinel are scattered between the olivine grains. Amphibole are present both as disseminated crystals (i.e. HP124; Fig. 3b) or in veins (i.e. HP121; Fig.3d), and are associated with rare phlogopite (HP124). The “layered” textural effect evidenced in some samples (i.e. HP143 or HP151; Figs. 3a, e) is marked by a trail of small irregular spinel within the olivine grains, and/or by the amphibole/clinopyroxene veins in clear textural disequilibrium with the dunite matrix (HP121; HP124 and HP143).

Secondary textures (i.e. glassy patches and sieved pyroxenes or with spongy rims) are rare in this group of ultramafic xenoliths. They consist of glassy thin *menisc* between minerals (including disseminated amphibole) or small pools (<100 microns) containing microlites of olivine, spinel and clinopyroxene (HP124, HP143, HP144, and HP151).

The predominant equigranular texture exhibited by Harrow Peaks xenoliths is completely absent in most of the xenolith suits from the same volcanic district (i.e. Baker Rocks and Greene Point), where the protogranular texture is commonly observed. In addition, secondary textures (i.e. glassy patches and sieved pyroxenes, spongy rims) are rarer with respect to other Antarctic xenolith occurrences (Coltorti et al., 2004; Pelorosso et al., 2016).

3. Analytical Methods

Bulk major and trace element analyses were precluded due to the small size of the xenoliths. Instead, thin and thick sections were prepared for in situ analytical protocols.

Major element compositions of minerals and glass were determined by a CAMECA SX100 electron microprobe equipped with four wavelengths dispersive (WD) and one Energy Dispersive (ED) spectrometer, at the Department of Lithospheric Research, University of Wien (Austria). The operating conditions were 15 kV accelerating voltage, 20 nA beam current and 20 s counting time on peak position.

To minimise Na and K loss, a 5µm defocused beam and 10 s counting time on peak position were applied for glass analyses. Moreover, for Ni and Ca the counting time was increased up to 40 s to improve their detection limits, at 500 ppm and 280 ppm respectively.

Natural and synthetic standards were used for calibration and PAP corrections were applied to the intensity data (Pouchou and Pichoir, 1991). Typical analytical uncertainties (relative standard deviation -RSD) are 0.2 to 0.6% for SiO_2, Al_2O_3, MgO, TiO_2, CaO; 1% for FeO; 2 to 3% for K_2O, Na_2O; 5 to 7% for P_2O_5, and 10 to 15% for MnO.

The concentrations of trace elements in pyroxene and glass were obtained by a Laser Ablation Microprobe-Inductively Coupled Plasma Mass Spectrometry (LAM-ICP-MS) at Geosciences Montpellier Université de Montpellier and at IGG- CNR, Pavia. Both laboratories applied the same analytical protocol and processing data system.

Each analysis took 120 s: 60 s for background acquisition (gas blank) and 60 s for sample acquisition. The analyses were corrected with internal standards using CaO for clinopyroxene and glass, and SiO_2 for orthopyroxene. The detection limit is a function of the ablation volume and counting time and is therefore calculated for each analysis. The ablation volume, in fact, greatly depends on the instrument configuration, consequently, the detection limit decreases if spot size, beam power and cell gas flow are reduced. A beam diameter of 40-100 µm and a scanning rate of 20 µm/s were used. The theoretical limit of detection ranges between 10 and 20 ppb for REE, Ba, Th, U, and Zr and 2 ppm for Ti.

Data were processed using the Glitter® software (van Achterbergh et al., 2001), and element concentrations were calibrated against the NIST612 certified reference material, using the values of Pearce et al. (1997).

4. Mineral chemistry

Major element data on olivine, pyroxene, spinel and amphibole are provided in the Supplementary material (Tables S1 to S5). Only for olivine, reported as the reference mineral, compositional averages *per* sample are listed in Table 2.

4.1 Mineral major element compositions

Olivine is the ubiquitous phase of the Harrow Peaks peridotites; however, despite the variety of the lithological types and the presence of composite xenoliths, it has a relatively narrow range of

composition. The forsterite (Fo) content, calculated as [Mg/(Mg+Fe_{tot}) x100 atomic formula units], varies from 86.18 to 90.76, and the NiO content from 0.26 to 0.47 wt %, reported as sample average (Fig. 4a; Tables 2 and S1 of Supplementary Material);

Olivine of orthopyroxenite HP163 and lherzolite HP164 are not included in this compositional range; they are in the range of Fo 79.00-86.33, with large grain to grain chemical zoning (Fig. 4a; Tables 2 and S1 of Supplementary Material).

Orthopyroxene vary in the range of $En_{66.62-83.89}Fs_{0.19-0.21}$-$Wo_{0.038-\ 0.17}$ with Mg# [Mg# = molar Mg/(Mg+Fe_{tot}) x100] = 82.54-89.56 showing textural equilibrium with the coexisting olivine as apparent cumulus phases in all the investigated samples. Orthopyroxene present Al_2O_3 contents mostly in the range of 1.24 to 3.32 wt %, and Cr_2O_3 and TiO_2 (as sample compositional averages) always <0.50 and <0.20 wt %, respectively (Fig. 4b; Table S2 of Supplementary Material).

Spinel are chemically heterogeneous, varying in composition from sample to sample without any clear relationship with the lithological types. In composite xenoliths HP124 and HP143 they show high variable Cr# [Cr# = molar Cr/(Cr + Al)x100] (37.33-59.48) and Mg# (49.13-60.81) values, with TiO_2 (0.5- 1.04 wt%) contents approaching the spinel composition of orthopyroxenite HP163. HP121 contains relatively low-Ti spinel (TiO_2=0.15-0.36 wt %) with the lowest Fe_2O_3 (0.71 wt % as sample average) recorded by the Harrow Peaks xenolith population (Fig.4c; Table S3 of Supplementary Material). Spinel from harzburgite HP144 and lherzolite HP151 show the highest and the lowest Cr# values, respectively, at similar low Fe_2O_3 (2.54 - 4.46 wt%) and (lowest) TiO_2 ($\leq$0.22 wt %) (Fig. 4c). Clinopyroxene occur in this group of ultramafic xenoliths in evident textural and chemical disequilibrium; they occur as small to very small grains, mostly pseudo-idiomorphic in shape, occupying triple junction positions between olivine - orthopyroxene and spinel (Figs. 4a, b, c.). They are Cr-rich augite following the Morimoto (1989) classification scheme, and heterogeneous in composition from one grain to another. Regardless of the lithology, Mg# values span from 85.18 to 94.06 with TiO_2< 0.55 wt % and Al_2O_3 < 4.13 wt % as sample averages (Figs., 5a, b; Table S4 of Supplementary Material).

Ortho- and clinopyroxene in all samples are widely out of Fe–Mg equilibrium with a $K_D \sim 0.6$ (as compared to the empirically determined equilibrium value of 1.09 ± 0.14; Putirka 2008).

Only a few grains of clinopyroxene concentrated in veins of both HP124 and HP143 dunites have TiO_2 and Al_2O_3 contents that reflect local interaction with the infiltrating host basalt (Figs. 5 a, b). Amphibole are texturally related to the clinopyroxene and generally occur as veins in dunites, while they are small and disseminated in lherzolites and the orthopyroxenite. They are chemically classified as kaersutite (HP121, HP143 and HP163), magnesio-hastingsite (HP124) and ferri-kaersutite (HP164), following the Leake et al. (1997) scheme, with Mg# ranging from 82.86 to 90.64 and TiO_2 and Al_2O_3 contents varying from 1.66 to 4.19 wt% and 11.43 to 14.86 %, respectively (Gentili et al., 2015, Figs. 5 c, d; Table S5 of Supplementary Material). The Harrow Peaks amphibole group had already been investigated for a crystallochemical study that led to the discovery of a new amphibole type: the ferri-kaersutite (Gentili et al. 2015).

Phlogopite grains occurring in HP124 appear chemically zoned (Mg# ~ 91-92), coherent with the observed variability of the other phases forming the vein. They have TiO_2 and Al_2O_3 contents between 1.41-2.19 wt% and 13.88-15.86 wt%, respectively; alkalis are instead constant (Na_2O ~0.60 wt%, K_2O ~ 9.60 wt%, Table S5 of Supplementary Material).

Glasses are extremely variable in composition (Table S6 of Supplementary Material) with SiO_2 contents ranging from 56.21 to 68.35 wt %, in relation to the textural position and adjacent mineral type, as well as the xenolith's lithology.

4.2 Pyroxene trace elements

Trace element concentrations of pyroxene averaged *per* sample are reported in Table 3, whereas all the LA-ICP-MS data are in Tables S7 –S10 of Supplementary Material.

In the chondrite-normalised REE+Sr+Zr+Hf+Ti+Y diagram, orthopyroxene display a H-MREE downward trend, with the slope increasing in the Yb and Lu region and with a ubiquitous positive

Ti anomaly (Fig. 6). Among dunites, only HP143 contains a few orthopyroxenes large enough for in situ trace element analyses. In detail, the chondrite-normalised trace element distribution of HP143 orthopyroxene mimics that of the HP164 lherzolite (clinopyroxene modal contents ~11 in volume %) and, to a lesser extent, that of the HP151 lherzolite (clinopyroxene ~9 in volume %), with Yb_N/Gd_N = 4.16 and remarkable Ti (Ti/Ti*=5.6) positive and Sr (Sr/Sr*=0.84) negative anomalies. HP166 lherzolite (clinopyroxene ~7 in volume %) displays orthopyroxene with high Zr, Hf (and Ti) and M-HREE contents, depicting a M-HREE chondrite normalised profile ~7 times higher, but LREE and LILE contents comparable to the orthopyroxene in lherzolites (and dunite). HP166 orthopyroxene show coupled strong Ti and Zr (Hf) positive anomalies. In turn, orthopyroxene in HP144 harzburgite (clinopyroxene ~3 and orthopyroxene ~13 in volume %) contains the lowest M-HREE (plus Ti), but the highest LREE and LILE concentrations of the entire xenolith population (Table 3), exhibiting almost flat or slightly L-REE enriched patterns (Ce_N/Nd_N ~ 2), (Fig. 6, Table 3).

Disseminated clinopyroxene are scarce in Harrow Peaks xenoliths. HP164 is the clinopyroxene-richest sample with 11 volume % of modal content (Table 1). Clinopyroxene are extremely variable in terms of trace element contents and, coherently with major elements behaviour, without any correlation with their modal contents. (Fig. 7a; Table 3). In the chondrite normalised incompatible multi-element variation diagram, clinopyroxene show negative Sr and Ti anomalies. The large compositional variability is even more evident in chondrite normalised REE diagrams (Fig. 7b) with overall enriched (La_N 9.02-89.9 and Yb_N 3.30-20.0 times chondrite) patterns, ranging from almost flat / slightly (i.e. HP143 La_N/Yb_N= 2.78) to highly (i.e HP124: La_N/Sm_N = 5.25; La_N/Yb_N= 10.47) LREE enriched. Strongly MREE enriched upward convex patterns (HP166: Gd_N/Yb_N=2.36; Gd_N/La_N=2.17) can also be observed. The clinopyroxene of HP151 and HP166 lherzolites display significant negative Eu anomalies (Fig. 7b).

Clinopyroxene (~6 volume%) in orthopyroxenite are compositionally variable; most of the grains reproduce the convex upward pattern shown in HP166 lherzolite (at a lower degree of enrichment,

Fig. 7b), and a few small crystals evidence a progressive LREE enrichment (La_N = 15.4-179, Fig. 7b).

Clinopyroxene concentrated in veins of HP143 and HP124 dunites have generally low HREE contents (Yb_N=3.3 for HP143 and 8.01 for HP124), with less pronounced or absent negative Sr and Ti anomalies with respect to the disseminated clinopyroxene of lherzolites and harzburgite. They share (almost) flat chondrite-normalised REE distribution patterns, but different degrees of LREE enrichments (La_N/Yb_N=2.78-10.47). As observed in lherzolites HP151 and HP166, an Eu anomaly also characterises the small clinopyroxene in the amphibole-bearing vein of HP121 composite xenolith.

4.3 Amphibole trace elements

Amphibole are characterised by incompatible trace element chondrite-normalised patterns of similar shape but with various degrees of trace element enrichment (i.e. Ba_N=13.2-95.6; Nd_N=11.1-46.1, Fig. 11a) and with systematic Nb and Ti positive anomalies (Fig. 8a). The lowest trace element concentrations are recorded by the rare amphibole in the thick clinopyroxene vein of the HP143 dunite (Figs, 3c and Fig. 8b). They perfectly mimic the coexisting clinopyroxene REE pattern (Fig. 8b). Conversely, the highest trace element concentrations are in the veined amphibole in the HP121 dunite that reflect a pure alkaline-like REE pattern (i.e. ~ La_N 43.1, Nd_N 46.1, Yb_N 11.3). Veined amphibole in the HP124 dunite is also characterised by a gently convex REE pattern (Fig. 8b), but depleted in LREEs with respect to the associated clinopyroxene. Finally, in the HP164 lherzolite, the disseminated amphibole roughly display a pattern similar to the coexisting clinopyroxene (Fig. 7b), but with higher LREE contents (i.e. amphibole: La_N= 32.2; clinopyroxene La_N=11.0, Figs. 7b and 8b). Overall, the Harrow Peaks amphibole appear more heterogeneous and trace element depleted with respect to that of the nearby Baker Rocks mantle xenolith population (Figs. 8a, b; Coltorti et al., 2004).

5. Discussion

Geochemical and textural features of Harrow Peaks ultramafic xenoliths highlighted remarkable differences between this locality and others in Antarctica. Primarily, the equigranular texture observed, is completely absent in most of the xenolith suits from the same volcanic district (i.e. Baker Rocks and Greene Point), where the protogranular texture is instead the predominant type; in addition, secondary textures (i.e. glassy patches and sieved pyroxenes, spongy rims) are rarer with respect to the other xenolith occurrences of this area (Coltorti et al., 2004; Pelorosso et al., 2016). Coherently, their modal compositions do not depict any trend attributable to a common mantle residual path (Fig. 2; Bodinier and Godard, 2003; Workman and Hart, 2005) and most important, the Fo content of olivine, in relation to the modal content, is difficult to ascribe to i) mantle residua as found in other localities in northern Victoria Land (Coltorti et al., 2004; Pelorosso et al., 2016, Fig.4a), or ii) alkaline cumulate rocks such as those sampled from Mt. Overlord (~ 50 Km from Harrow Peaks, Perinelli et al., 2017) or in thoeleiitic magmatic products as those of the Basement Sills (Bedard et al., 2007, Fig. 4a).

Spinels exhibit a large chemical variability, in terms of Cr/Al with respect to the Fo content-of the coexisting olivine, that makes the Fo - Spinel Cr# distribution unreproducible by melting, with the exception of dunite HP121, where spinel and olivine compositions intercept the mantle array curve relationships of Arai (1994) in a region that reflects a moderate fertile lherzolite (melting degree < 20%), inconsistent with the rock lithotype (Figs. 2 and 9). Conversely, they suggest a magmatic genesis, but tracing a possible spinel crystallization trend is unreasonable for this group of ultramafic cumulates (Fig. 9). At magmatic conditions, spinel Mg# is a function of melt Mg# and Al_2O_3, whereas at near- and post-magmatic conditions it is controlled by the rate of cooling and re-equilibration with coexisting silicates (Kamenesky et al., 2001), therefore the primary crystallization trend is hidden.

Moreover, clinopyroxene, which are extremely low in modal content, tend to have Mg# values comparable to those of the clinopyroxene from Antarctica mantle peridotites (Fig.5a, b), but without any relationship with potential residual (i.e. decreasing of Al_2O_3 with the increasing of Mg#) or metasomatic (i.e. enrichment in TiO_2 or Al_2O_3 at comparable Mg#) trends (Coltorti et al., 2004; Perinelli et al., 2006; 2008; 2011; Armienti and Perinelli 2010; Pelorosso et al., 2016, 2017).

Thus, all the mentioned characteristics suggest that xenoliths from Harrow Peaks do not represent a simple peridotite residuum after melt extraction. Consequently, we discuss the origin of these xenoliths as potentially representing cumulates that crystallised from various silicate melts migrating through the mantle and separated at mantle-crust boundary P-T conditions.

5.1 *Formation of Harrow Peaks xenoliths*

T-P-fO_2 equilibration conditions of the Harrow Peaks xenolith suite have been previously explored by Gentili et al. (2015), using a crystallochemical approach based on the amphibole dehydrogenation. The study highlighted a strong discrepancy between the redox conditions recorded by the amphibole dehydration equilibrium (ΔQFM = +5 - + 6.8) and those of the coexisting peridotite mineral assemblage (ΔQFM = – 2.78 - – 0.2) finally equilibrated at ~ 854 –940°C (calculated at P= 1.5 GPa). Using the same approach, this decoupling was not detected for the amphibole-bearing lherzolites and harzburgites of the nearby area of Baker Rocks where amphiboles and peridotite matrices converge to *f*O_2 values between QFM and ΔQFM –1.78 (Bonadiman et al., 2014).

Based on the crystallochemical model of Oberti et al. (2000), the Harrow Peaks amphibole present lattice parameters primarily ascribable to the magmatic-type (Gentili et al. 2015), whereas amphiboles from the rest of the Antarctic xenoliths have chemical and structural characteristics that fall within the "mantle-type" (Oberti et al. 2000; Bonadiman et al., 2014).

We re-examined the Harrow Peaks samples in view of the suggested possible magmatic origin and integrated previously determined thermobarometric results with new chemical data and new samples.

Temperature values calculated using the combination of olivine-spinel Fe-Mg exchange thermometers of Wood and Virgo (1989) and Ballhaus et al. (1991) in the lherzolites, harzburgite and dunites, respectively, suggest that these xenoliths finally equilibrated between 800 (orthopyroxenite HP163) and 1225°C (lherzolite HP151).

Presuming that the initial crystallisation of olivine was the main forming process of this group of xenoliths, the temperature of crystallisation was also calculated based on olivine/melt equilibrium, assuming that the Fe/Mg ratio of olivine (on sample average) was still close to the initial crystallization conditions. This is reasonable since they were extracted from the forming melts, and cumulated as monomineralic or bimineralic systems. Experimental determinations of Fe-Mg diffusivity in such a system reveal that for an olivine composition of Fo_{83-90} the closure temperature is reached quickly, and the estimated length scales for diffusion in a given time strongly decreased (Chakraborty 1997; Gordeychik et al., 2018).

The major oxides plus Ni (ppm) contents of the theoretical melt/s in equilibrium with olivine of the composite xenoliths were calculated by fitting various $^{Fe/Mg}Kd$- ^{Ni}Kd olivine/melt (Norman et al. 2002; 2005; Sobolev et al., 2005; Putirka et al. 2008; Laubier et al., 2014; Oeser et al. 2015) models. Using the equation [21] of Putirka (2008) and assigning a maximum H_2O content of 1 wt %, the best fit obtained for the high Mg# HP121 is a melt composition having Mg# 71.5. For HP124, HP143, the majority of lherzolites (Mg# 88) and the harzburgite (Mg# 89), the melt in equilibrium (melt 2) is obtained by fractionation of ca.4 % olivine and 0.8 % of spinel from melt 1 (Tables 4,5). Furthermore, the olivine in the orthopyroxenite sample (Mg# 80.54-84.49) are in equilibrium with a slightly evolved melt (melt 3) obtained by additional fractionation of ca. 5% of olivine, 4 % of orthopyroxene, 1 % of clinopyroxene and 0.5 of plagioclase from melt 2 (Table 5).

It is important to note that, the initial water content is included in the chemical parameters chosen in our calculations. This is because we had to consider that the measured water contents in tholeiites from a possible HP –related magmatic system is ~ 0.6-1 wt.% (Western Dronning Maud land; Heinonen and Luttinen 2010).

Overall, the calculated melts show compositions that span between high-Mg tholeiites (picrites?) and typical tholeiitic basalts, in a co-genetic evolution of the liquid line of descent. In this respect, the HP121 olivine represent the primitive crystallised product of the Kirkpatrick basalt precursor (Kyle, 1980; Fleming 1995). The olivine crystallisation temperature, obtained by iterative calculations using simultaneously melt composition and Fo-content (Putirka, 2008), is in the narrow range of 1314-1202± 27 °C, with, coherently, the highest values recorded for the olivine of HP121. The barometric conditions under which the Harrow Peak xenoliths were finally equilibrated were firstly deduced by the presence of spinel as the sole aluminium phase ($0.9 < P < 2.5$ GPa, Wood, 1974). However, an attempt to evaluate the region where the crystallised phases olivine, olivine + (orthopyroxene) and orthopyroxene + (olivine) separated from the hypothetical (calculated melt/s) was carried out applying the geobarometers of Putirka (2008) and Nimis and Ulmer (1998), based on orthopyroxene/melt and clinopyroxene/melt equilibrium, respectively. The values obtained (Table 4) limit the stationing of Harrow Peaks cumulates in the P field of 1.3 (HP143) – 0.5 (HP163) GPa. Considering that the estimated error (for the method) is ± 0.2 GPa, the values obtained are coherent with those reported by Perinelli et al. (2011, 2017), which constrain the crust/mantle boundary (Moho).

Experiments and data from a deep-seated layered-ultramafic intrusion (Cawthorn, 2018) showed that the Al_2O_3 content of orthopyroxene is a powerful tool to inspect the accumulation processes and relative motions in confined intrusive bodies (Cawthorn, 2018). It is well known that the Al_2O_3 content increases with increasing pressure, whereas Al_2O_3 positive correlations with Mg# are related to the falling temperature and differentiation (Gasparik, 1987; Maier and Eales;1997, Cawthorn, 2018). On the basis of experimental results and natural findings, Al_2O_3 in orthopyroxene is assumed

to vary in the order of 0.5 -0.6 wt% /0.1GPa (0.2 wt% *per* Km) in layered intrusive complexes (i.e. Bushveld; Cawthorn, 2018).

The wide range in Al_2O_3 values at near-constant Mg# (as shown in Fig. 4b) as observed for HP orthopyroxene could represent formation over a pressure range similar to that of the grain-magma two-phase assemblage. Hence, it is suggested that the Al_2O_3 variations of orthopyroxene from dunites to harzburgite/lherzolites (Fig. 4b) record possible movements towards a shallow lithospheric level and the orthopyroxene zoning within each sample is attributable to the cumulus/intercumulus grain-magma boundary (Cawthorn, 2018). In this context, the orthopyroxenite represents the end of the accumulation process at a shallow level (3 Km above) in the crust.

5.2 *Parental Melt modelling*

The predominant mineral assemblages (olivine+spinel) of the composite xenoliths, the occurrence of orthopyroxenite and the calculated olivine (and orthopyroxene)/melt equilibrium, reveal that the parental liquid had a high MgO content (Mg# 72) and was close to silica saturation. Such melts are associated with an anomalous high temperature (excess T_{ex}) melting of the Phanerozoic mantle (picrites) or the Archean cratons (komatiites). Picrites and komatiites either present cumulitic olivine or are olivine-saturated even at high pressure, so that they can reach such high MgO, Mg# (Lee et al., 2006; Class, 2008) and Ni contents (Sobolev et al., 2005).

All the studied Harrow Peaks xenoliths (including orthopyroxenite HP163), have olivine as cumulus phase, whose composition differs from most of the Antarctic ultramafic olivine cumulates, commonly ascribed to the Cenozoic alkaline magmatism of the West Antarctic Ridge System (Fig.4a; Gamble and Kyle, 1987; Gamble et al., 1988; Perinelli et al., 2017). Harrow Peaks' rocks instead, represent products crystallised at mantle depth, close to the Moho discontinuity, from the precursor melt/s of the Ferrar Group tholeiitic magmatism (Kyle 1990, Fleming 1995), or from the

high Mg-tholeiites (low Ti –picrites), similar to those of Vestfallja (Heinonen and Luttinen, 2008; 2010).

The calculated primitive melt forming the dunite matrix of HP121 has Mg# (up to 72) higher than any documented melt (Mg# 59-68), directly or indirectly (i.e. mantle metasomatic melt) related to the Cenozoic magmatic system, which is responsible for xenoliths rising to the surface (Coltorti, et. al. 2004; Perinelli et al. 2008; Nardini et al., 2009). In this respect, the HP121 dunite represents the primitive crystallised product of the Kirkpatrick basalt (Ferrar Group) precursor (low Ti picrites), whereas HP124 and HP143 dunites and harzburgite/lherzolite samples are fractionated and accumulated by melt/s close in composition to the exposed Ferrar thoeleiitic magmas (i.e. Kirkpatrick basalt; dolerites; Kyle 1980; Fleming 1995) in a co-genetic liquid line of descent (Table 5). The scarceness of olivine and the low Mg# of orthopyroxene in HP163 orthopyroxenite, point towards a cumulate of the same evolved melt (Table 5).

The calculated Harrow Peaks initial melt is high in Mg# and SiO_2, therefore orthopyroxene are expected to become liquidus phase since the initial stage of crystallization. This was observed in this group of samples, where orthopyroxene are absent or rare in dunites, while modally relevant in harzburgites and lherzolites (Table 1). In our model, the fractionation process (crystallisation and accumulation) is stopped at the early stage of evolution, with a predominant two-phase assemblage Ol (*sp*) +Opx (*cpx*) (Tables 1 and 5). Olivine (and spinel) are highly refractory to accept most of the incompatible trace elements of the basaltic geochemical system; the sole trace elements that, at maximum concentrations, are above the detection limits (LAM-ICP-MS; SIMs) are Ti, Zr, Y and HREE (De Hoog et al., 2010; Spandler and O'Neill, 2010). Consequently, the most fractionated melts in our model (melts 2 - 3; Table 5) preserve the pristine incompatible trace element budget, that is finally partitioned mainly in orthopyroxene and, to a lesser extent, in the rarer disseminated clinopyroxene. Orthopyroxene thus cannot depict a clear trace element fractionation trend in the multi-element-diagram, (Fig. 8), but if we consider those elements that are initially "partitioned" in olivine, (Ti, Zr Y and Yb) the fractionation line emerges (Fig.8).

In this situation, it is not easy to understand the role of clinopyroxene (and amphibole). The few clinopyroxene grains of HP121 and those concentrated in amphibole-bearing veins in HP124 and HP143, as well as the clinopyroxene occurring in harzburgite and lherzolites, generally show high Mg# (90-91) and Fe/Mg clinopyroxene/olivine distribution coefficients ($^{Fe/Mg}$Kd 0.59-0.97), out of the range of equilibrium values ($^{Fe/Mg}$Kd clinopyroxene/olivine = 0.83-0.86, Putirka 2008). Applying the $^{Fe/Mg}$Kd clinopyroxene/melt formulation of Putirka et al. (2008) and Mollo et al. (2017) to the previously calculated Harrow Peaks parental melts, the ideal liquidus clinopyroxene has a $^{Fe/Mg}$Kd clinopyroxene/melt of 0.24-0.27. The Harrow Peaks clinopyroxene instead, are characterised by $^{Fe/Mg}$Kd values (0.18-0.32) that cannot be equilibrated with most of the calculated melts (Table 4). This is clear for the HP121 and HP124 composite xenoliths ($^{Fe/Mg}$Kd clinopyroxene/melt = 0.18-0.15), whereas the HP143, where the clinopyroxene almost entirely form the monomineralic large vein (Fig. 3), is the only sample that records a potential equilibrium of clinopyroxene with the matrix olivine, and with a calculated melt ($^{Fe/Mg}$Kd clinopyroxene/melt = 0.27) having Mg#~68 (Table 5). HP143 clinopyroxene are characterised by notably lower REE contents with a slight LREE-enrichment and flat M-REE patterns (La_N/Ce_N=1.04). Moreover, they do not present the high Eu negative anomaly, which instead characterises most of the Harrow Peaks clinopyroxenes. Overall, the HP143 REE profile would confirm equilibrium with a tholeiite-like forming melt and is clearly distinct from the alkaline-type clinopyroxene of HP121 and HP124 dunites (Fig.9b).

Furthermore, we use the REE of the HP143 clinopyroxene to evaluate the HP143 parental melt REE contents. The ^{REE}Kd clinopyroxene/melt dataset used for the calculations is reported in Table S11 of Supplementary Material. The resulting profile mimics those of the Ferrar tholeiites and, coherently with the major element results, it suggests a potential equilibrium between the HP143 clinopyroxene and a parental thoeleiitic melt (Fig. 10).

To sum up, HP121 and HP163 are cumulates from hypothetical parental melts that represent two extremes: the most primitive and the most evolved terms of a hypothetical very short liquid line of descent, respectively. This suggests that the parental melt of the Kirkpatrick basalt was a (low

alkaline) picrite, which stationed in the shallow mantle. The melt system, modified in time and space, produced the rest of the Harrow Peaks ultramafic rocks, including the orthopyroxenite, at a shallower level. For all, but HP143, clinopyroxene (and amphibole) were formed by a different magmatic or metasomatic episode/s associated with more evolved melts that reasonably also crystallised plagioclase; this phase, even if not present in these cumulus fragments, may have imprinted the scattered Eu negative anomaly (Fig.9).

Despite the successful model in reproducing such ultramafic cumulates, we cannot exclude the possibility that each composition represents segregates of different melts. Considering that melts from Mg#72 to Mg# 60 close to silica saturation, may account for olivine spanning from Fo_{90} to Fo_{83} with the Ni content varying from 0.39 to 0.30 (on sample average), we could also argue that they are all primitive magmas derived from mantle sources with a variable contribution of a pyroxenite component (Sobolev et a., 2005; 2007; Matzen et al., 2014).

Considering the starting point of hypothetical fractionation lines, the most primitive HP olivine (highest NiO content= 0.39 wt% and T=1300 °C) is in equilibrium with a peridotite derived melt (Fig. 4a) and far from an initial melt of a pure pyroxenite source. As a raw consideration, it is also difficult to outline a possible mixing between the two sources to produce the HP121 olivine crystallising melt (Fig.4a).

Finally, we must consider that we are dealing with the chemistry of crystallised and accumulate minerals, thus, the nature of the mantle source of their forming melt is difficult to identify.

5.3 *Geodynamic implications*

The study of the Harrow Peaks xenoliths is clearly relevant as they represent the initial stages of the Ferrar magmatism. The importance of the Ferrar magmatism in West Antarctica is widely attested to (Kyle 1980; Fleming 1992; Elliot 1999); the large volume of magmas generated by this event

permeated part of the lithospheric domains beneath northern Victoria Land, refertilising the residual peridotitic upper mantle (Pelorosso et al., 2016).

The Ferrar large igneous system includes various magmatic bodies; among them, the doleritic Basement Sill from the McMurdo Dry Valleys represents the plumbing system of the Ferrar flood basalt eruptions (Bedard et al., 2007). The rock forming the sill displays a cumulate texture similar to that observed in layered intrusions and is characterised by an "orthopyroxene enriched base" (Bedard et al., 2007); hence, the orthopyroxenite HP163 could be representative of the same basement.

Orthopyroxenites are quite rare among the Antarctica xenoliths suites. To the best of our knowledge the only other one documented is associated with clinopyroxenites and peridotite xenoliths hosted in basalts of the Mount Morning eruptive centre (Martin et al., 2015).

In northern Victoria Land, orthopyroxenites were also found as part of the layered sequence from the Niagara Icefall (northern Victoria Land, Tribuzio et al., 2008); they were interpreted as cumulates of a boninitic melt related to the development of a back-arc basin in an active continental margin. Similarities between the Harrow Peaks ultramafic cumulates and the Niagara Icefall layered rocks include: i) the occurrence of high Mg# dunites (Mg# value ~90) coexisting with orthopyroxenites (Mg# values ~83-84); ii) the matching of REE abundances and profiles of clinopyroxenes from the Niagara Icefall gabbronorite with that of the HP143 clinopyroxene (Fig. 11). Therefore, considering the mentioned examples from different geodynamic settings, we cannot exclude *a priori* that the Harrow Peaks cumulates represent fragments of cumulus "layers" crystallised and separated from tholeiitic or boninitic melts. However, Harrow Peaks cumulates are hosted in lavas sampled in the Wilson Terrane, where the Ferrar outcrops are represented by the Ferrar Dolerite Dufek Intrusions and the Kirkpatrick Basalts (Hergt et al., 1989; Fleming et al., 1995; Elliot et al., 1999). Thus, the hypothesis that the investigated suite of samples could represent cumulus rocks from the most primitive Ferrar melt seems the most plausible.

Tracing the origin of Harrow Peaks cumulates back to the Jurassic, it is reasonable that they remained located within the shallow lithospheric mantle (*P* ~1 GPa) up to the Cenozoic (~ 50 Ma), when the alkaline magmatism associated with the West Antarctic Rift brought them to the surface. The Cenozoic (late stage) alkaline metasomatism pervaded large portions of mantle domains and cumulates suites in Victoria Land (Coltorti et al., 2004; Perinelli et al., 2006, 2008, 2011; Martin et al., 2015; Pelorosso et al., 2016, 2017), and affected the Harrow Peaks lithospheric portion, as testified by the presence of alkaline-like amphiboles (phlogopite) and the LREE-enrichment in clinopyroxene (HP121 and HP124).

Conclusions

1. The textural and geochemical characteristics of Harrow Peaks xenoliths evidence that these ultramafic rocks represent deep crustal/mantle cumulates crystallised from a primitive high Mg-melt with primitive olivine crystallising at temperature ~ 1300 °C;
2. The presence of orthopyroxenite in the system demonstrates that the inferred initial melt was either silica-saturated or rapidly evolved towards silica-saturation;
3. The mineral/melt equilibrium allowed the identification of parental melt as corresponding to the first stages of the Ferrar magmatism;
4. The peculiar olivine composition and the related mineral assemblage of this group of rocks suggest that a possible source of such primitive melts could be a peridotite with the (very limited) contribution of pyroxenite component.
5. During Cenozoic, the lithospheric mantle beneath Victoria Land was variably affected by an alkaline metasomatism related to the magmatic system, which was responsible for the xenoliths' sampling. This process also affected the Harrow Peaks district as testified by the occurrence of hydrous phases in complete geochemical disequilibrium with the anhydrous cumulus matrix.

Acknowledgements

We would like to thank two anonymous reviewers for their careful reading of the manuscript. In particular, we would thank Reviewer#1 for the detailed and helpful comments, which helped us to enrich the discussion of our results. In addition, the valuable remarks and editorial handling improved the clarity of our arguments and the presentation of this manuscript.

The authors would like to thank Barbara Galassi and Steve Deforie (Brighton, UK) for checking the English language in this paper.

This work was funded by PNRA (National Programme Antarctic Research) project: 2013-2015 "Hydrous phases stability in the lithospheric mantle of the large continental rift systems: a petrological/experimental study of the mantle xenoliths and lavas of the Northern Victoria Land (principal investigator; C.B)

B.P was supported by MIUR-2015 20158A9CBM Grant (principal investigator: C.B).

References

Arai S (1994) Characterization of spinel peridotites by olivine-spinel compositional relationships: review and interpretation. Chem Geol 113: 191-204

Armienti P, Perinelli C (2010) Cenozoic thermal evolution of lithospheric mantle in northern Victoria Land (Antarctica): evidences from mantle xenoliths. Tectonophysics 486: 28–35

Balestrieri ML, Bigazzi G, Ghezzo C, Lombardo B (1994) Fission track dating of apatites from the Granite Harbour Intrusive suite and uplift/denudation history of the Transantarctic Mountains in the area between David and Mariner Glaciers (Northern Victoria Land, Antarctica). Terra Antarctica 1 (1): 82-87

Ballhaus C, Berry RF, Green DH (1991) High pressure experiment calibration of the olivine-orthopyroxene-spinel oxygen barometer: implication for the oxidation state of the mantle. Contrib Mineral Petrol 107: 27-40

Bannister S, Yu J, Leitner B, Kennett BLN (2003) Variations in crustal structure across the transition from West to East Antarctica, Southern Victoria Land, Variations in crustal structure across the transition from West to East Antarctica, Southern Victoria Land, Geophys J Int 155: 870–880.

Beccaluva L, Coltorti M, Orsi G, Saccani E., Siena F (1991) Nature and evolution of subcontinental lithospheric mantle of Antarctica: evidence from ultramafic xenoliths of the Melbourne volcanic province (northern Victoria Land, Antarctica). Mem Soc Geo Ita 46: 353-370

Bédard JH, Marsh BD, Hersum TG, Naslund HR, Mukasa SB (2007) Large-scale mechanical redistribution of orthopyroxene and plagioclase in the Basement Sill, Ferrar dolerites, Antarctica: petrological, mineral-chemical and field evidence for channelized movement of crystals and melt. J Petrol 48: 2289-2326

Bodinier JL, Godard M, Carlson RW (2003) Orogenic, ophiolitic, and abyssal peridotites, Treatise on Geochemistry. 2. Geochemistry of the Mantle and Core, Amsterdam Elsevier, 103-170

Bonadiman B, Hao Y, Coltorti M, Dallai L, Faccini B, Huang Y, Xia Q (2009) Water contents of pyroxenes in intraplate lithospheric mantle. Eur J Mineral 21: 637-647

Bonadiman C, Coltorti M, Beccaluva L, Griffin WL, O'Reilly SY, and Siena F (2011) Metasomatism vs host magma infiltration: A case study of Sal mantle xenoliths, Cape Verde Archipelago, in Coltorti, M., and Gregoire, M., eds., Metasomatism in Oceanic and Continental Lithospheric Mantle: Geol Soc Spec Pap 478: 283–305

Bonadiman C, Nazzareni S, Coltorti M, Comodi P, Giuli G, and Faccini B (2014) Crystal chemistry of amphiboles: implications for oxygen fugacity and water activity in lithospheric mantle beneath Victoria Land, Antarctica. Contrib Mineral Petrol 167: 1-17

Cawthorn RG (2018) A non-horizontal floor during accumulation of the Bushveld Complex – Evidence and implications. Lithos 323-329.

Chakraborty S (1997) Rates and mechanisms of Fe–Mg interdiffusion in olivine at 980–1300 °C. J Geophys Res 102: 12317-12331

Collins TJ (2007) ImageJ for microscopy. Biotechniques 43: S25-S30

Coltorti M, Beccaluva L, Bonadiman C, Faccini B, Ntaflos T, Siena F (2004) Amphibole genesis via metasomatic reaction with clinopyroxene in mantle xenoliths from Victoria Land, Antarctica. Lithos 75: 115-139

Cooper AF, Adam LJ, Coulter RF, Eby G N and McIntosh WC (2007) Geology, geochronology and geochemistry of a basanitic volcano, White Island, Ross Sea, Antarctica. J Volcanol Geotherm Res 165: 189–216

Costa F. and Dungan M (2005) Short time scales of magmatic assimilation from diffusion modeling of multiple elements in olivine. Geology 33: 837–840

De Hoog JC M, Gall L and Cornell DH (2010) Trace-element geochemistry of mantle olivine and application to mantle petrogenesis and geothermobarometry. Chem Geol 270: 196–215

Elliot DH (1999) Paleovolcanological setting of the middle Jurassic Mawson Formation: evidence from the Prince Albert Mountains, Victoria Land. Paper Presented at the 8th International Symposium on Antarctic Earth Sciences. Victoria Univ., Wellington, New Zealand

Elliot DH and Fleming TH (2000) Weddell triple junction: the principal focus of Ferrar and Karoo magmatism during initial breakup of Gondwana. Geology 28: 539–542

Elliott DH and Fleming TH (2004) Occurrence and dispersal of magmas in the Jurassic Ferrar large igneous province, Antarctica. Gondwana Res 7: 223-237

Estrada S, Läufer A, Eckelmann K, Hofmann M, Gärtner A, Linnemann U (2016) Continuous Neoproterozoic to Ordovician sedimentation at the East Gondwana margin – implications

from detrital zircons of the Ross Orogen in northern Victoria Land, Antarctica. Gondwana Res, 37: 426-448. doi: 10.1016/j.gr.2015.10.006

Finn C, Moore D, Damaske D, Mackey T (1999) Aeromagnetic legacy of early subduction along the Pacific margin of Gondwana. Geology 27: 1087-1090

Fitzgerald PG (1994) Thermochronologic constraints on post-Paleozoic tectonic evolution of the central Transantarctic Mountains, Antarctica. Tectonics 13: 818-836

Fitzgerald PG, Stump E (1997) Cretaceous and Cenozoic episodic denudation of the Transantarctic Mountains, Antarctica: new constraints from apatite fission track thermochronology in the Scott Glacier region. J Geophys Res 102 (B4): 7747-7765

Fleming TH, Elliot DH, Jones LM, Bowman JR, Siders MA (1992) Chemical and isotopic variations in an iron-rich lava flow from the Kirkpatrick Basalt, north Victoria Land, Antarctica: implications for low-temperature alteration. Contrib Mineral Petrol 111: 440-457

Fleming TH, Foland KA, Elliot DH (1995) Isotopic and chemical constraints on the crustal evolution and source signature of Ferrar magmas, north Victoria Land, Antarctica. Contrib Mineral Petrol 121: 217–236

Gamble JA and Kyle PR (1987) The origins of glass and amphibole in spinel-wehrlite xenoliths from Foster Crater, McMurdo Volcanic Group, Antarctica. J Petrol 28: 755–779

Gamble JA, McGibbon F, Kyle PR, Menzies MA, Kirsch (1988) Metasomatized xenoliths from Foster Crater, Antarctica: implications for lithosphere structure and processes beneath the Transantarctic Mountains. In: Menzies, M.A., Cox, K.G. (Eds.). Oceanic and Continental Lithosphere: Similarities and Differences. J Petrol Special Issue 1, 109–138

Gentili S, Bonadiman C, Biagioni C, Comodi P, Coltorti M, Zucchini A, Ottolini L (2015) Oxo-amphiboles in mantle xenoliths: evidence for H2O-rich melt interacting with the lithospheric mantle of Harrow Peaks (Northern Victoria Land, Antarctica). Mineral Petrol 109: 741–759

Gibson GM, Wright TO (1985) Importance of thrust faulting in the tectonic development of northern Victoria Land, Antarctica. Nature 315: 480–483

Gleadow AJW, Fitzgerald PF (1987) Uplift history and structure of the Transantarctic Mountains: new evidence from fission track dating of basement apatites in the Dry Valleys area, southern Victoria Land. Earth and Planet Sci Lett 82: 1-14

Gordeychik B, Churikova T, Kronz A, Sundermeyer C., Simakin A., Wörner G (2018) Growth of, and diffusion in, olivine in ultra-fast ascending basalt magmas from Shiveluch volcano. Sci Rep 8 (11775): 1-15.

Gavrilenko M, Ozerov A, Kyle PR, Carr MJ, Nikulin A, Vidito C, Danyushevsky L (2016) Abrupt transition from fractional crystallization to magma mixing at Gorely volcano (Kamchatka) after caldera collapse. Bull Volcanol 78: 47

Heinonen JS, Luttinen AV (2008) Jurassic dikes of Vestfjella, western Dronning Maud Land, Antarctica: Geochemical tracing of ferropicrite sources. Lithos 105: 347-364

Heinonen JS, Luttinen AV (2010) Mineral chemical evidence for extremely magnesian subalkaline melts from the Antarctic extension of the Karoo large igneous province. Mineral Petrol 99: 201-217

Hergt JM, Chappell BW, Faure G, Mensing TM (1989) The geochemistry of Jurassic dolerites from Portal Peak, Antarctica. Contrib Mineral Petrol 102: 298-305

Herzberg C (2004) Geodynamic information in peridotite petrology: J Petrol 45: 2507–2530, doi:10.1093/petrology/egh039

Herzberg C, Gasparik T (1991) Garnet and pyroxenes in the mantle: a test of the majorite fractionation hypothesis. J Geophys Res 96: 16263–16274

Herzberg C, Ratteron P, Zhang J (2000) New experimental observations on the anhydrous solidus for peridotite KLB-1. Geochem Geophys. 1, paper no. 2000GC000089

Jennings ES, Holland TJB (2015) A Simple Thermodynamic Model for Melting of Peridotite in the System NCFMASOCr, J Petrol 56 (5): 869–892

Kamenetsky VS, Crawford AJ, Meffre S (2001) Factors controlling chemistry of magmatic spinel: An empirical study of associated olivine, Cr-spinel and melt inclusions from primitive rocks J Petrol 42: 655–671.

Kyle PR (1980) Development of heterogeneities in the subcontinental mantle: evidence from the Ferrar Group, Antarctica. Contrib Mineral Petrol 73: 89–104. LeMasurier WE, Thomson J W (Eds.) 1990. Volcanoes of the Antarctic Plate and Southern Oceans. Antarctic Research Series, Washington, DC AGU 48, 487

Leake BE, Woolley AR, Arps CES, Birch WD, Gilbert MC, Grice JD, Hawthorne FC, Kato A, Kisch HJ, Krivovichev VG, Linthout K, Laird J, Mandarino JA, Maresch WV, Nickel EH, Rock NMS, Schumacher JC, Smith DC, Stephenson NCN, Ungaretti L, Whittaker EJW, and Youzhi G (1997) Nomenclature of amphiboles: Report of the Subcommittee on Amphiboles of the International Mineralogical Association, Commission on New Minerals and Mineral Names. Amer Miner 82: 1019–1037

Lee C-TA, Cheng X, Horodyskyj U (2006) The development and refinement of continental arcs by primary basaltic magmatism, garnet pyroxenite accumulation, basaltic recharge and delamination: insights from the Sierra Nevada, California. Contrib Mineral Petrol 151: 222–242

Martin A P, Price RC, Cooper AF, McCammon CA (2015) Petrogenesis of the Rifted Southern Victoria Land Lithospheric Mantle, Antarctica, Inferred from Petrography, Geochemistry, Thermobarometry and Oxybarometry of Peridotite and Pyroxenite Xenoliths from the Mount Morning Eruptive Centre. J Petrol 56: 193–226

Mc Donough WF and Sun S.-s. (1995) The composition of the Earth. Chem Geol 120: 223-253.

Matzen AK, Baker MB, Beckett JR, Stolper EM (2013) The temperature and pressure dependence of nickel partitioning between olivine and silicate melt J Petrol 54: 2521–2545

Melchiorre M, Coltorti M, Bonadiman B, Faccini B, O'Reilly SY and Pearson N (2011). The role of eclogite in the rift-related metasomatism and Cenozoic magmatism of Northern Victoria Land, Antarctica. Lithos 124: 319-330

Mercier, J.C., Nicolas, A., 1975. Textures and Fabrics of the Upper-Mantle Peridotites as illustrated by Xenoliths from Basalts. J Petrol 16: 454-487

Mollo S, Blundy JD, Giacomoni P, Nazzari M, Scarlato P, Coltorti M, Langone A, Andronico D (2017) Clinopyroxene-melt element partitioning during interaction between trachybasaltic magma and siliceous crust: Clues from quartzite enclaves at Mt. Etna volcano. Lithos 284: 447–461

Nardini I, Armienti P, Rocchi S, Dallai L, Harrison D (2009) Sr–Nd–Pb–He–O isotopeand geochemical constraints to the genesis of Cenozoic magmas from the West Antarctic rift. J Petrol 50: 1359–1375

Nimis P, Ulmer P (1998) Clinopyroxene geobarometry of magmatic rocks: part 1. An expanded structural geobarometer for anhydrous and hydrous, basic and ultrabasic systems. Contrib Mineral Petrol 133: 122–135

Norman MD, Garcia MO, Kamenetsky VS, Nielsen RL (2002) Olivine-hosted melt inclusions in Hawaiian picrites: equilibration, melting, and plume source characteristics. Chem Geol 183: 143-168

Oberti R, Vannucci R, Zanetti A, Tiepolo M, Brumm RC (2000) A crystal-chemical re-evaluation of amphibole/melt and amphibole/ clinopyroxene D Ti in petrogenetic studies. Amer Miner 85: 407–419

Park K, HiChoi S, Cho M, Lee DC (2017) Evolution of the lithospheric mantle beneath Mt. Baekdu (Changbaishan): Constraints from geochemical and Sr–Nd–Hf isotopic studies on peridotite xenoliths in trachybasalt. Lithos 286-287: 330_ 344

Pearce N JG, Perkins WT, Westgate JA, Gorton MP, Jackson SE, Neal CR and Chenery SP (1997) A compilation of new and published major and trace data for NIST SRM 610 and NIST SRM 612 glass reference materials. Geostand Newslett 21, no. 1, 115–144

Oeser M, Dohmen R, Horn I, Schuth S and Weyer S (2015) Processes and time scales of magmatic evolution as revealed by Fe-Mg chemical and isotopic zoning in natural olivines. Geochim Cosmochim Acta 154: 130–150

Pelorosso B, Bonadiman C, Coltorti M, Faccini B, Melchiorre M, Ntaflos T and Gregoire M (2016) Pervasive, tholeiitic refertilisation and heterogeneous metasomatism in northern Victoria Land lithospheric mantle (Antarctica). Lithos 248–251: 493–505

Pelorosso B, Bonadiman C, Coltorti M, Melchiorre M, Giacomoni PP, Ntaflos T, Gregoire M, Benoit M (2017) Role of percolating melts in Antarctic subcontinental lithospheric mantle: New insights from Handler Ridge mantle xenoliths (northern Victoria Land, Antarctica), in Bianchini G, Bodinier J-L, Braga R, and Wilson M, eds., The Crust-Mantle and Lithosphere-Asthenosphere Boundaries: Insights from Xenoliths, Orogenic Deep Sections, and Geophysical Studies: Geol Soc Am Special Paper 526: 133–150

Perinelli C, Armienti P, Dallai L (2006) Geochemical and O-isotope constraints on the evolution of lithospheric mantle in the Ross Sea rift area (Antarctica). Contrib Mineral Petrol 151: 245-266

Perinelli C, Orlando A, Conte AM, Armienti P, Borrini D, Faccini B, and Misiti V (2008) Metasomatism induced by alkaline magma on upper mantle of the Northern Victoria Land (Antarctica): an experimental approach. In: Coltorti, M. and Gregoire, M. (eds) Mantle Metasomatism in Intra-plate and Suprasubduction Settings. Geol Soc London Spec Publ 293: 197-221

Perinelli C, Armienti P, Dallai L (2011) Thermal evolution of the lithosphere in a rift environment as inferred from the geochemistry of mantle cumulates; Northern Victoria Land, Antarctica. J Petrol 52: 665-690

Perinelli C, Andreozzi GB, Conte AM, Oberti R, Armienti P (2012) Redox state of subcontinental lithospheric mantle and relationships with metasomatism: insights from spinel peridotites from northern Victoria Land (Antarctica). Contrib Mineral Petrol 164: 1053-1067

Perinelli C, Gaeta M, Armienti P (2017) Cumulate xenoliths from Mt. Overlord, northern Victoria Land, Antarctica: A window into high pressure storage and differentiation of mantle-derived basalts. Lithos 268–271: 225–239

Popp RK, Hibbert HA, Lamb WM (2006) Oxy-amphibole equilibria in Ti-bearing calcic amphiboles: experimental investigation and petrologic implications for mantle-derived amphiboles. Am Mineral 91: 54–66

Pouchou JL, Pichoir F (1991) Quantitative Analysis of Homogeneous or Stratified Microvolumes Applying the Model "PAP". In: Heinrich K.F.J., Newbury D.E. (eds) Electron Probe Quantitation. Springer, Boston, MA. 31-75

Putirka K.D (2008) Thermometers and barometers for volcanic systems. In: Putirka, K.D., Tepley III, F.J. (Eds.). Minerals, Inclusions and Volcanic Processes, Reviews in Mineralogy and Geochemistry vol 69: pp. 61–120

Rocchi S, Tonarini S, Armienti P, Innocenti F, Manetti P (1998) Geochemical and isotopic structure of the early Palaeozoic active margin of Gondwana in northern Victoria Land, Antarctica. Tectonophysics 284: 261–281

Rocchi S, Armienti P, D'Orazio M, Tonarini S, Wijbrans J, Di Vincenzo GD (2002) Cenozoic magmatism in the western Ross Embayment: role of mantle plume vs. plate dynamics in the development of the West Antarctic Rift System. J Geophys Res 107 (B9), 2195

Sato H (1977) Nickel content of basalticmagmas: identification of primarymagmas and a measure of the degree of olivine fraction. Lithos 10: 113–120

Schmidt DL, Rowley, PD (1986) Continental rifting and transform faulting along the Jurassic Transantarctic Rift, Antarctica. Tectonics 5: 279-291

Sobolev, AV, Hofmann, AW, Sobolev, SV, Nikogosian, IK (2005) An olivine-free mantle source of Hawaiian shield basalts. Nature 434, 590-597

Sobolev AV, Hofmann AW, Kuzmin DV, Yaxley GM, Arndt NT, Chung, SL, Danyushevsky LV, Elliott T, Frey FA, Garcia MO, Gurenko AA, Kamenetsky VS, Kerr AC, Krivolutskaya NA, Matvienkov VV, Nikogosian IK, Rocholl A, Sigurdsson IA, Sushchevskaya NM, Teklay M (2007) The amount of recycled crust in sources of mantle-derived melts. Science 316:412-417.

Spandler C and O'Neill HStC (2010) Diffusion and partition coefficients of minor and trace elements in San Carlos olivine at 1,300 °C with some geochemical implications. Contrib Mineral Petrol 159: 791–818.

Storey BC, Alabaster T (1991) Tectonomagmatic controls on Gondwana break-up models: evidence from the proto-Pacific margin of Antarctica. Tectonics 10 (6): 1274-1288.

Storey BC and Kyle PR (1997) An active mantle mechanism for Gondwana break-up, South African J Geol 100: 283–290

Storey BC, Vaughan AP and Riley TR (2013) The links between large igneous provinces, continental break-up and environmental change: evidence reviewed from Antarctica. Earth and Environmental Science Transactions of the Royal Society of Edinburgh 104: 17–30

Stump E, Fitzgerald PG (1992) Episodic uplift of the Transantarctic Mountains. Geology 20: 161-164

Tribuzio R, Tiepolo M, Fiameni S (2008) A mafic-ultramafic cumulate sequence derived from boninite-type melts (Niagara Icefalls, northern Victoria Land, Antarctica). Contrib Mineral Petrol 155: 619-633

van Achterbergh E, Griffin WL, and Stiefenhofer J (2001) Metasomatism in mantle xenoliths from the Letlhakane kimberlites: Estimation of element fluxes: Contrib Mineral Petrol 141: 397–414

Wang Z and Gaetani GA (2008) Partitioning of Ni between olivine and siliceous eclogite partial melt: experimental constraints on the mantle source of Hawaiian basalts. Contrib Mineral Petrol 156: 661–678

Wood BJ and Virgo D (1989) Upper mantle oxidation state: Ferric iron contents of lherzolite spinels by Mossbauer spectroscopy and resultant oxygen fugacities. Geochim Cosmochim Acta 53: 1277-1291

Workman RK and Hart SR (2005) Major and trace element composition of the depleted MORB mantle (DMM). Earth Planet Sci Lett 231: 53- 72

Zipfel J and Wörner G (1992) Four- and five-phase peridotites from a continental rift system: evidence for upper mantle uplift and cooling at the Ross Sea margin (Antarctica). Contrib Mineral Petrol 111: 24-36

Figure Captions

Figure 1. Sketch map of northern Victoria Land and location of Harrow Peaks outcrop (red circle). Greene Point (Melchiorre et al., 2011; Pelorosso et al., 2016), Baker Rocks (Coltorti et al., 2004; Perinelli et al., 2006, 2008) and Handler Ridge (Pelorosso et al., 2017) are also reported (black circles). The map of northern Victoria Land is modified from Estrada et al. (2016), the Antarctica view is from Google Earth (US Dept of State Geographer. Image Landsat/Copernicus. Image U.S. Geological Survey Data SIO, NOAA, U.S. Navy, NGA, GEBCO).

Figure 2. Harrow Peaks xenoliths in the olivine-orthopyroxene-clinopyroxene IUGS classification diagram. (*) Composite xenoliths. Due to the uncertainties of modal determinations, composite

xenoliths are all attributable to dunite. The residual path (annotated by melting %) from PM (Primordial Mantle, McDonough and Sun, 1995) to clinopyroxene consumption is also calculated (dashed line) using theoretical and experimental results of Jensing and Holland (2015) and Herzberg (2004).

Figure 3. Photomicrographs of representative microstructures from Harrow Peaks xenoliths. Polygonal large olivine with boundaries-converging at 120° (a, b), detail of the large clinopyroxene vein with embryonic amphibole (c). Tabular olivine zone and amphibole vein in sample HP121 (d). Lherzolite HP166 characterised by equigranular olivine, orthopyroxene and small clinopyroxene (e). Large orthopyroxene in the orthopyroxenite HP163 (f)

Figure 4. Chemical composition of (a) olivine (NiO *vs.* Fo) 1, 2 and 3 are fractional crystallisation trends for Hawaiian tholeiites, Hawaiian basalts and from a pyroxenite source (Sato, 1977; Wang and Gaetani, 2008 and Gavrilenko and al. 2016); (b) orthopyroxene (Al_2O_3 *vs.* Mg#), the black arrow indicates the large Al_2O_3 compositional zoning due to cumulus processes; (c) spinel (Mg# *vs.* Cr#); Compositional fields defined by Victoria Land peridotites (Coltorti et al., 2004; Martin et al., 2015; Pelorosso et al., 2016, 2017), Mt Overlord cumulates (Perinelli et al., 2017) and Basement sill leucotroctolites (Bedard et al., 2007) are reported for comparison.

Figure 5. Harrow Peaks clinopyroxene (a, b) and amphibole (c, d) compositions in term of Mg# *vs.* TiO_2 and *vs.* Al_2O_3. Compositional fields reported for comparison in (a, b) are as in Figure 4.

Figure 6. Chondrite-normalized trace element (REE+Sr+Zr+Hf+Ti+Y) distribution for Harrow Peaks orthopyroxene (represented as sample average). Chondrite values from McDonough and Sun (2005)

Figure 7. Chondrite-normalized trace-element patterns a) and Rare Earth Elements (REE) patterns b) for Harrow Peaks clinopyroxene represented ad sample average, except for HP163 (orthopyroxenite). Due to the large trace element variability, all the analyses of the few HP163 clinopyroxenes are reported. Chondrite values from McDonough and Sun (2005)

Figure 8. Chondrite-normalized trace-element patterns (a) and REE patterns (b) of amphibole. For comparison, the compositional field defined by the amphibole from northern Victoria Land peridotites (Coltorti et al., 2004) is also reported. Chondrite values from McDonough and Sun (2005)

Figure 9. Plot of spinel Cr# *vs* Fo content of coexisting olivine of Harrow Peaks ultramafic xenoliths. (*) Composite xenoliths. Due to the uncertainties of modal determinations, composite xenoliths are all attributable to dunite. The olivine–spinel mantle array is from Arai (1994). Melting trend (annotated by melting %) is from Park et al. (2017); peridotite fields are modified from Park et al. (2017). Sample HP163 is not reported, having Cr# spinel and Mg# olivine at 0.43 and 81.9 out of the diagram's scale.

Figure 10. Trace element composition modelling of melt 2, as calculated (major elements) in Table 5. The reconstructed melt 2, assumed in equilibrium with HP143 clinopyroxene, is obtained using REE $Kd^{cpx/melt}$ data from GERM (Table S11). The resulting profile converges on a tholeiitic melt that resembles the Ferrar basalt (Kyle 1980; Fleming et al., 1995). In turn, HP143 clinopyroxene profile mimics those occurring in the ultramafic sequence (cumulates) from Niagara Ice Falls (Tribuzio et al., 2008). Chondrite-normalized values from McDonough and Sun (2005).

Figure S1. Thin sections of Harrow Peaks mantle xenoliths, which are mainly characterised by equigranular textural type. HP143, HP124, HP121composite xenoliths (a, b, c) consist of large

clinopyroxene and amphibole veins cross-cutting a dunitic matrix. a) HP143 with evident spinel trails. Important to note that the real modal content of spinel do not correspond to the black areas as in the thin section. b) HP124 is characterised by dunitic matrix and the thinnest vein containing also phlogopite. c) HP121 with the largest monomineralic vein that has been partly removed for crystallochemical investigations (Gentili et al., 2015). Harzburgite HP144 (d) and high clinopyroxene lherzolite (e). High orthopyroxene lherzolites (f, g) and orthopyroxenite (h).

An insight into the first stages of the Ferrar magmatism: ultramafic cumulates from Harrow Peaks, northern Victoria Land, Antarctica.

Beatrice Pelorosso [a], Costanza Bonadiman[a*],
Theodoros Ntaflos[b], Michel Gregoire[c], Silvia Gentili[d] , Alberto Zanetti[e], Massimo Coltorti[a]

a Dipartimento di Fisica e Scienze della Terra, Università di Ferrara, Italy
b Department of Lithospheric Research, University of Vienna, Austria
c GET, Université de Toulouse, CNRS, CNES, IRD, UPS, (Toulouse), France
d Dipartimento di Fisica e Geologia, Università di Perugia, Piazza dell'Università 1, 06123 Perugia, Italy
e CNR-IGG, Sezione di Pavia, via Ferrata 1, I-27100 Pavia, Italy

*corresponding author : costanza.bonadiman@unife.it ; bdc@unife.it

Key words: ultramafic xenoliths; high-Mg magmatic olivines; orthopyroxenite; Karoo-Ferrar large igneous province.

Abstract

A group of ultramafic xenoliths hosted in Cenozoic hypabyssal rocks from Harrow Peaks (northern Victoria Land, Antarctica) show textural and geochemical features far removed from anything previously observed in mantle xenoliths of this region and elsewhere in Antarctica. They consist of spinel bearing lherzolites and harzburgites, characterised by a predominant equigranular texture with orthopyroxene modal contents remarkably higher in lherzolites (18 - 26 volume. %) with respect to the harzburgite (13 vol. %), one orthopyroxenite and three composite xenoliths. The latter are formed by an olivine–dominant assemblage (olivine > 70 %) crosscut by large monomineralic (amphibole or clinopyroxene) or bimineralic (amphibole+clinopyroxene) veins.

No significant correlation was observed between the lithology and the Fo content (90.21-82.81) of olivine, suggesting that these rocks could be derived from a cumulus process.

The presence of the orthopyroxenite suggests that the inferred melt/s from which they stemmed, was close (or even above) to silica saturation. Based on major and trace element mineral/melt and

mineral/mineral equilibrium modelling, these rocks were formed by progressive extraction of olivine from a high magnesium (Mg=72) - high temperature (~1300 °C) melt following a very short fractionation line. Thermo-barometric results indicate the stationing of Harrow Peaks cumulates in the P field of 1.3 ± 0.2 (dunites) – 0.5 ± 0.2 (orthopyroxenite) GPa. These values well match the crust/mantle boundary (Moho) of the region. The combined geochemical and petrological data suggest that Harrow Peaks melts could be related to the initial stage of the Jurassic Ferrar magmatism, whose deep cumulates were subsequently affected by the Cenozoic alkaline metasomatism, widely detected in the northern Victoria Land lithosphere and responsible for the formation of the late amphibole /amphibole+clinopyroxene veins.

1. Introduction

The West Antarctic Rift system (WARS) is one of the largest continental rift areas in the world and is comparable to the East African Rift in scale (Martin et al., 2015; Le Masurier and Thomson 1990). Since the Cenozoic it was affected by alkaline magmatism represented by the Mc. Murdo volcanic and Meander intrusive rocks (Kyle 1980). The most primitive volcanic products from Victoria Land contain mafic and ultramafic xenoliths in a large spectrum of lithologies that testify for a complex mantle/crust evolution of the Subcontinental Lithospheric Mantle (SCLM). Evidence of mantle partial melting and enrichment events (due to both alkaline metasomatism and refertilisation by tholeiitic melts) as well as crystallization of alkaline melts at the Moho depth have been widely documented (Gamble et al., 1988; Beccaluva et al., 1991; Cooper et al., 2007; Martin et al., 2015; Pelorosso et al., 2016). Geochemical and isotopic data trace back the refertilisation process of SCLM in the northern Victoria Land to before the Cenozoic began (Melchiorre et al., 2011; Pelorosso et al., 2016), suggesting a possible connection with the most important magmatic activity in Antarctica, which occurred before the Cenozoic: the Jurassic magmatism, part of the Karoo-Ferrar Large Igneous Province. The Jurassic magmatism produced outcrops that stretch over 3500

km from the Theron Mountains of Antarctica to southeast Australia (Elliot & Fleming 2004), including several volcanic bodies such as mafic sills, flood basalts (i.e. Kirkpatrick basalt, Vestfjella ferropicrites), phreatomagmatic volcanic rocks, layered mafic intrusions (i.e. Ferrar dolerite sill) and mafic dykes (Kyle et al., 1989; Fleming 1995; Elliot et al., 1999; Storey et al., 2013; Heinonen and Luttinen, 2010; Bedard et al., 2007). At Harrow Peaks (74.0 2785°S 164.47466°E, Fig. 1), where the alkaline Cenozoic magmatism is dominant as well as in many other northern Victoria Land magmatic localities, lavas brought to the surface ultramafic xenoliths.

The samples available for this study were collected during the XX Italian Expedition organised by PNRA (Programma Nazionale Ricerche in Antartide) in the 2004/05 Austral summer. They are mainly (amphibole bearing) spinel peridotites, but composite xenoliths are also abundant. The Harrow Peaks samples include dunites and one orthopyroxenite, which are rarely observed or absent in the xenolith populations sampled in the region and carried by the same magmatic system (Perinelli et al., 2011; 2018; Coltorti 2004; Martin 2015 and reference therein).

A few of these xenoliths were studied by Gentili et al. (2015) to evaluate the role of amphibole formation in the modification of the original redox condition of this mantle domain. The quoted authors revealed extremely high redox conditions (Δlog QFM fO_2 = ~ +5, +7) for the amphibole formation, in clear disequilibrium with the peridotite matrix.

In this paper, we present new petrological and geochemical data of this unique group of ultramafic xenoliths, which provide evidence for a magmatic origin. Moreover, they show to what extent these rocks also experienced metasomatic event(s) that are attributable to large scale processes that occurred in Victoria Land SCLM.

2. Sample description and Petrography

The ultramafic xenoliths found in the Harrow Peaks lavas are rather small (< 10 cm) and sub-rounded in shape.

The mineral modal proportion was determined by point counting, averaging two runs with more than 2,000 points for each thin section (2.5 x 4.0 cm), Table 1. Based on the classification diagram for mafic and ultramafic rocks (Fig. 2; Streickeisen, 1974), the Harrow Peaks xenoliths consist of spinel-bearing lherzolites (HP151, HP164 and HP166), one harzburgite (HP144) and one orthopyroxenite (HP163).

Three out of the eight samples selected for this study are composite xenoliths formed by an olivine –dominant assemblage (olivine > 70 %) crosscut by large monomineralic or bimineralic veins. They combine various lithologies that make it difficult to apply the standard nomenclature for ultramafic rocks. Two composite samples are made up of a dunite matrix crossed by clinopyroxene (HP143, Fig. 1S) and clinopyroxene + amphibole + rare phlogopite (HP124, Fig.1S) veins. HP121 is also composite, with a harzburgite matrix (containing up to 6% and 4% of modal orthopyroxene and clinopyroxene, respectively) crosscut by a large amphibole vein (Fig. 1S). Considering the uncertainties of the modal content, we cannot attribute to this sample an unequivocal classification term (Fig. 2; Table1), therefore we equate the HP121 sample with the rest of the composite dunites. Hydrous phases (mainly amphibole) occur in all samples, showing significant different grain sizes and modal contents from sample to sample.

Regardless of the lithology, most of the samples are tabular to equigranular (Mercier & Nicolas 1975) with equidimensional, polygonal in shape olivine (1 mm) delimited by boundaries often converging at 120° (i.e. Figs. 3a, b). The modal content of the orthopyroxene is higher in lherzolites (18 - 26 volume. %) with respect to the harzburgite (13 vol. %). The clinopyroxene in lherzolites/harzburgite are small and interstitial (Fig. 3e); small irregular spinel are scattered between the olivine grains. Amphibole are present both as disseminated crystals (i.e. HP124; Fig. 3b) or in veins (i.e. HP121; Fig.3d), and are associated with rare phlogopite (HP124). The “layered” textural effect evidenced in some samples (i.e. HP143 or HP151; Figs. 3a, e) is marked by a trail of small irregular spinel within the olivine grains, and/or by the amphibole/clinopyroxene veins in clear textural disequilibrium with the dunite matrix (HP121; HP124 and HP143).

Secondary textures (i.e. glassy patches and sieved pyroxenes or with spongy rims) are rare in this group of ultramafic xenoliths. They consist of glassy thin *menisc* between minerals (including disseminated amphibole) or small pools (<100 microns) containing microlites of olivine, spinel and clinopyroxene (HP124, HP143, HP144, and HP151).

The predominant equigranular texture exhibited by Harrow Peaks xenoliths is completely absent in most of the xenolith suits from the same volcanic district (i.e. Baker Rocks and Greene Point), where the protogranular texture is commonly observed. In addition, secondary textures (i.e. glassy patches and sieved pyroxenes, spongy rims) are rarer with respect to other Antarctic xenolith occurrences (Coltorti et al., 2004; Pelorosso et al., 2016).

3. Analytical Methods

Bulk major and trace element analyses were precluded due to the small size of the xenoliths. Instead, thin and thick sections were prepared for in situ analytical protocols.

Major element compositions of minerals and glass were determined by a CAMECA SX100 electron microprobe equipped with four wavelengths dispersive (WD) and one Energy Dispersive (ED) spectrometer, at the Department of Lithospheric Research, University of Wien (Austria). The operating conditions were 15 kV accelerating voltage, 20 nA beam current and 20 s counting time on peak position.

To minimise Na and K loss, a 5μm defocused beam and 10 s counting time on peak position were applied for glass analyses. Moreover, for Ni and Ca the counting time was increased up to 40 s to improve their detection limits, at 500 ppm and 280 ppm respectively.

Natural and synthetic standards were used for calibration and PAP corrections were applied to the intensity data (Pouchou and Pichoir, 1991). Typical analytical uncertainties (relative standard deviation -RSD) are 0.2 to 0.6% for SiO_2, Al_2O_3, MgO, TiO_2, CaO; 1% for FeO; 2 to 3% for K_2O, Na_2O; 5 to 7% for P_2O_5, and 10 to 15% for MnO.

The concentrations of trace elements in pyroxene and glass were obtained by a Laser Ablation Microprobe-Inductively Coupled Plasma Mass Spectrometry (LAM-ICP-MS) at Geosciences Montpellier Université de Montpellier and at IGG- CNR, Pavia. Both laboratories applied the same analytical protocol and processing data system.

Each analysis took 120 s: 60 s for background acquisition (gas blank) and 60 s for sample acquisition. The analyses were corrected with internal standards using CaO for clinopyroxene and glass, and SiO_2 for orthopyroxene. The detection limit is a function of the ablation volume and counting time and is therefore calculated for each analysis. The ablation volume, in fact, greatly depends on the instrument configuration, consequently, the detection limit decreases if spot size, beam power and cell gas flow are reduced. A beam diameter of 40-100 µm and a scanning rate of 20 µm/s were used. The theoretical limit of detection ranges between 10 and 20 ppb for REE, Ba, Th, U, and Zr and 2 ppm for Ti.

Data were processed using the Glitter® software (van Achterbergh et al., 2001), and element concentrations were calibrated against the NIST612 certified reference material, using the values of Pearce et al. (1997).

4. Mineral chemistry

Major element data on olivine, pyroxene, spinel and amphibole are provided in the Supplementary material (Tables S1 to S5). Only for olivine, reported as the reference mineral, compositional averages *per* sample are listed in Table 2.

4.1 Mineral major element compositions

Olivine is the ubiquitous phase of the Harrow Peaks peridotites; however, despite the variety of the lithological types and the presence of composite xenoliths, it has a relatively narrow range of

composition. The forsterite (Fo) content, calculated as [Mg/(Mg+Fe_{tot}) x100 atomic formula units], varies from 86.18 to 90.76, and the NiO content from 0.26 to 0.47 wt %, reported as sample average (Fig. 4a; Tables 2 and S1 of Supplementary Material);

Olivine of orthopyroxenite HP163 and lherzolite HP164 are not included in this compositional range; they are in the range of Fo 79.00-86.33, with large grain to grain chemical zoning (Fig. 4a; Tables 2 and S1 of Supplementary Material).

Orthopyroxene vary in the range of $En_{66.62-83.89}Fs_{0.19-0.21}$-$Wo_{0.038-\ 0.17}$ with Mg# [Mg# = molar Mg/(Mg+Fe_{tot}) x100] = 82.54-89.56 showing textural equilibrium with the coexisting olivine as apparent cumulus phases in all the investigated samples. Orthopyroxene present Al_2O_3 contents mostly in the range of 1.24 to 3.32 wt %, and Cr_2O_3 and TiO_2 (as sample compositional averages) always <0.50 and <0.20 wt %, respectively (Fig. 4b; Table S2 of Supplementary Material).

Spinel are chemically heterogeneous, varying in composition from sample to sample without any clear relationship with the lithological types. In composite xenoliths HP124 and HP143 they show high variable Cr# [Cr# = molar Cr/(Cr + Al)x100] (37.33-59.48) and Mg# (49.13-60.81) values, with TiO_2 (0.5- 1.04 wt%) contents approaching the spinel composition of orthopyroxenite HP163. HP121 contains relatively low-Ti spinel (TiO_2=0.15-0.36 wt %) with the lowest Fe_2O_3 (0.71 wt % as sample average) recorded by the Harrow Peaks xenolith population (Fig.4c; Table S3 of Supplementary Material). Spinel from harzburgite HP144 and lherzolite HP151 show the highest and the lowest Cr# values, respectively, at similar low Fe_2O_3 (2.54 - 4.46 wt%) and (lowest) TiO_2 ($\leq$0.22 wt %) (Fig. 4c). Clinopyroxene occur in this group of ultramafic xenoliths in evident textural and chemical disequilibrium; they occur as small to very small grains, mostly pseudo-idiomorphic in shape, occupying triple junction positions between olivine - orthopyroxene and spinel (Figs. 4a, b, c.). They are Cr-rich augite following the Morimoto (1989) classification scheme, and heterogeneous in composition from one grain to another. Regardless of the lithology, Mg# values span from 85.18 to 94.06 with TiO_2< 0.55 wt % and Al_2O_3 < 4.13 wt % as sample averages (Figs., 5a, b; Table S4 of Supplementary Material).

Ortho- and clinopyroxene in all samples are widely out of Fe–Mg equilibrium with a $K_D \sim 0.6$ (as compared to the empirically determined equilibrium value of 1.09 ± 0.14; Putirka 2008).

Only a few grains of clinopyroxene concentrated in veins of both HP124 and HP143 dunites have TiO_2 and Al_2O_3 contents that reflect local interaction with the infiltrating host basalt (Figs. 5 a, b). Amphibole are texturally related to the clinopyroxene and generally occur as veins in dunites, while they are small and disseminated in lherzolites and the orthopyroxenite. They are chemically classified as kaersutite (HP121, HP143 and HP163), magnesio-hastingsite (HP124) and ferri-kaersutite (HP164), following the Leake et al. (1997) scheme, with Mg# ranging from 82.86 to 90.64 and TiO_2 and Al_2O_3 contents varying from 1.66 to 4.19 wt% and 11.43 to 14.86 %, respectively (Gentili et al., 2015, Figs. 5 c, d; Table S5 of Supplementary Material). The Harrow Peaks amphibole group had already been investigated for a crystallochemical study that led to the discovery of a new amphibole type: the ferri-kaersutite (Gentili et al. 2015).

Phlogopite grains occurring in HP124 appear chemically zoned (Mg# ~ 91-92), coherent with the observed variability of the other phases forming the vein. They have TiO_2 and Al_2O_3 contents between 1.41-2.19 wt% and 13.88-15.86 wt%, respectively; alkalis are instead constant (Na_2O ~0.60 wt%, K_2O ~ 9.60 wt%, Table S5 of Supplementary Material).

Glasses are extremely variable in composition (Table S6 of Supplementary Material) with SiO_2 contents ranging from 56.21 to 68.35 wt %, in relation to the textural position and adjacent mineral type, as well as the xenolith's lithology.

4.2 Pyroxene trace elements

Trace element concentrations of pyroxene averaged *per* sample are reported in Table 3, whereas all the LA-ICP-MS data are in Tables S7 –S10 of Supplementary Material.

In the chondrite-normalised REE+Sr+Zr+Hf+Ti+Y diagram, orthopyroxene display a H-MREE downward trend, with the slope increasing in the Yb and Lu region and with a ubiquitous positive

Ti anomaly (Fig. 6). Among dunites, only HP143 contains a few orthopyroxenes large enough for in situ trace element analyses. In detail, the chondrite-normalised trace element distribution of HP143 orthopyroxene mimics that of the HP164 lherzolite (clinopyroxene modal contents ~11 in volume %) and, to a lesser extent, that of the HP151 lherzolite (clinopyroxene ~9 in volume %), with Yb_N/Gd_N = 4.16 and remarkable Ti (Ti/Ti*=5.6) positive and Sr (Sr/Sr*=0.84) negative anomalies. HP166 lherzolite (clinopyroxene ~7 in volume %) displays orthopyroxene with high Zr, Hf (and Ti) and M-HREE contents, depicting a M-HREE chondrite normalised profile ~7 times higher, but LREE and LILE contents comparable to the orthopyroxene in lherzolites (and dunite). HP166 orthopyroxene show coupled strong Ti and Zr (Hf) positive anomalies. In turn, orthopyroxene in HP144 harzburgite (clinopyroxene ~3 and orthopyroxene ~13 in volume %) contains the lowest M-HREE (plus Ti), but the highest LREE and LILE concentrations of the entire xenolith population (Table 3), exhibiting almost flat or slightly L-REE enriched patterns (Ce_N/Nd_N ~ 2), (Fig. 6, Table 3).

Disseminated clinopyroxene are scarce in Harrow Peaks xenoliths. HP164 is the clinopyroxene-richest sample with 11 volume % of modal content (Table 1). Clinopyroxene are extremely variable in terms of trace element contents and, coherently with major elements behaviour, without any correlation with their modal contents. (Fig. 7a; Table 3). In the chondrite normalised incompatible multi-element variation diagram, clinopyroxene show negative Sr and Ti anomalies. The large compositional variability is even more evident in chondrite normalised REE diagrams (Fig. 7b) with overall enriched (La_N 9.02-89.9 and Yb_N 3.30-20.0 times chondrite) patterns, ranging from almost flat / slightly (i.e. HP143 La_N/Yb_N= 2.78) to highly (i.e HP124: La_N/Sm_N = 5.25; La_N/Yb_N= 10.47) LREE enriched. Strongly MREE enriched upward convex patterns (HP166: Gd_N/Yb_N=2.36; Gd_N/La_N=2.17) can also be observed. The clinopyroxene of HP151 and HP166 lherzolites display significant negative Eu anomalies (Fig. 7b).

Clinopyroxene (~6 volume%) in orthopyroxenite are compositionally variable; most of the grains reproduce the convex upward pattern shown in HP166 lherzolite (at a lower degree of enrichment,

Fig. 7b), and a few small crystals evidence a progressive LREE enrichment (La_N = 15.4-179, Fig. 7b).

Clinopyroxene concentrated in veins of HP143 and HP124 dunites have generally low HREE contents (Yb_N=3.3 for HP143 and 8.01 for HP124), with less pronounced or absent negative Sr and Ti anomalies with respect to the disseminated clinopyroxene of lherzolites and harzburgite. They share (almost) flat chondrite-normalised REE distribution patterns, but different degrees of LREE enrichments (La_N/Yb_N=2.78-10.47). As observed in lherzolites HP151 and HP166, an Eu anomaly also characterises the small clinopyroxene in the amphibole-bearing vein of HP121 composite xenolith.

4.3 Amphibole trace elements

Amphibole are characterised by incompatible trace element chondrite-normalised patterns of similar shape but with various degrees of trace element enrichment (i.e. Ba_N=13.2-95.6; Nd_N=11.1-46.1, Fig. 11a) and with systematic Nb and Ti positive anomalies (Fig. 8a). The lowest trace element concentrations are recorded by the rare amphibole in the thick clinopyroxene vein of the HP143 dunite (Figs, 3c and Fig. 8b). They perfectly mimic the coexisting clinopyroxene REE pattern (Fig. 8b). Conversely, the highest trace element concentrations are in the veined amphibole in the HP121 dunite that reflect a pure alkaline-like REE pattern (i.e. ~ La_N 43.1, Nd_N 46.1, Yb_N 11.3). Veined amphibole in the HP124 dunite is also characterised by a gently convex REE pattern (Fig. 8b), but depleted in LREEs with respect to the associated clinopyroxene. Finally, in the HP164 lherzolite, the disseminated amphibole roughly display a pattern similar to the coexisting clinopyroxene (Fig. 7b), but with higher LREE contents (i.e. amphibole: La_N= 32.2; clinopyroxene La_N=11.0, Figs. 7b and 8b). Overall, the Harrow Peaks amphibole appear more heterogeneous and trace element depleted with respect to that of the nearby Baker Rocks mantle xenolith population (Figs. 8a, b; Coltorti et al., 2004).

5. Discussion

Geochemical and textural features of Harrow Peaks ultramafic xenoliths highlighted remarkable differences between this locality and others in Antarctica. Primarily, the equigranular texture observed, is completely absent in most of the xenolith suits from the same volcanic district (i.e. Baker Rocks and Greene Point), where the protogranular texture is instead the predominant type; in addition, secondary textures (i.e. glassy patches and sieved pyroxenes, spongy rims) are rarer with respect to the other xenolith occurrences of this area (Coltorti et al., 2004; Pelorosso et al., 2016). Coherently, their modal compositions do not depict any trend attributable to a common mantle residual path (Fig. 2; Bodinier and Godard, 2003; Workman and Hart, 2005) and most important, the Fo content of olivine, in relation to the modal content, is difficult to ascribe to i) mantle residua as found in other localities in northern Victoria Land (Coltorti et al., 2004; Pelorosso et al., 2016, Fig.4a), or ii) alkaline cumulate rocks such as those sampled from Mt. Overlord (~ 50 Km from Harrow Peaks, Perinelli et al., 2017) or in thoeleiitic magmatic products as those of the Basement Sills (Bedard et al., 2007, Fig. 4a).

Spinels exhibit a large chemical variability, in terms of Cr/Al with respect to the Fo content-of the coexisting olivine, that makes the Fo - Spinel Cr# distribution unreproducible by melting, with the exception of dunite HP121, where spinel and olivine compositions intercept the mantle array curve relationships of Arai (1994) in a region that reflects a moderate fertile lherzolite (melting degree < 20%), inconsistent with the rock lithotype (Figs. 2 and 9). Conversely, they suggest a magmatic genesis, but tracing a possible spinel crystallization trend is unreasonable for this group of ultramafic cumulates (Fig. 9). At magmatic conditions, spinel Mg# is a function of melt Mg# and Al_2O_3, whereas at near- and post-magmatic conditions it is controlled by the rate of cooling and re-equilibration with coexisting silicates (Kamenesky et al., 2001), therefore the primary crystallization trend is hidden.

Moreover, clinopyroxene, which are extremely low in modal content, tend to have Mg# values comparable to those of the clinopyroxene from Antarctica mantle peridotites (Fig.5a, b), but without any relationship with potential residual (i.e. decreasing of Al_2O_3 with the increasing of Mg#) or metasomatic (i.e. enrichment in TiO_2 or Al_2O_3 at comparable Mg#) trends (Coltorti et al., 2004; Perinelli et al., 2006; 2008; 2011; Armienti and Perinelli 2010; Pelorosso et al., 2016, 2017).

Thus, all the mentioned characteristics suggest that xenoliths from Harrow Peaks do not represent a simple peridotite residuum after melt extraction. Consequently, we discuss the origin of these xenoliths as potentially representing cumulates that crystallised from various silicate melts migrating through the mantle and separated at mantle-crust boundary P-T conditions.

5.1 *Formation of Harrow Peaks xenoliths*

T-P-fO_2 equilibration conditions of the Harrow Peaks xenolith suite have been previously explored by Gentili et al. (2015), using a crystallochemical approach based on the amphibole dehydrogenation. The study highlighted a strong discrepancy between the redox conditions recorded by the amphibole dehydration equilibrium (ΔQFM = +5 - + 6.8) and those of the coexisting peridotite mineral assemblage (ΔQFM = – 2.78 - – 0.2) finally equilibrated at ~ 854 –940°C (calculated at P= 1.5 GPa). Using the same approach, this decoupling was not detected for the amphibole-bearing lherzolites and harzburgites of the nearby area of Baker Rocks where amphiboles and peridotite matrices converge to *f*O_2 values between QFM and ΔQFM –1.78 (Bonadiman et al., 2014).

Based on the crystallochemical model of Oberti et al. (2000), the Harrow Peaks amphibole present lattice parameters primarily ascribable to the magmatic-type (Gentili et al. 2015), whereas amphiboles from the rest of the Antarctic xenoliths have chemical and structural characteristics that fall within the "mantle-type" (Oberti et al. 2000; Bonadiman et al., 2014).

We re-examined the Harrow Peaks samples in view of the suggested possible magmatic origin and integrated previously determined thermobarometric results with new chemical data and new samples.

Temperature values calculated using the combination of olivine-spinel Fe-Mg exchange thermometers of Wood and Virgo (1989) and Ballhaus et al. (1991) in the lherzolites, harzburgite and dunites, respectively, suggest that these xenoliths finally equilibrated between 800 (orthopyroxenite HP163) and 1225°C (lherzolite HP151).

Presuming that the initial crystallisation of olivine was the main forming process of this group of xenoliths, the temperature of crystallisation was also calculated based on olivine/melt equilibrium, assuming that the Fe/Mg ratio of olivine (on sample average) was still close to the initial crystallization conditions. This is reasonable since they were extracted from the forming melts, and cumulated as monomineralic or bimineralic systems. Experimental determinations of Fe-Mg diffusivity in such a system reveal that for an olivine composition of Fo_{83-90} the closure temperature is reached quickly, and the estimated length scales for diffusion in a given time strongly decreased (Chakraborty 1997; Gordeychik et al., 2018).

The major oxides plus Ni (ppm) contents of the theoretical melt/s in equilibrium with olivine of the composite xenoliths were calculated by fitting various $^{Fe/Mg}Kd$- ^{Ni}Kd olivine/melt (Norman et al. 2002; 2005; Sobolev et al., 2005; Putirka et al. 2008; Laubier et al., 2014; Oeser et al. 2015) models. Using the equation [21] of Putirka (2008) and assigning a maximum H_2O content of 1 wt %, the best fit obtained for the high Mg# HP121 is a melt composition having Mg# 71.5. For HP124, HP143, the majority of lherzolites (Mg# 88) and the harzburgite (Mg# 89), the melt in equilibrium (melt 2) is obtained by fractionation of ca.4 % olivine and 0.8 % of spinel from melt 1 (Tables 4,5). Furthermore, the olivine in the orthopyroxenite sample (Mg# 80.54-84.49) are in equilibrium with a slightly evolved melt (melt 3) obtained by additional fractionation of ca. 5% of olivine, 4 % of orthopyroxene, 1 % of clinopyroxene and 0.5 of plagioclase from melt 2 (Table 5).

It is important to note that, the initial water content is included in the chemical parameters chosen in our calculations. This is because we had to consider that the measured water contents in tholeiites from a possible HP –related magmatic system is ~ 0.6-1 wt.% (Western Dronning Maud land; Heinonen and Luttinen 2010).

Overall, the calculated melts show compositions that span between high-Mg tholeiites (picrites?) and typical tholeiitic basalts, in a co-genetic evolution of the liquid line of descent. In this respect, the HP121 olivine represent the primitive crystallised product of the Kirkpatrick basalt precursor (Kyle, 1980; Fleming 1995). The olivine crystallisation temperature, obtained by iterative calculations using simultaneously melt composition and Fo-content (Putirka, 2008), is in the narrow range of 1314-1202± 27 °C, with, coherently, the highest values recorded for the olivine of HP121. The barometric conditions under which the Harrow Peak xenoliths were finally equilibrated were firstly deduced by the presence of spinel as the sole aluminium phase ($0.9 < P < 2.5$ GPa, Wood, 1974). However, an attempt to evaluate the region where the crystallised phases olivine, olivine + (orthopyroxene) and orthopyroxene + (olivine) separated from the hypothetical (calculated melt/s) was carried out applying the geobarometers of Putirka (2008) and Nimis and Ulmer (1998), based on orthopyroxene/melt and clinopyroxene/melt equilibrium, respectively. The values obtained (Table 4) limit the stationing of Harrow Peaks cumulates in the P field of 1.3 (HP143) – 0.5 (HP163) GPa. Considering that the estimated error (for the method) is ± 0.2 GPa, the values obtained are coherent with those reported by Perinelli et al. (2011, 2017), which constrain the crust/mantle boundary (Moho).

Experiments and data from a deep-seated layered-ultramafic intrusion (Cawthorn, 2018) showed that the Al_2O_3 content of orthopyroxene is a powerful tool to inspect the accumulation processes and relative motions in confined intrusive bodies (Cawthorn, 2018). It is well known that the Al_2O_3 content increases with increasing pressure, whereas Al_2O_3 positive correlations with Mg# are related to the falling temperature and differentiation (Gasparik, 1987; Maier and Eales;1997, Cawthorn, 2018). On the basis of experimental results and natural findings, Al_2O_3 in orthopyroxene is assumed

to vary in the order of 0.5 -0.6 wt% /0.1GPa (0.2 wt% *per* Km) in layered intrusive complexes (i.e. Bushveld; Cawthorn, 2018).

The wide range in Al_2O_3 values at near-constant Mg# (as shown in Fig. 4b) as observed for HP orthopyroxene could represent formation over a pressure range similar to that of the grain-magma two-phase assemblage. Hence, it is suggested that the Al_2O_3 variations of orthopyroxene from dunites to harzburgite/lherzolites (Fig. 4b) record possible movements towards a shallow lithospheric level and the orthopyroxene zoning within each sample is attributable to the cumulus/intercumulus grain-magma boundary (Cawthorn, 2018). In this context, the orthopyroxenite represents the end of the accumulation process at a shallow level (3 Km above) in the crust.

5.2 *Parental Melt modelling*

The predominant mineral assemblages (olivine+spinel) of the composite xenoliths, the occurrence of orthopyroxenite and the calculated olivine (and orthopyroxene)/melt equilibrium, reveal that the parental liquid had a high MgO content (Mg# 72) and was close to silica saturation. Such melts are associated with an anomalous high temperature (excess T_{ex}) melting of the Phanerozoic mantle (picrites) or the Archean cratons (komatiites). Picrites and komatiites either present cumulitic olivine or are olivine-saturated even at high pressure, so that they can reach such high MgO, Mg# (Lee et al., 2006; Class, 2008) and Ni contents (Sobolev et al., 2005).

All the studied Harrow Peaks xenoliths (including orthopyroxenite HP163), have olivine as cumulus phase, whose composition differs from most of the Antarctic ultramafic olivine cumulates, commonly ascribed to the Cenozoic alkaline magmatism of the West Antarctic Ridge System (Fig.4a; Gamble and Kyle, 1987; Gamble et al., 1988; Perinelli et al., 2017). Harrow Peaks' rocks instead, represent products crystallised at mantle depth, close to the Moho discontinuity, from the precursor melt/s of the Ferrar Group tholeiitic magmatism (Kyle 1990, Fleming 1995), or from the

high Mg-tholeiites (low Ti –picrites), similar to those of Vestfallja (Heinonen and Luttinen, 2008; 2010).

The calculated primitive melt forming the dunite matrix of HP121 has Mg# (up to 72) higher than any documented melt (Mg# 59-68), directly or indirectly (i.e. mantle metasomatic melt) related to the Cenozoic magmatic system, which is responsible for xenoliths rising to the surface (Coltorti, et. al. 2004; Perinelli et al. 2008; Nardini et al., 2009). In this respect, the HP121 dunite represents the primitive crystallised product of the Kirkpatrick basalt (Ferrar Group) precursor (low Ti picrites), whereas HP124 and HP143 dunites and harzburgite/lherzolite samples are fractionated and accumulated by melt/s close in composition to the exposed Ferrar thoeleiitic magmas (i.e. Kirkpatrick basalt; dolerites; Kyle 1980; Fleming 1995) in a co-genetic liquid line of descent (Table 5). The scarceness of olivine and the low Mg# of orthopyroxene in HP163 orthopyroxenite, point towards a cumulate of the same evolved melt (Table 5).

The calculated Harrow Peaks initial melt is high in Mg# and SiO_2, therefore orthopyroxene are expected to become liquidus phase since the initial stage of crystallization. This was observed in this group of samples, where orthopyroxene are absent or rare in dunites, while modally relevant in harzburgites and lherzolites (Table 1). In our model, the fractionation process (crystallisation and accumulation) is stopped at the early stage of evolution, with a predominant two-phase assemblage Ol (*sp*) +Opx (*cpx*) (Tables 1 and 5). Olivine (and spinel) are highly refractory to accept most of the incompatible trace elements of the basaltic geochemical system; the sole trace elements that, at maximum concentrations, are above the detection limits (LAM-ICP-MS; SIMs) are Ti, Zr, Y and HREE (De Hoog et al., 2010; Spandler and O'Neill, 2010). Consequently, the most fractionated melts in our model (melts 2 - 3; Table 5) preserve the pristine incompatible trace element budget, that is finally partitioned mainly in orthopyroxene and, to a lesser extent, in the rarer disseminated clinopyroxene. Orthopyroxene thus cannot depict a clear trace element fractionation trend in the multi-element-diagram, (Fig. 8), but if we consider those elements that are initially "partitioned" in olivine, (Ti, Zr Y and Yb) the fractionation line emerges (Fig.8).

In this situation, it is not easy to understand the role of clinopyroxene (and amphibole). The few clinopyroxene grains of HP121 and those concentrated in amphibole-bearing veins in HP124 and HP143, as well as the clinopyroxene occurring in harzburgite and lherzolites, generally show high Mg# (90-91) and Fe/Mg clinopyroxene/olivine distribution coefficients ($^{Fe/Mg}$Kd 0.59-0.97), out of the range of equilibrium values ($^{Fe/Mg}$Kd clinopyroxene/olivine = 0.83-0.86, Putirka 2008). Applying the $^{Fe/Mg}$Kd clinopyroxene/melt formulation of Putirka et al. (2008) and Mollo et al. (2017) to the previously calculated Harrow Peaks parental melts, the ideal liquidus clinopyroxene has a $^{Fe/Mg}$Kd clinopyroxene/melt of 0.24-0.27. The Harrow Peaks clinopyroxene instead, are characterised by $^{Fe/Mg}$Kd values (0.18-0.32) that cannot be equilibrated with most of the calculated melts (Table 4). This is clear for the HP121 and HP124 composite xenoliths ($^{Fe/Mg}$Kd clinopyroxene/melt = 0.18-0.15), whereas the HP143, where the clinopyroxene almost entirely form the monomineralic large vein (Fig. 3), is the only sample that records a potential equilibrium of clinopyroxene with the matrix olivine, and with a calculated melt ($^{Fe/Mg}$Kd clinopyroxene/melt = 0.27) having Mg#~68 (Table 5). HP143 clinopyroxene are characterised by notably lower REE contents with a slight LREE-enrichment and flat M-REE patterns ($La_N/Ce_{N=}1.04$). Moreover, they do not present the high Eu negative anomaly, which instead characterises most of the Harrow Peaks clinopyroxenes. Overall, the HP143 REE profile would confirm equilibrium with a tholeiite-like forming melt and is clearly distinct from the alkaline-type clinopyroxene of HP121 and HP124 dunites (Fig.9b).

Furthermore, we use the REE of the HP143 clinopyroxene to evaluate the HP143 parental melt REE contents. The ^{REE}Kd clinopyroxene/melt dataset used for the calculations is reported in Table S11 of Supplementary Material. The resulting profile mimics those of the Ferrar tholeiites and, coherently with the major element results, it suggests a potential equilibrium between the HP143 clinopyroxene and a parental thoeleiitic melt (Fig. 10).

To sum up, HP121 and HP163 are cumulates from hypothetical parental melts that represent two extremes: the most primitive and the most evolved terms of a hypothetical very short liquid line of descent, respectively. This suggests that the parental melt of the Kirkpatrick basalt was a (low

alkaline) picrite, which stationed in the shallow mantle. The melt system, modified in time and space, produced the rest of the Harrow Peaks ultramafic rocks, including the orthopyroxenite, at a shallower level. For all, but HP143, clinopyroxene (and amphibole) were formed by a different magmatic or metasomatic episode/s associated with more evolved melts that reasonably also crystallised plagioclase; this phase, even if not present in these cumulus fragments, may have imprinted the scattered Eu negative anomaly (Fig.9).

Despite the successful model in reproducing such ultramafic cumulates, we cannot exclude the possibility that each composition represents segregates of different melts. Considering that melts from Mg#72 to Mg# 60 close to silica saturation, may account for olivine spanning from Fo_{90} to Fo_{83} with the Ni content varying from 0.39 to 0.30 (on sample average), we could also argue that they are all primitive magmas derived from mantle sources with a variable contribution of a pyroxenite component (Sobolev et a., 2005; 2007; Matzen et al., 2014).

Considering the starting point of hypothetical fractionation lines, the most primitive HP olivine (highest NiO content= 0.39 wt% and T=1300 °C) is in equilibrium with a peridotite derived melt (Fig. 4a) and far from an initial melt of a pure pyroxenite source. As a raw consideration, it is also difficult to outline a possible mixing between the two sources to produce the HP121 olivine crystallising melt (Fig.4a).

Finally, we must consider that we are dealing with the chemistry of crystallised and accumulate minerals, thus, the nature of the mantle source of their forming melt is difficult to identify.

5.3 *Geodynamic implications*

The study of the Harrow Peaks xenoliths is clearly relevant as they represent the initial stages of the Ferrar magmatism. The importance of the Ferrar magmatism in West Antarctica is widely attested to (Kyle 1980; Fleming 1992; Elliot 1999); the large volume of magmas generated by this event

permeated part of the lithospheric domains beneath northern Victoria Land, refertilising the residual peridotitic upper mantle (Pelorosso et al., 2016).

The Ferrar large igneous system includes various magmatic bodies; among them, the doleritic Basement Sill from the McMurdo Dry Valleys represents the plumbing system of the Ferrar flood basalt eruptions (Bedard et al., 2007). The rock forming the sill displays a cumulate texture similar to that observed in layered intrusions and is characterised by an "orthopyroxene enriched base" (Bedard et al., 2007); hence, the orthopyroxenite HP163 could be representative of the same basement.

Orthopyroxenites are quite rare among the Antarctica xenoliths suites. To the best of our knowledge the only other one documented is associated with clinopyroxenites and peridotite xenoliths hosted in basalts of the Mount Morning eruptive centre (Martin et al., 2015).

In northern Victoria Land, orthopyroxenites were also found as part of the layered sequence from the Niagara Icefall (northern Victoria Land, Tribuzio et al., 2008); they were interpreted as cumulates of a boninitic melt related to the development of a back-arc basin in an active continental margin. Similarities between the Harrow Peaks ultramafic cumulates and the Niagara Icefall layered rocks include: i) the occurrence of high Mg# dunites (Mg# value ~90) coexisting with orthopyroxenites (Mg# values ~83-84); ii) the matching of REE abundances and profiles of clinopyroxenes from the Niagara Icefall gabbronorite with that of the HP143 clinopyroxene (Fig. 11). Therefore, considering the mentioned examples from different geodynamic settings, we cannot exclude *a priori* that the Harrow Peaks cumulates represent fragments of cumulus "layers" crystallised and separated from tholeiitic or boninitic melts. However, Harrow Peaks cumulates are hosted in lavas sampled in the Wilson Terrane, where the Ferrar outcrops are represented by the Ferrar Dolerite Dufek Intrusions and the Kirkpatrick Basalts (Hergt et al., 1989; Fleming et al., 1995; Elliot et al., 1999). Thus, the hypothesis that the investigated suite of samples could represent cumulus rocks from the most primitive Ferrar melt seems the most plausible.

Tracing the origin of Harrow Peaks cumulates back to the Jurassic, it is reasonable that they remained located within the shallow lithospheric mantle (*P* ~1 GPa) up to the Cenozoic (~ 50 Ma), when the alkaline magmatism associated with the West Antarctic Rift brought them to the surface. The Cenozoic (late stage) alkaline metasomatism pervaded large portions of mantle domains and cumulates suites in Victoria Land (Coltorti et al., 2004; Perinelli et al., 2006, 2008, 2011; Martin et al., 2015; Pelorosso et al., 2016, 2017), and affected the Harrow Peaks lithospheric portion, as testified by the presence of alkaline-like amphiboles (phlogopite) and the LREE-enrichment in clinopyroxene (HP121 and HP124).

Conclusions

1. The textural and geochemical characteristics of Harrow Peaks xenoliths evidence that these ultramafic rocks represent deep crustal/mantle cumulates crystallised from a primitive high Mg-melt with primitive olivine crystallising at temperature ~ 1300 °C;
2. The presence of orthopyroxenite in the system demonstrates that the inferred initial melt was either silica-saturated or rapidly evolved towards silica-saturation;
3. The mineral/melt equilibrium allowed the identification of parental melt as corresponding to the first stages of the Ferrar magmatism;
4. The peculiar olivine composition and the related mineral assemblage of this group of rocks suggest that a possible source of such primitive melts could be a peridotite with the (very limited) contribution of pyroxenite component.
5. During Cenozoic, the lithospheric mantle beneath Victoria Land was variably affected by an alkaline metasomatism related to the magmatic system, which was responsible for the xenoliths' sampling. This process also affected the Harrow Peaks district as testified by the occurrence of hydrous phases in complete geochemical disequilibrium with the anhydrous cumulus matrix.

Acknowledgements

We would like to thank two anonymous reviewers for their careful reading of the manuscript. In particular, we would thank Reviewer#1 for the detailed and helpful comments, which helped us to enrich the discussion of our results. In addition, the valuable remarks and editorial handling improved the clarity of our arguments and the presentation of this manuscript.

The authors would like to thank Barbara Galassi and Steve Deforie (Brighton, UK) for checking the English language in this paper.

This work was funded by PNRA (National Programme Antarctic Research) project: 2013-2015 "Hydrous phases stability in the lithospheric mantle of the large continental rift systems: a petrological/experimental study of the mantle xenoliths and lavas of the Northern Victoria Land (principal investigator; C.B)

B.P was supported by MIUR-2015 20158A9CBM Grant (principal investigator: C.B).

References

Arai S (1994) Characterization of spinel peridotites by olivine-spinel compositional relationships: review and interpretation. Chem Geol 113: 191-204

Armienti P, Perinelli C (2010) Cenozoic thermal evolution of lithospheric mantle in northern Victoria Land (Antarctica): evidences from mantle xenoliths. Tectonophysics 486: 28–35

Balestrieri ML, Bigazzi G, Ghezzo C, Lombardo B (1994) Fission track dating of apatites from the Granite Harbour Intrusive suite and uplift/denudation history of the Transantarctic Mountains in the area between David and Mariner Glaciers (Northern Victoria Land, Antarctica). Terra Antarctica 1 (1): 82-87

Ballhaus C, Berry RF, Green DH (1991) High pressure experiment calibration of the olivine-orthopyroxene-spinel oxygen barometer: implication for the oxidation state of the mantle. Contrib Mineral Petrol 107: 27-40

Bannister S, Yu J, Leitner B, Kennett BLN (2003) Variations in crustal structure across the transition from West to East Antarctica, Southern Victoria Land, Variations in crustal structure across the transition from West to East Antarctica, Southern Victoria Land, Geophys J Int 155: 870–880.

Beccaluva L, Coltorti M, Orsi G, Saccani E., Siena F (1991) Nature and evolution of subcontinental lithospheric mantle of Antarctica: evidence from ultramafic xenoliths of the Melbourne volcanic province (northern Victoria Land, Antarctica). Mem Soc Geo Ita 46: 353-370

Bédard JH, Marsh BD, Hersum TG, Naslund HR, Mukasa SB (2007) Large-scale mechanical redistribution of orthopyroxene and plagioclase in the Basement Sill, Ferrar dolerites, Antarctica: petrological, mineral-chemical and field evidence for channelized movement of crystals and melt. J Petrol 48: 2289-2326

Bodinier JL, Godard M, Carlson RW (2003) Orogenic, ophiolitic, and abyssal peridotites, Treatise on Geochemistry. 2. Geochemistry of the Mantle and Core, Amsterdam Elsevier, 103-170

Bonadiman B, Hao Y, Coltorti M, Dallai L, Faccini B, Huang Y, Xia Q (2009) Water contents of pyroxenes in intraplate lithospheric mantle. Eur J Mineral 21: 637-647

Bonadiman C, Coltorti M, Beccaluva L, Griffin WL, O'Reilly SY, and Siena F (2011) Metasomatism vs host magma infiltration: A case study of Sal mantle xenoliths, Cape Verde Archipelago, in Coltorti, M., and Gregoire, M., eds., Metasomatism in Oceanic and Continental Lithospheric Mantle: Geol Soc Spec Pap 478: 283–305

Bonadiman C, Nazzareni S, Coltorti M, Comodi P, Giuli G, and Faccini B (2014) Crystal chemistry of amphiboles: implications for oxygen fugacity and water activity in lithospheric mantle beneath Victoria Land, Antarctica. Contrib Mineral Petrol 167: 1-17

Cawthorn RG (2018) A non-horizontal floor during accumulation of the Bushveld Complex – Evidence and implications. Lithos 323-329.

Chakraborty S (1997) Rates and mechanisms of Fe–Mg interdiffusion in olivine at 980–1300 °C. J Geophys Res 102: 12317-12331

Collins TJ (2007) ImageJ for microscopy. Biotechniques 43: S25-S30

Coltorti M, Beccaluva L, Bonadiman C, Faccini B, Ntaflos T, Siena F (2004) Amphibole genesis via metasomatic reaction with clinopyroxene in mantle xenoliths from Victoria Land, Antarctica. Lithos 75: 115-139

Cooper AF, Adam LJ, Coulter RF, Eby G N and McIntosh WC (2007) Geology, geochronology and geochemistry of a basanitic volcano, White Island, Ross Sea, Antarctica. J Volcanol Geotherm Res 165: 189–216

Costa F. and Dungan M (2005) Short time scales of magmatic assimilation from diffusion modeling of multiple elements in olivine. Geology 33: 837–840

De Hoog JC M, Gall L and Cornell DH (2010) Trace-element geochemistry of mantle olivine and application to mantle petrogenesis and geothermobarometry. Chem Geol 270: 196–215

Elliot DH (1999) Paleovolcanological setting of the middle Jurassic Mawson Formation: evidence from the Prince Albert Mountains, Victoria Land. Paper Presented at the 8th International Symposium on Antarctic Earth Sciences. Victoria Univ., Wellington, New Zealand

Elliot DH and Fleming TH (2000) Weddell triple junction: the principal focus of Ferrar and Karoo magmatism during initial breakup of Gondwana. Geology 28: 539–542

Elliott DH and Fleming TH (2004) Occurrence and dispersal of magmas in the Jurassic Ferrar large igneous province, Antarctica. Gondwana Res 7: 223-237

Estrada S, Läufer A, Eckelmann K, Hofmann M, Gärtner A, Linnemann U (2016) Continuous Neoproterozoic to Ordovician sedimentation at the East Gondwana margin – implications

from detrital zircons of the Ross Orogen in northern Victoria Land, Antarctica. Gondwana Res, 37: 426-448. doi: 10.1016/j.gr.2015.10.006

Finn C, Moore D, Damaske D, Mackey T (1999) Aeromagnetic legacy of early subduction along the Pacific margin of Gondwana. Geology 27: 1087-1090

Fitzgerald PG (1994) Thermochronologic constraints on post-Paleozoic tectonic evolution of the central Transantarctic Mountains, Antarctica. Tectonics 13: 818-836

Fitzgerald PG, Stump E (1997) Cretaceous and Cenozoic episodic denudation of the Transantarctic Mountains, Antarctica: new constraints from apatite fission track thermochronology in the Scott Glacier region. J Geophys Res 102 (B4): 7747-7765

Fleming TH, Elliot DH, Jones LM, Bowman JR, Siders MA (1992) Chemical and isotopic variations in an iron-rich lava flow from the Kirkpatrick Basalt, north Victoria Land, Antarctica: implications for low-temperature alteration. Contrib Mineral Petrol 111: 440-457

Fleming TH, Foland KA, Elliot DH (1995) Isotopic and chemical constraints on the crustal evolution and source signature of Ferrar magmas, north Victoria Land, Antarctica. Contrib Mineral Petrol 121: 217–236

Gamble JA and Kyle PR (1987) The origins of glass and amphibole in spinel-wehrlite xenoliths from Foster Crater, McMurdo Volcanic Group, Antarctica. J Petrol 28: 755–779

Gamble JA, McGibbon F, Kyle PR, Menzies MA, Kirsch (1988) Metasomatized xenoliths from Foster Crater, Antarctica: implications for lithosphere structure and processes beneath the Transantarctic Mountains. In: Menzies, M.A., Cox, K.G. (Eds.). Oceanic and Continental Lithosphere: Similarities and Differences. J Petrol Special Issue 1, 109–138

Gentili S, Bonadiman C, Biagioni C, Comodi P, Coltorti M, Zucchini A, Ottolini L (2015) Oxo-amphiboles in mantle xenoliths: evidence for H2O-rich melt interacting with the lithospheric mantle of Harrow Peaks (Northern Victoria Land, Antarctica). Mineral Petrol 109: 741–759

Gibson GM, Wright TO (1985) Importance of thrust faulting in the tectonic development of northern Victoria Land, Antarctica. Nature 315: 480–483

Gleadow AJW, Fitzgerald PF (1987) Uplift history and structure of the Transantarctic Mountains: new evidence from fission track dating of basement apatites in the Dry Valleys area, southern Victoria Land. Earth and Planet Sci Lett 82: 1-14

Gordeychik B, Churikova T, Kronz A, Sundermeyer C., Simakin A., Wörner G (2018) Growth of, and diffusion in, olivine in ultra-fast ascending basalt magmas from Shiveluch volcano. Sci Rep 8 (11775): 1-15.

Gavrilenko M, Ozerov A, Kyle PR, Carr MJ, Nikulin A, Vidito C, Danyushevsky L (2016) Abrupt transition from fractional crystallization to magma mixing at Gorely volcano (Kamchatka) after caldera collapse. Bull Volcanol 78: 47

Heinonen JS, Luttinen AV (2008) Jurassic dikes of Vestfjella, western Dronning Maud Land, Antarctica: Geochemical tracing of ferropicrite sources. Lithos 105: 347-364

Heinonen JS, Luttinen AV (2010) Mineral chemical evidence for extremely magnesian subalkaline melts from the Antarctic extension of the Karoo large igneous province. Mineral Petrol 99: 201-217

Hergt JM, Chappell BW, Faure G, Mensing TM (1989) The geochemistry of Jurassic dolerites from Portal Peak, Antarctica. Contrib Mineral Petrol 102: 298-305

Herzberg C (2004) Geodynamic information in peridotite petrology: J Petrol 45: 2507–2530, doi:10.1093/petrology/egh039

Herzberg C, Gasparik T (1991) Garnet and pyroxenes in the mantle: a test of the majorite fractionation hypothesis. J Geophys Res 96: 16263–16274

Herzberg C, Ratteron P, Zhang J (2000) New experimental observations on the anhydrous solidus for peridotite KLB-1. Geochem Geophys. 1, paper no. 2000GC000089

Jennings ES, Holland TJB (2015) A Simple Thermodynamic Model for Melting of Peridotite in the System NCFMASOCr, J Petrol 56 (5): 869–892

Kamenetsky VS, Crawford AJ, Meffre S (2001) Factors controlling chemistry of magmatic spinel: An empirical study of associated olivine, Cr-spinel and melt inclusions from primitive rocks J Petrol 42: 655–671.

Kyle PR (1980) Development of heterogeneities in the subcontinental mantle: evidence from the Ferrar Group, Antarctica. Contrib Mineral Petrol 73: 89–104. LeMasurier WE, Thomson J W (Eds.) 1990. Volcanoes of the Antarctic Plate and Southern Oceans. Antarctic Research Series, Washington, DC AGU 48, 487

Leake BE, Woolley AR, Arps CES, Birch WD, Gilbert MC, Grice JD, Hawthorne FC, Kato A, Kisch HJ, Krivovichev VG, Linthout K, Laird J, Mandarino JA, Maresch WV, Nickel EH, Rock NMS, Schumacher JC, Smith DC, Stephenson NCN, Ungaretti L, Whittaker EJW, and Youzhi G (1997) Nomenclature of amphiboles: Report of the Subcommittee on Amphiboles of the International Mineralogical Association, Commission on New Minerals and Mineral Names. Amer Miner 82: 1019–1037

Lee C-TA, Cheng X, Horodyskyj U (2006) The development and refinement of continental arcs by primary basaltic magmatism, garnet pyroxenite accumulation, basaltic recharge and delamination: insights from the Sierra Nevada, California. Contrib Mineral Petrol 151: 222–242

Martin A P, Price RC, Cooper AF, McCammon CA (2015) Petrogenesis of the Rifted Southern Victoria Land Lithospheric Mantle, Antarctica, Inferred from Petrography, Geochemistry, Thermobarometry and Oxybarometry of Peridotite and Pyroxenite Xenoliths from the Mount Morning Eruptive Centre. J Petrol 56: 193–226

Mc Donough WF and Sun S.-s. (1995) The composition of the Earth. Chem Geol 120: 223-253.

Matzen AK, Baker MB, Beckett JR, Stolper EM (2013) The temperature and pressure dependence of nickel partitioning between olivine and silicate melt J Petrol 54: 2521–2545

Melchiorre M, Coltorti M, Bonadiman B, Faccini B, O'Reilly SY and Pearson N (2011). The role of eclogite in the rift-related metasomatism and Cenozoic magmatism of Northern Victoria Land, Antarctica. Lithos 124: 319-330

Mercier, J.C., Nicolas, A., 1975. Textures and Fabrics of the Upper-Mantle Peridotites as illustrated by Xenoliths from Basalts. J Petrol 16: 454-487

Mollo S, Blundy JD, Giacomoni P, Nazzari M, Scarlato P, Coltorti M, Langone A, Andronico D (2017) Clinopyroxene-melt element partitioning during interaction between trachybasaltic magma and siliceous crust: Clues from quartzite enclaves at Mt. Etna volcano. Lithos 284: 447–461

Nardini I, Armienti P, Rocchi S, Dallai L, Harrison D (2009) Sr–Nd–Pb–He–O isotopeand geochemical constraints to the genesis of Cenozoic magmas from the West Antarctic rift. J Petrol 50: 1359–1375

Nimis P, Ulmer P (1998) Clinopyroxene geobarometry of magmatic rocks: part 1. An expanded structural geobarometer for anhydrous and hydrous, basic and ultrabasic systems. Contrib Mineral Petrol 133: 122–135

Norman MD, Garcia MO, Kamenetsky VS, Nielsen RL (2002) Olivine-hosted melt inclusions in Hawaiian picrites: equilibration, melting, and plume source characteristics. Chem Geol 183: 143-168

Oberti R, Vannucci R, Zanetti A, Tiepolo M, Brumm RC (2000) A crystal-chemical re-evaluation of amphibole/melt and amphibole/ clinopyroxene D Ti in petrogenetic studies. Amer Miner 85: 407–419

Park K, HiChoi S, Cho M, Lee DC (2017) Evolution of the lithospheric mantle beneath Mt. Baekdu (Changbaishan): Constraints from geochemical and Sr–Nd–Hf isotopic studies on peridotite xenoliths in trachybasalt. Lithos 286-287: 330_ 344

Pearce N JG, Perkins WT, Westgate JA, Gorton MP, Jackson SE, Neal CR and Chenery SP (1997) A compilation of new and published major and trace data for NIST SRM 610 and NIST SRM 612 glass reference materials. Geostand Newslett 21, no. 1, 115–144

Oeser M, Dohmen R, Horn I, Schuth S and Weyer S (2015) Processes and time scales of magmatic evolution as revealed by Fe-Mg chemical and isotopic zoning in natural olivines. Geochim Cosmochim Acta 154: 130–150

Pelorosso B, Bonadiman C, Coltorti M, Faccini B, Melchiorre M, Ntaflos T and Gregoire M (2016) Pervasive, tholeiitic refertilisation and heterogeneous metasomatism in northern Victoria Land lithospheric mantle (Antarctica). Lithos 248–251: 493–505

Pelorosso B, Bonadiman C, Coltorti M, Melchiorre M, Giacomoni PP, Ntaflos T, Gregoire M, Benoit M (2017) Role of percolating melts in Antarctic subcontinental lithospheric mantle: New insights from Handler Ridge mantle xenoliths (northern Victoria Land, Antarctica), in Bianchini G, Bodinier J-L, Braga R, and Wilson M, eds., The Crust-Mantle and Lithosphere-Asthenosphere Boundaries: Insights from Xenoliths, Orogenic Deep Sections, and Geophysical Studies: Geol Soc Am Special Paper 526: 133–150

Perinelli C, Armienti P, Dallai L (2006) Geochemical and O-isotope constraints on the evolution of lithospheric mantle in the Ross Sea rift area (Antarctica). Contrib Mineral Petrol 151: 245-266

Perinelli C, Orlando A, Conte AM, Armienti P, Borrini D, Faccini B, and Misiti V (2008) Metasomatism induced by alkaline magma on upper mantle of the Northern Victoria Land (Antarctica): an experimental approach. In: Coltorti, M. and Gregoire, M. (eds) Mantle Metasomatism in Intra-plate and Suprasubduction Settings. Geol Soc London Spec Publ 293: 197-221

Perinelli C, Armienti P, Dallai L (2011) Thermal evolution of the lithosphere in a rift environment as inferred from the geochemistry of mantle cumulates; Northern Victoria Land, Antarctica. J Petrol 52: 665-690

Perinelli C, Andreozzi GB, Conte AM, Oberti R, Armienti P (2012) Redox state of subcontinental lithospheric mantle and relationships with metasomatism: insights from spinel peridotites from northern Victoria Land (Antarctica). Contrib Mineral Petrol 164: 1053-1067

Perinelli C, Gaeta M, Armienti P (2017) Cumulate xenoliths from Mt. Overlord, northern Victoria Land, Antarctica: A window into high pressure storage and differentiation of mantle-derived basalts. Lithos 268–271: 225–239

Popp RK, Hibbert HA, Lamb WM (2006) Oxy-amphibole equilibria in Ti-bearing calcic amphiboles: experimental investigation and petrologic implications for mantle-derived amphiboles. Am Mineral 91: 54–66

Pouchou JL, Pichoir F (1991) Quantitative Analysis of Homogeneous or Stratified Microvolumes Applying the Model "PAP". In: Heinrich K.F.J., Newbury D.E. (eds) Electron Probe Quantitation. Springer, Boston, MA. 31-75

Putirka K.D (2008) Thermometers and barometers for volcanic systems. In: Putirka, K.D., Tepley III, F.J. (Eds.). Minerals, Inclusions and Volcanic Processes, Reviews in Mineralogy and Geochemistry vol 69: pp. 61–120

Rocchi S, Tonarini S, Armienti P, Innocenti F, Manetti P (1998) Geochemical and isotopic structure of the early Palaeozoic active margin of Gondwana in northern Victoria Land, Antarctica. Tectonophysics 284: 261–281

Rocchi S, Armienti P, D'Orazio M, Tonarini S, Wijbrans J, Di Vincenzo GD (2002) Cenozoic magmatism in the western Ross Embayment: role of mantle plume vs. plate dynamics in the development of the West Antarctic Rift System. J Geophys Res 107 (B9), 2195

Sato H (1977) Nickel content of basalticmagmas: identification of primarymagmas and a measure of the degree of olivine fraction. Lithos 10: 113–120

Schmidt DL, Rowley, PD (1986) Continental rifting and transform faulting along the Jurassic Transantarctic Rift, Antarctica. Tectonics 5: 279-291

Sobolev, AV, Hofmann, AW, Sobolev, SV, Nikogosian, IK (2005) An olivine-free mantle source of Hawaiian shield basalts. Nature 434, 590-597

Sobolev AV, Hofmann AW, Kuzmin DV, Yaxley GM, Arndt NT, Chung, SL, Danyushevsky LV, Elliott T, Frey FA, Garcia MO, Gurenko AA, Kamenetsky VS, Kerr AC, Krivolutskaya NA, Matvienkov VV, Nikogosian IK, Rocholl A, Sigurdsson IA, Sushchevskaya NM, Teklay M (2007) The amount of recycled crust in sources of mantle-derived melts. Science 316:412-417.

Spandler C and O'Neill HStC (2010) Diffusion and partition coefficients of minor and trace elements in San Carlos olivine at 1,300 °C with some geochemical implications. Contrib Mineral Petrol 159: 791–818.

Storey BC, Alabaster T (1991) Tectonomagmatic controls on Gondwana break-up models: evidence from the proto-Pacific margin of Antarctica. Tectonics 10 (6): 1274-1288.

Storey BC and Kyle PR (1997) An active mantle mechanism for Gondwana break-up, South African J Geol 100: 283–290

Storey BC, Vaughan AP and Riley TR (2013) The links between large igneous provinces, continental break-up and environmental change: evidence reviewed from Antarctica. Earth and Environmental Science Transactions of the Royal Society of Edinburgh 104: 17–30

Stump E, Fitzgerald PG (1992) Episodic uplift of the Transantarctic Mountains. Geology 20: 161-164

Tribuzio R, Tiepolo M, Fiameni S (2008) A mafic-ultramafic cumulate sequence derived from boninite-type melts (Niagara Icefalls, northern Victoria Land, Antarctica). Contrib Mineral Petrol 155: 619-633

van Achterbergh E, Griffin WL, and Stiefenhofer J (2001) Metasomatism in mantle xenoliths from the Letlhakane kimberlites: Estimation of element fluxes: Contrib Mineral Petrol 141: 397–414

Wang Z and Gaetani GA (2008) Partitioning of Ni between olivine and siliceous eclogite partial melt: experimental constraints on the mantle source of Hawaiian basalts. Contrib Mineral Petrol 156: 661–678

Wood BJ and Virgo D (1989) Upper mantle oxidation state: Ferric iron contents of lherzolite spinels by Mossbauer spectroscopy and resultant oxygen fugacities. Geochim Cosmochim Acta 53: 1277-1291

Workman RK and Hart SR (2005) Major and trace element composition of the depleted MORB mantle (DMM). Earth Planet Sci Lett 231: 53- 72

Zipfel J and Wörner G (1992) Four- and five-phase peridotites from a continental rift system: evidence for upper mantle uplift and cooling at the Ross Sea margin (Antarctica). Contrib Mineral Petrol 111: 24-36

Figure Captions

Figure 1. Sketch map of northern Victoria Land and location of Harrow Peaks outcrop (red circle). Greene Point (Melchiorre et al., 2011; Pelorosso et al., 2016), Baker Rocks (Coltorti et al., 2004; Perinelli et al., 2006, 2008) and Handler Ridge (Pelorosso et al., 2017) are also reported (black circles). The map of northern Victoria Land is modified from Estrada et al. (2016), the Antarctica view is from Google Earth (US Dept of State Geographer. Image Landsat/Copernicus. Image U.S. Geological Survey Data SIO, NOAA, U.S. Navy, NGA, GEBCO).

Figure 2. Harrow Peaks xenoliths in the olivine-orthopyroxene-clinopyroxene IUGS classification diagram. (*) Composite xenoliths. Due to the uncertainties of modal determinations, composite

xenoliths are all attributable to dunite. The residual path (annotated by melting %) from PM (Primordial Mantle, McDonough and Sun, 1995) to clinopyroxene consumption is also calculated (dashed line) using theoretical and experimental results of Jensing and Holland (2015) and Herzberg (2004).

Figure 3. Photomicrographs of representative microstructures from Harrow Peaks xenoliths. Polygonal large olivine with boundaries-converging at 120° (a, b), detail of the large clinopyroxene vein with embryonic amphibole (c). Tabular olivine zone and amphibole vein in sample HP121 (d). Lherzolite HP166 characterised by equigranular olivine, orthopyroxene and small clinopyroxene (e). Large orthopyroxene in the orthopyroxenite HP163 (f)

Figure 4. Chemical composition of (a) olivine (NiO *vs.* Fo) 1, 2 and 3 are fractional crystallisation trends for Hawaiian tholeiites, Hawaiian basalts and from a pyroxenite source (Sato, 1977; Wang and Gaetani, 2008 and Gavrilenko and al. 2016); (b) orthopyroxene (Al_2O_3 *vs.* Mg#), the black arrow indicates the large Al_2O_3 compositional zoning due to cumulus processes; (c) spinel (Mg# *vs.* Cr#); Compositional fields defined by Victoria Land peridotites (Coltorti et al., 2004; Martin et al., 2015; Pelorosso et al., 2016, 2017), Mt Overlord cumulates (Perinelli et al., 2017) and Basement sill leucotroctolites (Bedard et al., 2007) are reported for comparison.

Figure 5. Harrow Peaks clinopyroxene (a, b) and amphibole (c, d) compositions in term of Mg# *vs.* TiO_2 and *vs*. Al_2O_3. Compositional fields reported for comparison in (a, b) are as in Figure 4.

Figure 6. Chondrite-normalized trace element (REE+Sr+Zr+Hf+Ti+Y) distribution for Harrow Peaks orthopyroxene (represented as sample average). Chondrite values from McDonough and Sun (2005)

Figure 7. Chondrite-normalized trace-element patterns a) and Rare Earth Elements (REE) patterns b) for Harrow Peaks clinopyroxene represented ad sample average, except for HP163 (orthopyroxenite). Due to the large trace element variability, all the analyses of the few HP163 clinopyroxenes are reported. Chondrite values from McDonough and Sun (2005)

Figure 8. Chondrite-normalized trace-element patterns (a) and REE patterns (b) of amphibole. For comparison, the compositional field defined by the amphibole from northern Victoria Land peridotites (Coltorti et al., 2004) is also reported. Chondrite values from McDonough and Sun (2005)

Figure 9. Plot of spinel Cr# *vs* Fo content of coexisting olivine of Harrow Peaks ultramafic xenoliths. (*) Composite xenoliths. Due to the uncertainties of modal determinations, composite xenoliths are all attributable to dunite. The olivine–spinel mantle array is from Arai (1994). Melting trend (annotated by melting %) is from Park et al. (2017); peridotite fields are modified from Park et al. (2017). Sample HP163 is not reported, having Cr# spinel and Mg# olivine at 0.43 and 81.9 out of the diagram's scale.

Figure 10. Trace element composition modelling of melt 2, as calculated (major elements) in Table 5. The reconstructed melt 2, assumed in equilibrium with HP143 clinopyroxene, is obtained using REE $Kd^{cpx/melt}$ data from GERM (Table S11). The resulting profile converges on a tholeiitic melt that resembles the Ferrar basalt (Kyle 1980; Fleming et al., 1995). In turn, HP143 clinopyroxene profile mimics those occurring in the ultramafic sequence (cumulates) from Niagara Ice Falls (Tribuzio et al., 2008). Chondrite-normalized values from McDonough and Sun (2005).

Figure S1. Thin sections of Harrow Peaks mantle xenoliths, which are mainly characterised by equigranular textural type. HP143, HP124, HP121composite xenoliths (a, b, c) consist of large

clinopyroxene and amphibole veins cross-cutting a dunitic matrix. a) HP143 with evident spinel trails. Important to note that the real modal content of spinel do not correspond to the black areas as in the thin section. b) HP124 is characterised by dunitic matrix and the thinnest vein containing also phlogopite. c) HP121 with the largest monomineralic vein that has been partly removed for crystallochemical investigations (Gentili et al., 2015). Harzburgite HP144 (d) and high clinopyroxene lherzolite (e). High orthopyroxene lherzolites (f, g) and orthopyroxenite (h).

Figure1_rev

Click here to access/download;Figure;Fig.1_rev.tif

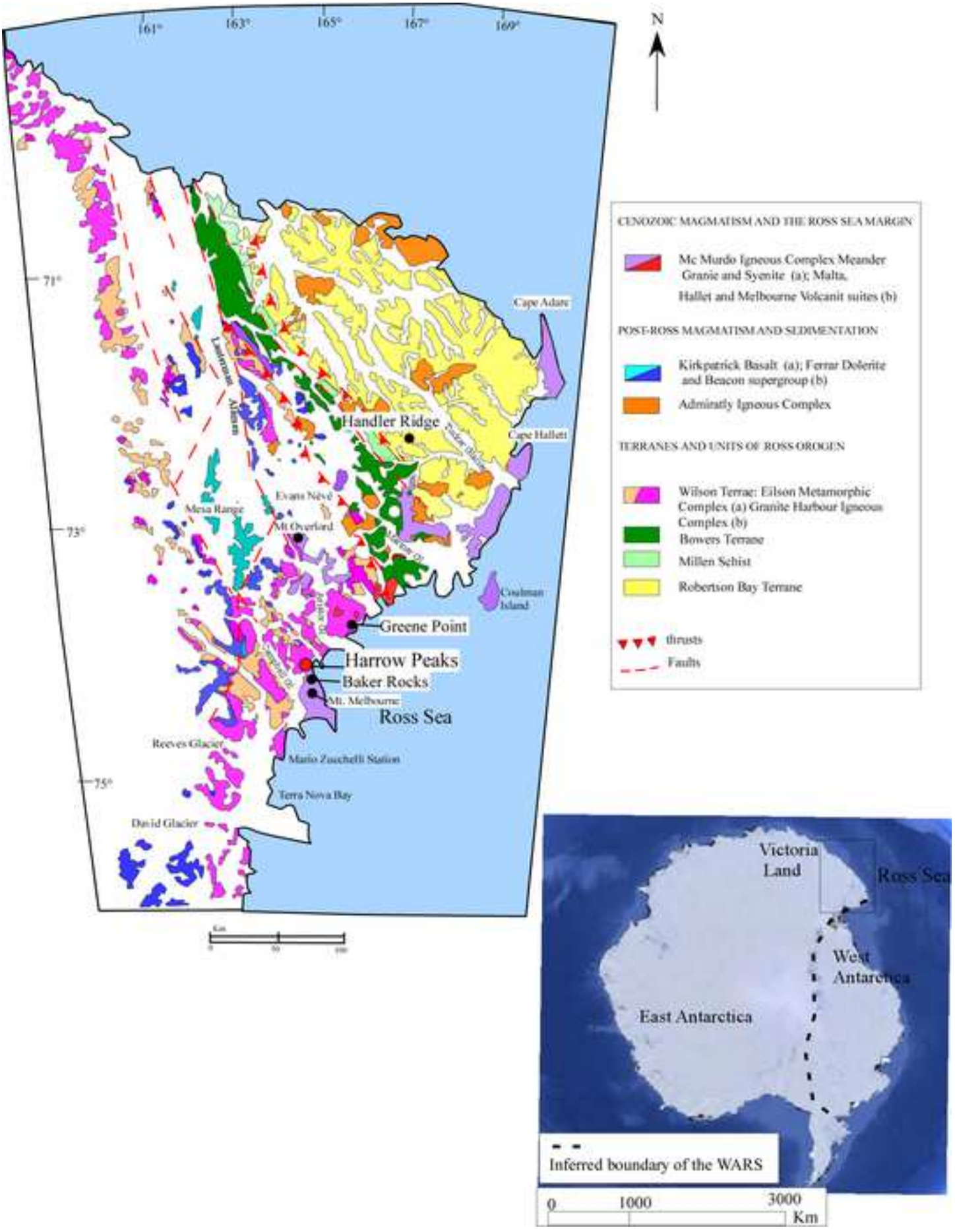

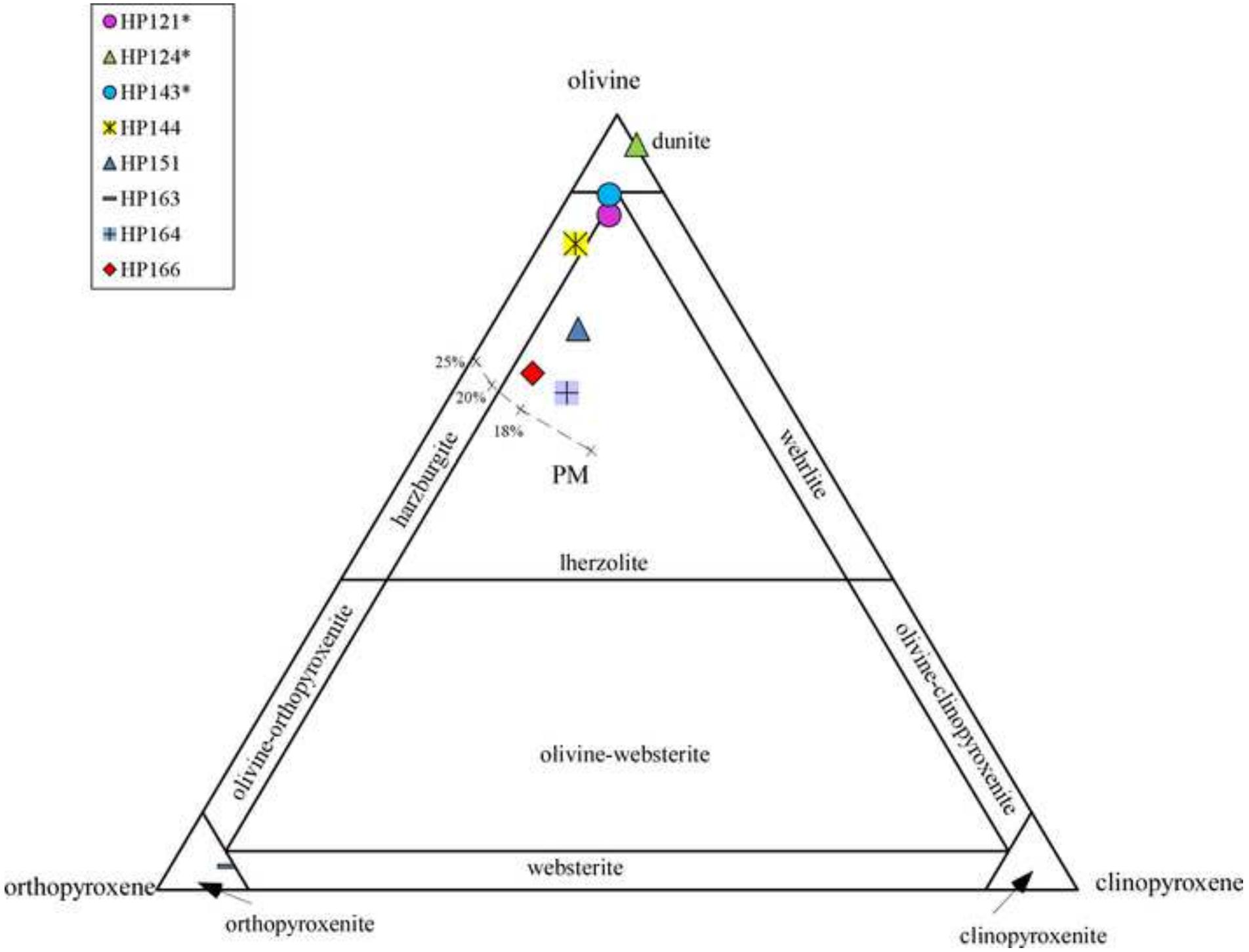

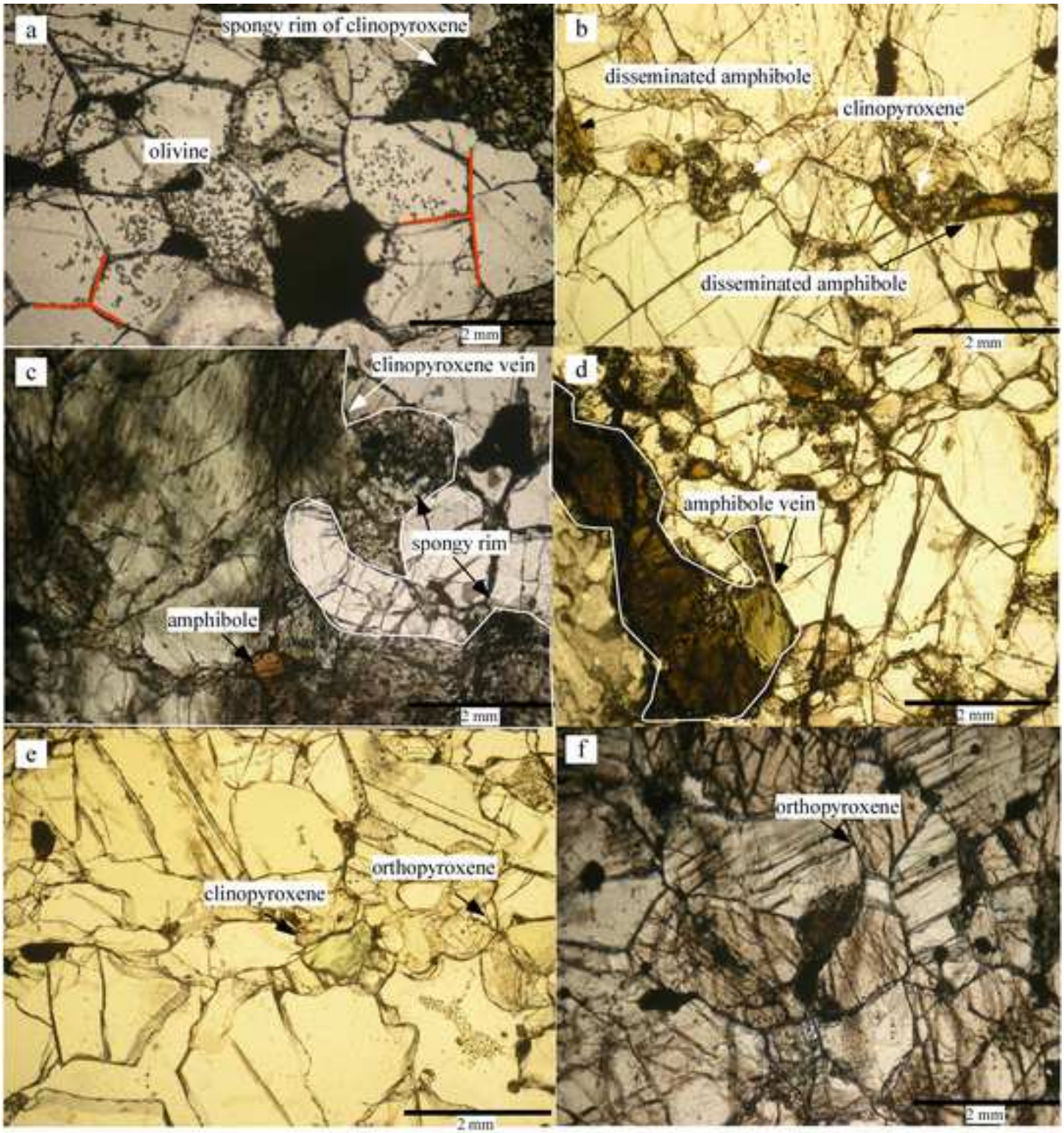

Figure4_rev

Click here to access/download;Figure;Fig.4_rev.tif

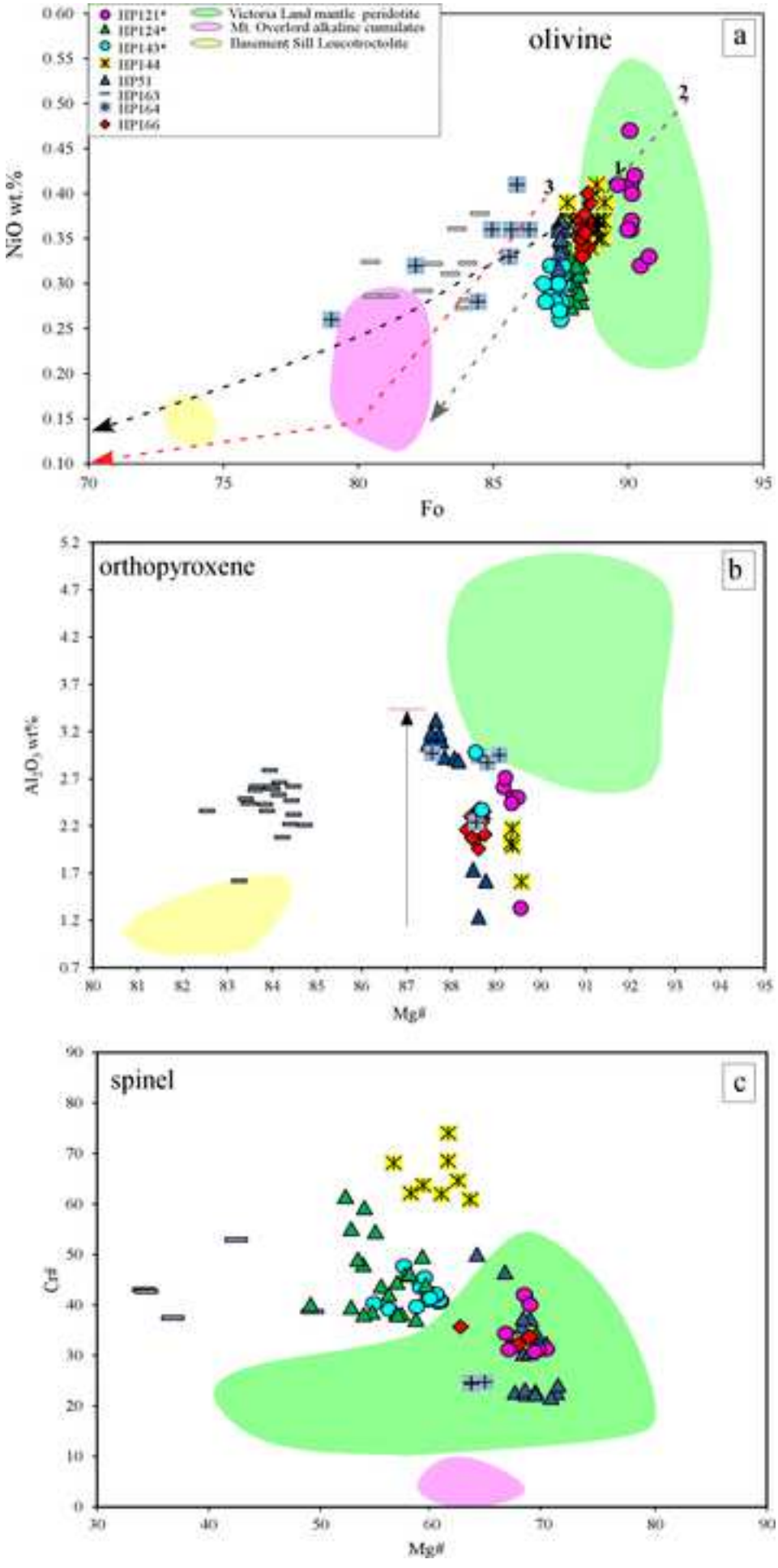

Figure5_rev

Click here to access/download;Figure;Fig.5_rev.tif

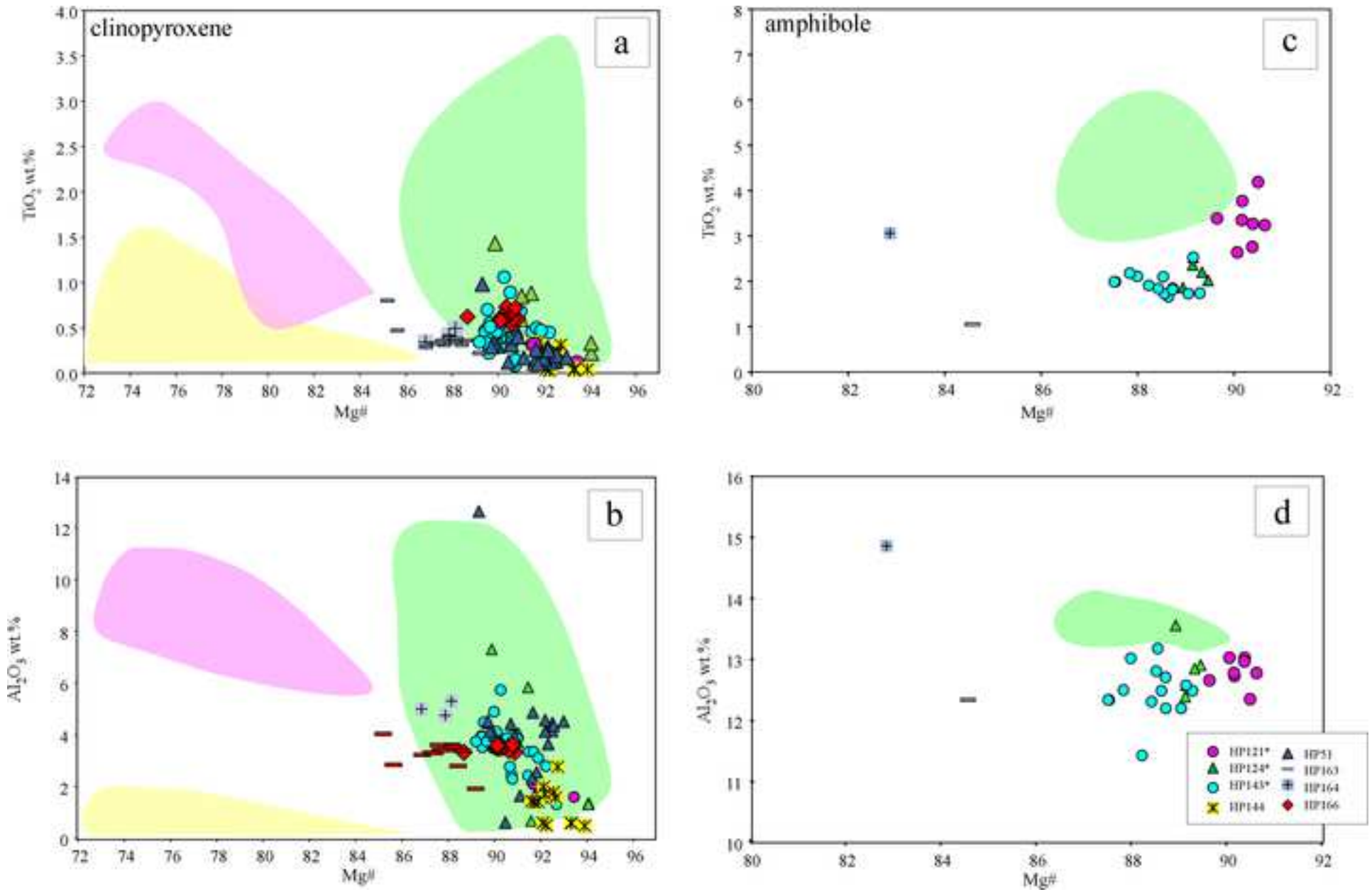

Figure6_rev

Click here to access/download;Figure;Fig.6_rev.tif

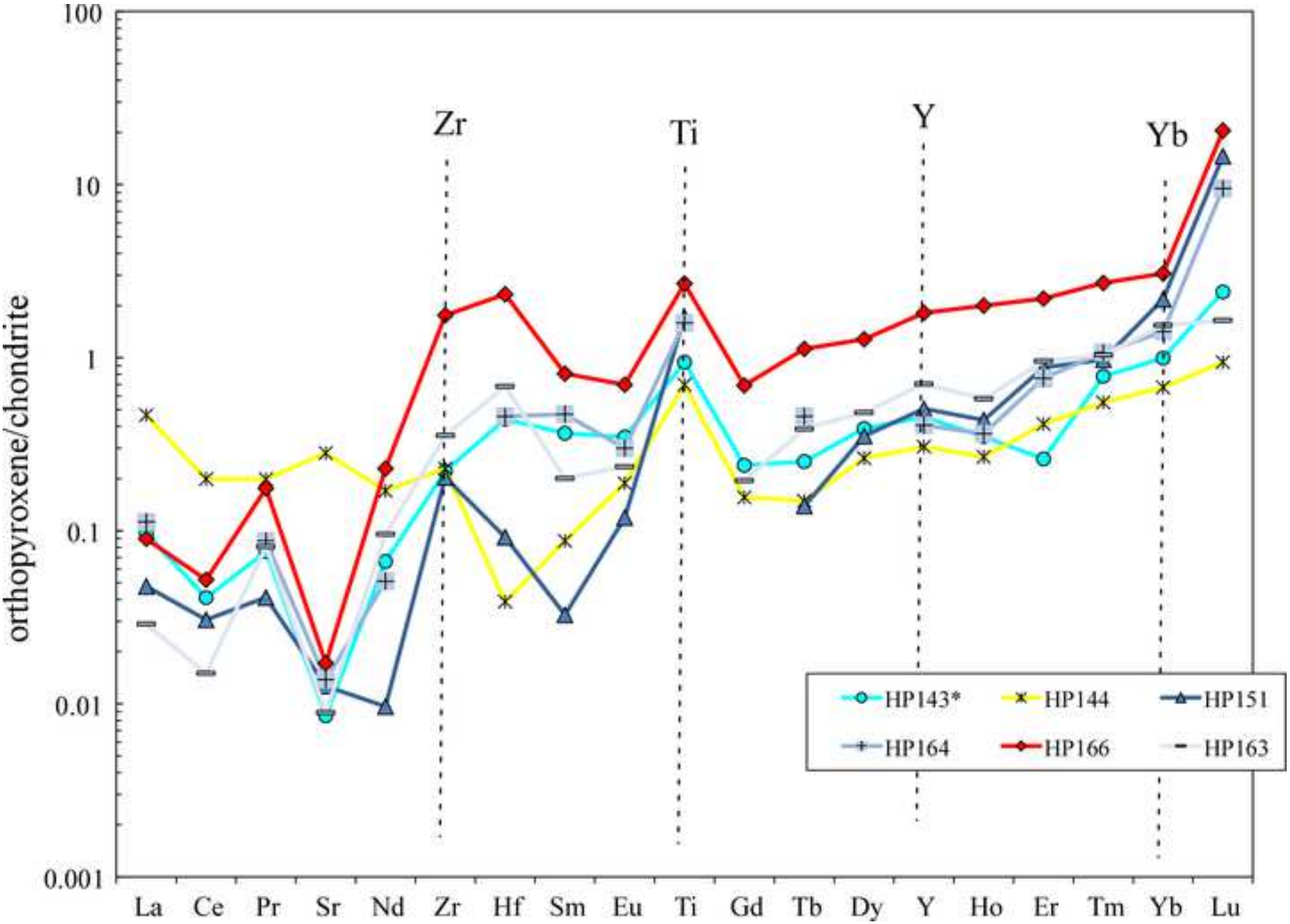

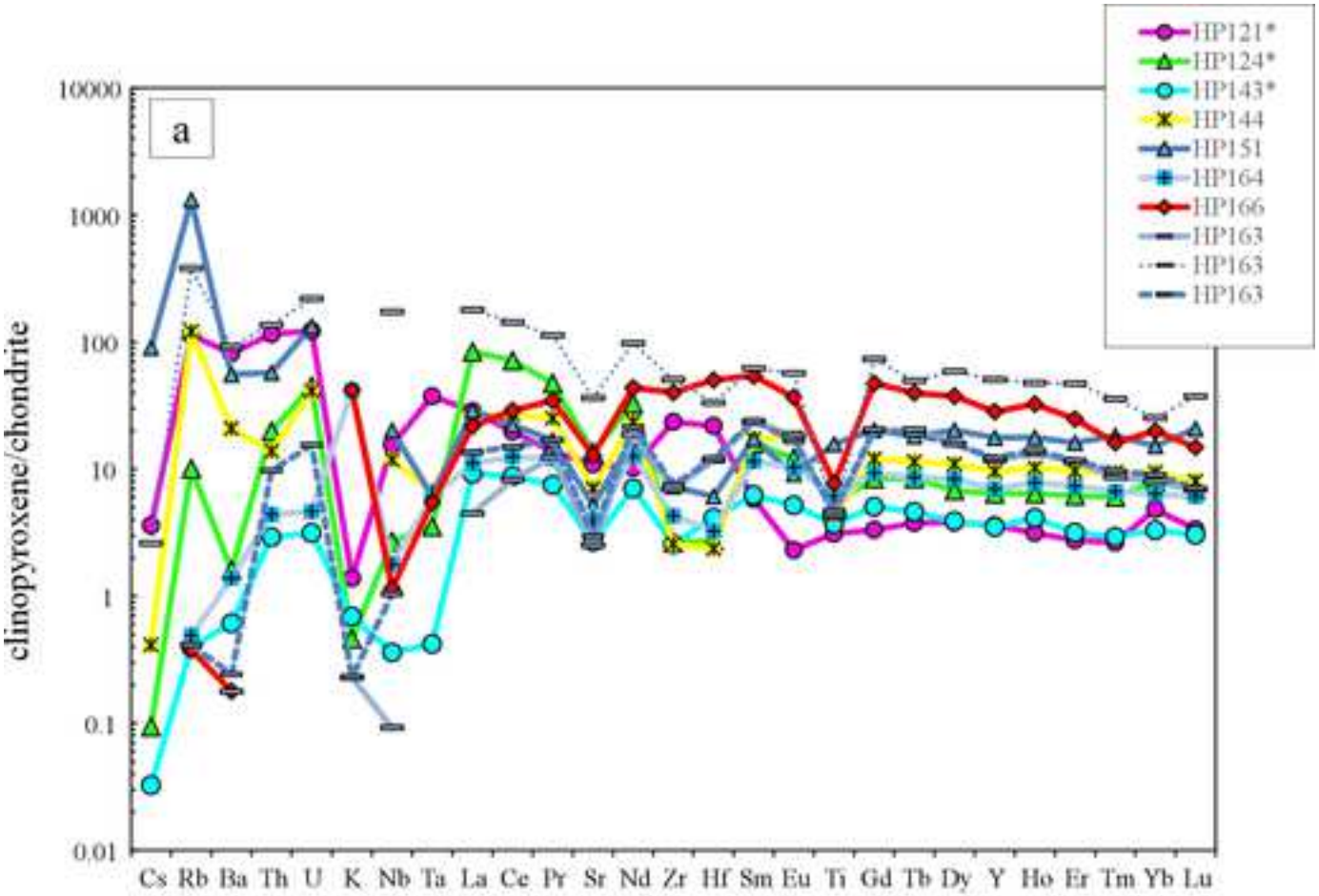

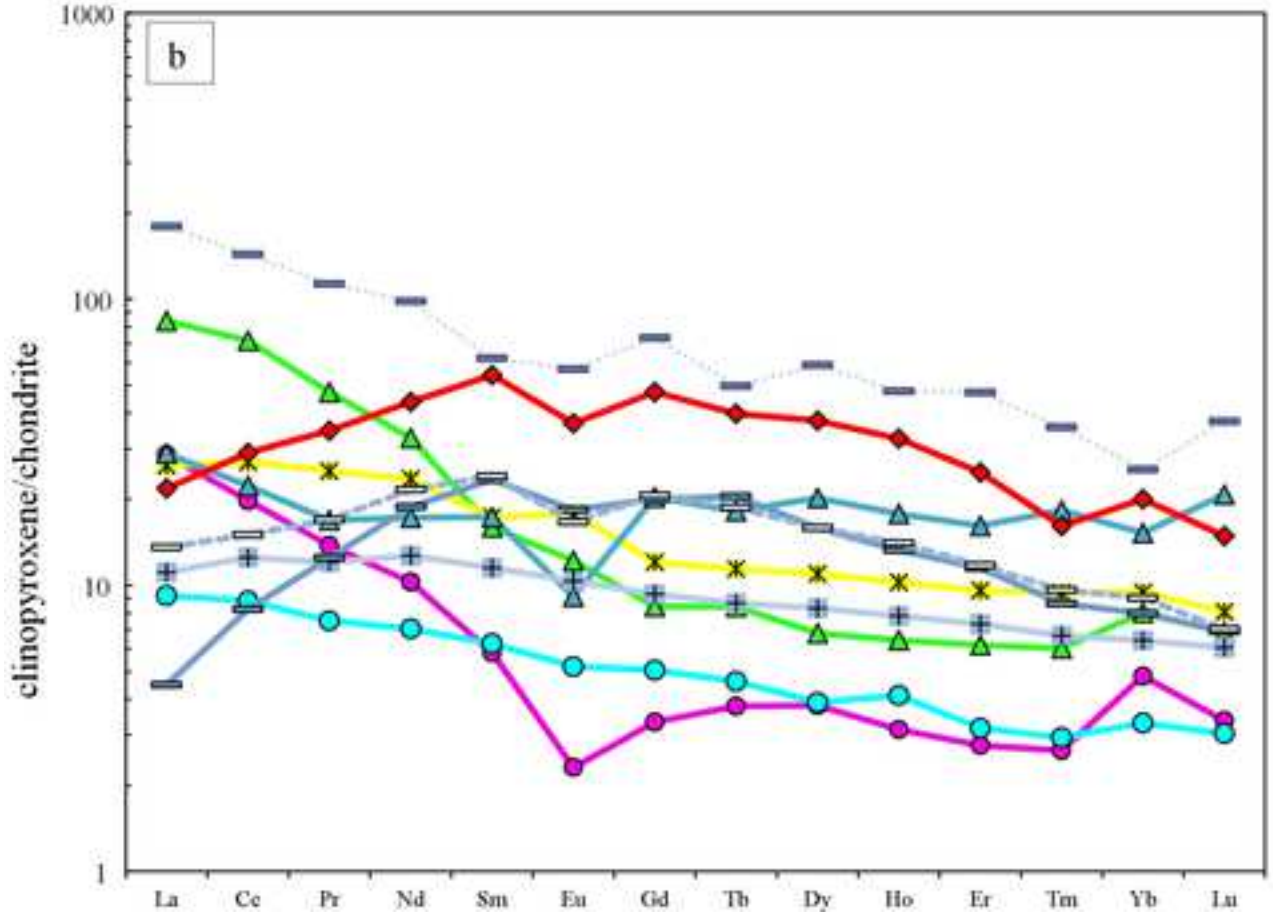

Figure8_rev

Click here to access/download;Figure;Fig.8_rev.tif

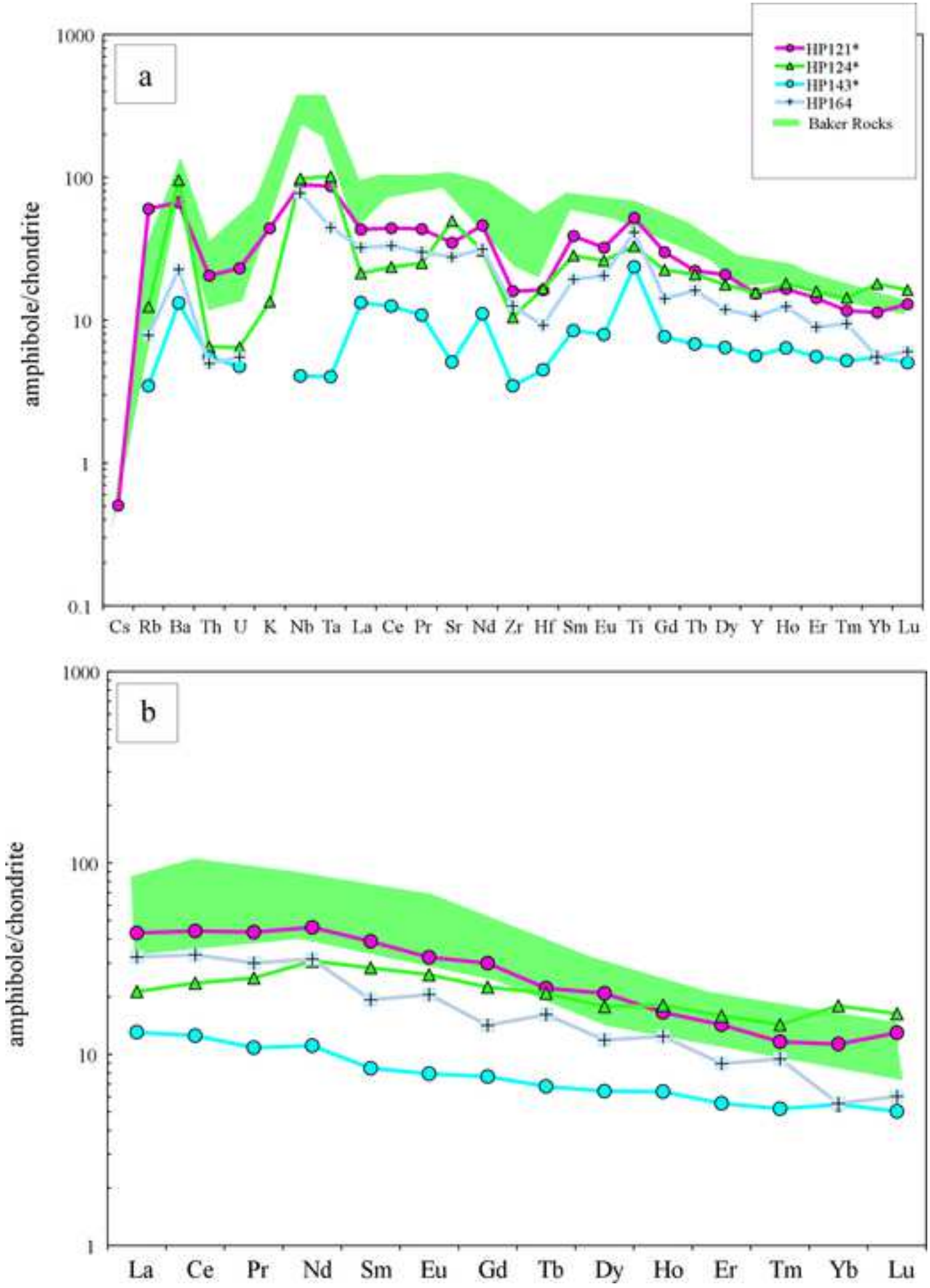

Figure9_rev

Click here to access/download;Figure;Fig.9_rev.tif

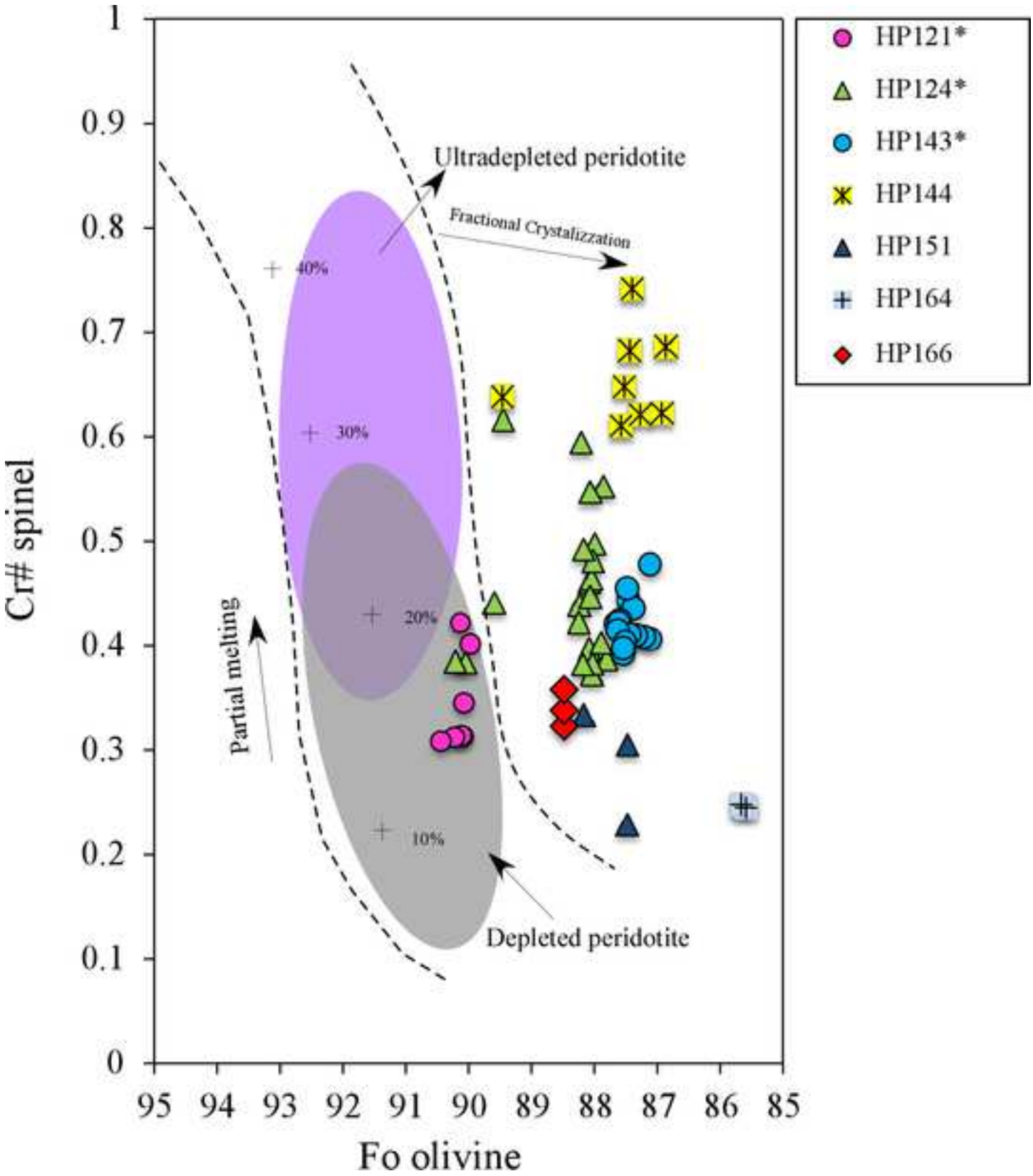

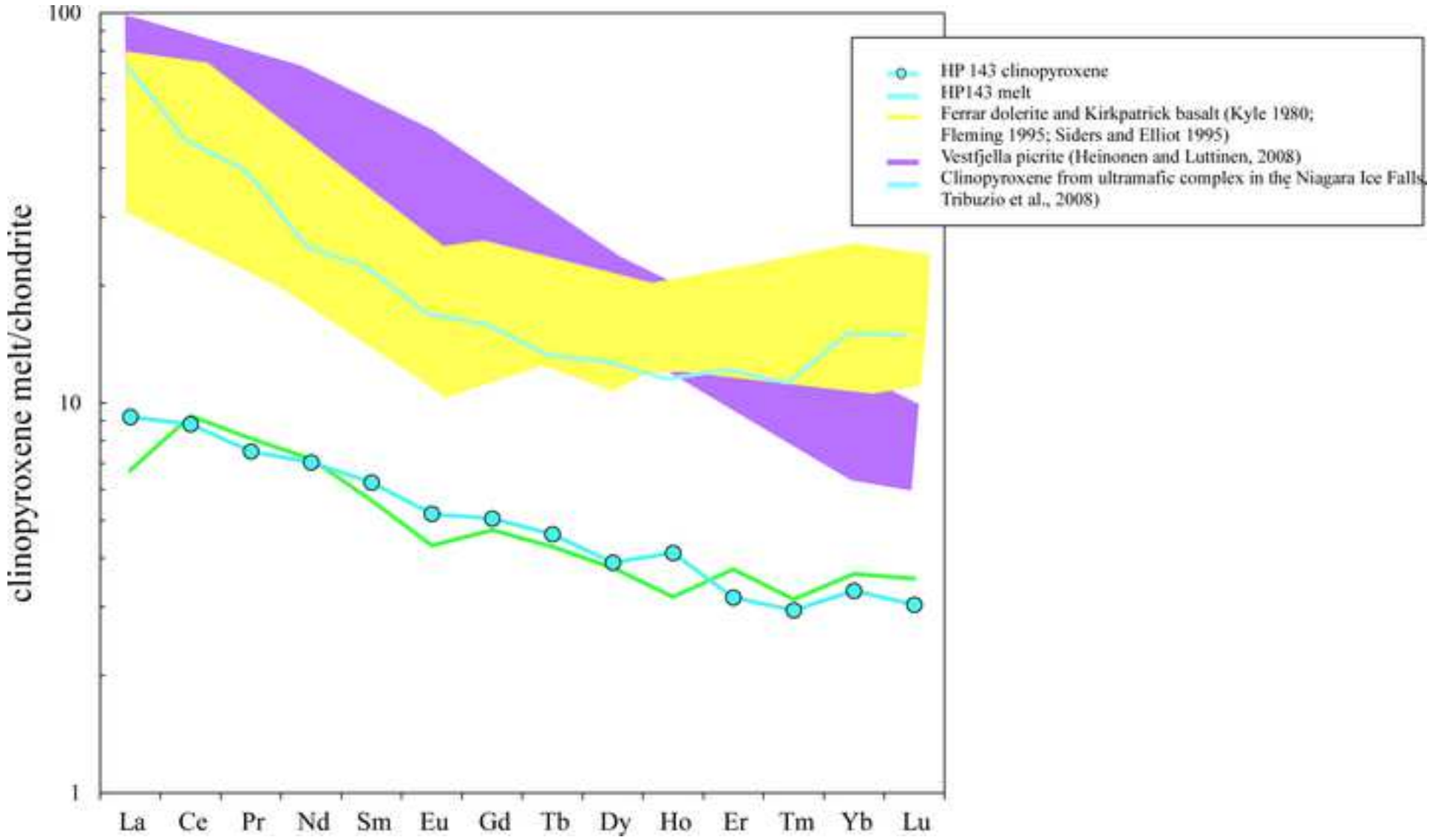

Table 1: Basic textural and geochemical features of Harrow Peaks xenoliths

Sample	lithology	texture	ol	opx	sp	cpx°	cpx+	amph°	amph+	phl +	Fo ol	Mg# opx	Cr# sp	T °C
HP121*	dunite	equigranular	70	6	0	4	1		19		90.15	89.36	32.47	904
HP124*	dunite	equigranular	85	-	1	3	6	5		0.5	88.14		41.47	952
HP143*	dunite	mosaic-equigranular	73	5	2	3	13	4			87.39	88.61	43.19	998
HP144	harzburgite	equigranular	84	13	0	3		trace			88.26	88.69	63.28	1188
HP151	lherzolite	equigranular	72	18	1	9		trace			87.50	88.04	44.83	1225
HP163	orthopyroxenite	equigranular	3	90		6		1			82.80	83.93	38.76	769
HP164	lherzolite	equigranular	63	23	1	11		2			84.25	88.53	24.79	912
HP166	lherzolite	equigranular	67	26		7		trace			88.39	88.59	34.02	1003

* Composite xenoliths. Due to the uncertainties of modal determinations, composite xenoliths are all attributable to dunites

°Disseminated

+Vein

T estimated by Fe/Mg equilibrium

ol= olivine; opx= orthopyroxene; sp= spinel; cpx= clinopyroxene; amph: amphibole; phl=phlogopite

Mg# = molar Mg/(Mg+Fetot) x100

Cr# = molar [Cr/(Cr+Al) x100]

Table 2: Major elements content (wt. %) of Harrow Peaks Olivine (on sample average)

Sample	HP121*		HP124 *		HP143 *		HP144		HP151		HP163		HP164		HP166	
Host rock	Du		Du		Du		Lh		Lh		Opxte		Lh		Lh	
	M	2σ	M	2σ	M	2σ	M	2σ	M	2σ	M	2σ	M	2σ	M	2σ
SiO2	41.28	0.5	40.45	0.30	40.31	0.31	40.49	0.42	40.36	0.23	39.57	0.61	40.02	0.97	40.58	0.31
TiO2	0.01	0.0	0.01	0.01	0.00	0.01	0.00	0.01	0.01	0.02	0.01	0.02	0.01	0.02	0.01	0.02
FeO	9.43	0.5	11.30	0.68	12.05	0.45	11.19	2.28	11.93	0.12	15.91	2.39	14.66	4.34	11.07	0.26
MnO	0.12	0.1	0.17	0.01	0.18	0.03	0.18	0.08	0.17	0.03	0.24	0.04	0.21	0.05	0.16	0.03
MgO	48.45	0.6	47.13	0.38	46.83	0.49	47.26	1.86	46.88	0.15	43.04	2.66	44.06	3.34	47.31	0.34
CaO	0.04	0.0	0.04	0.11	0.06	0.02	0.04	0.08	0.03	0.02	0.21	0.29	0.08	0.04	0.02	0.02
NiO	0.39	0.1	0.31	0.04	0.30	0.05	0.36	0.07	0.35	0.03	0.31	0.07	0.34	0.10	0.36	0.04
Tot	99.78	0.8	99.42	0.45	99.75	0.53	99.57	0.38	99.74	0.32	99.46	0.78	99.41	0.87	99.54	0.69
Mg#	90.15	0.6	88.14	0.70	87.39	0.49	88.26	2.52	87.50	0.11	82.80	2.97	84.25	4.98	88.39	0.24

* Composite xenoliths. Due to the uncertainties of modal determinations, composite xenoliths are all attributable to dunites

Du is for Dunite; Hz is for harzburgite; Lh: lherzolite; Opxte: orthopyroxenite

Table 3: Average Trace elements (ppm) contents of Harrow Peaks mineral phases

Sample	HP143*	HP144*		HP151	HP163		HP164		HP166		HP121		HP124		HP143*	
host rock	Du	Hz		Lh	Opxte		Lh		Lh		Du		Du		Du	
	matrix	matrix		matrix	matrix		matrix		matrix		matrix		vein		vein	
phase	opx	opx		opx	opx		opx		opx		cpx		cpx		cpx	
n	1	2	2σ	1	5	2σ	6	2σ	4	2σ	2	2σ	3	2σ	3	2σ
Cs	bdl	0.020	0.005	0.006	0.008	0.002	0.022	0.021	0.019	0.004	0.677	0.147	0.018	0.013	0.006	0.006
Rb	0.041	7.33	9.86	0.012	0.049	0.039	0.009	0.024	0.048	0.012	39.7	3.78	3.53	5.30	0.139	0.011
Ba	0.016	11.9	8.10	0.010	0.047	0.045	0.005	0.009	0.024	0.008	197	3.72	3.88	8.41	1.48	1.17
Th	0.011	0.064	0.020	0.012	bdl		0.002	0.010	0.021	0.006	3.35	0.141	0.577	0.834	0.084	0.017
U	0.017	0.058	0.044	0.010	bdl		bdl		0.025	0.006	0.980	0.134	0.360	0.330	0.025	0.015
Nb	0.018	0.689	0.709	0.027	0.010	0.002	0.431	0.443	0.025	0.008	3.83	0.127	0.664	0.87	0.09	0.017
Ta	0.013	0.019	0.013	0.002	bdl		0.081	0.083	0.017	0.006	0.524	0.044	0.049	0.07	0.01	0.001
La	0.023	0.110	0.118	0.011	0.009	0.002	0.033	0.012	0.021	0.005	6.78	0.453	19.9	17.4	2.18	0.158
Ce	0.025	0.122	0.121	0.019	0.023	0.005	0.009	0.024	0.032	0.015	12.1	0.311	43.8	37.3	5.40	0.424
Pr	0.007	0.019	0.021	0.004	0.008	0.001	0.010	0.006	0.017	0.006	1.31	0.208	4.50	3.17	0.713	0.093
Sr	0.062	2.04	1.14	0.092	0.065	0.043	0.103	0.042	0.125	0.064	79.2	6.039	99.0	11.1	19.5	2.86
Nd	0.031	0.079	0.076	0.005	0.045	0.020	0.032	0.038	0.107	0.013	4.80	0.325	15.3	9.7	3.29	0.226
Zr	0.854	0.885	1.00	0.787	1.37	0.12	0.010	5.070	6.81	0.768	91.2	0.127	10.3	7.5	9.97	0.778
Hf	0.047	0.004	0.001	0.010	0.073	0.020	0.064	0.084	0.248	0.061	2.34	0.509	0.290	0.401	0.442	0.074
Sm	0.056	0.013	0.001	0.005	0.031	0.006	0.099	0.074	0.124	0.024	0.89	0.679	2.44	0.26	0.957	0.079
Eu	0.020	0.011	0.001	0.007	0.014	0.001	0.022	0.014	0.040	0.009	0.134	0.102	0.708	0.198	0.302	0.033
Ti	420	311	90.66	762	456	138	683	236	1189	44	1379	2035	2418	4993	1649	1272
Gd	0.049	0.032	0.013	bdl	0.060		0.056	0.028	0.142	0.094	0.684	0.208	1.73	0.57	1.04	0.668
Tb	0.009	0.006	0.001	0.005	0.014	0.002	0.022	0.018	0.042	0.017	0.142	0.033	0.315	0.117	0.173	0.052
Dy	0.099	0.067	0.043	0.090	0.123	0.016	0.071	0.140	0.324	0.073	0.966	0.124	1.73	0.585	0.990	0.051
Y	0.712	0.480	0.185	0.796	1.11	0.05	0.577	0.767	2.85	0.463	5.67	0.481	10.0	3.99	5.49	0.566
Ho	0.020	0.015	0.004	0.025	0.033	0.005	0.019	0.049	0.113	0.025	0.178	0.018	0.364	0.161	0.234	0.010
Er	0.043	0.068	0.023	0.145	0.158	0.008	0.118	0.132	0.364	0.071	0.456	0.464	1.02	0.598	0.525	0.236
Tm	0.020	0.014	0.001	0.025	0.026	0.002	0.028	0.023	0.069	0.014	0.068	0.018	0.154	0.075	0.075	0.009
Yb	0.169	0.115	0.033	0.370	0.261	0.062	0.189	0.106	0.520	0.129	0.820	0.482	1.36	1.02	0.561	0.136
Lu	0.061	0.024	0.008	0.067	0.042	0.007	0.007	0.034	0.091	0.014	0.086	0.049	0.174	0.168	0.077	0.006

* Composite xenoliths. Due to the uncertainties of modal determinations, composite xenoliths are all attributable to dunites

n: number of averaged analyses; bdl: below detection limit

Du is for Dunite; Hz is for harzburgite; Lh: lherzolite; Opxte: orthopyroxenite

opx: orthopyroxene; cpx: clinopyroxene; amph: amphibole

Table 3 continued

Sample	HP144		HP151	HP163		HP163		HP163	HP164		HP166		HP121*		HP124*		HP143		HP164
host rock	Hz		Lh	Opxte		Opxte		Opxte	Lh		Lh		Du		Du		Du		Lh
	matrix		matrix	matrix		matrix		matrix	matrix		matrix		vein		vein		vein		matrix
phase	cpx		cpx	cpx		cpx		cpx	cpx		cpx		amph		amph		amph		amph
n	3	2σ	1	3	2σ	3	2σ	1	2	2σ	3	2σ	3	2σ	3	2σ	2	2σ	1
Cs	0.077	0.051	16.9	0.025	0.015	0.022	0.025	0.490	0.048		bdl		0.095	0.223	0.010	0.003	0.006		bdl
Rb	42.4	70.1	461	0.099	0.097	0.145	0.144	133	0.172	0.441	0.132	0.183	21.0	54.3	4.21	0.261	1.22	0.187	2.74
Ba	50.4	63.2	134	0.427	0.461	0.584	0.439	223	3.34	7.66	0.430	1.057	162	94	205	44	31.7	11.3	54.5
Th	0.401	0.043	1.66	0.081	0.070	0.283	0.160	3.95	0.127	0.039	0.069	0.010	0.594	0.435	0.200	0.027	0.159	0.074	0.144
U	0.331	0.202	1.06	0.050	0.033	0.124	0.062	1.75	0.037	0.007	0.083	0.124	0.185	0.219	0.045	0.017	0.038	0.021	0.044
Nb	2.91	2.70	4.97	0.023	0.007	0.256	0.194	42.6	0.439	0.21	0.283	0.041	21.9	4.2	23.3	1.73	1.00	0.007	19.1
Ta	0.094	0.103	0.086	bdl		bdl		bdl	0.085	0.008	0.076	0.043	1.21	0.56	1.34	0.141	0.056	0.028	0.623
La	6.20	2.40	6.85	1.06	0.09	3.22	1.46	42.6	2.63	1.41	5.17	1.04	10.2	5.70	5.03	0.078	3.14	0.198	7.64
Ce	16.5	4.53	13.6	5.05	0.33	9.19	4.29	87.7	7.65	2.63	17.8	2.82	27.0	10.8	14.2	0.301	7.66	0.000	20.3
Pr	2.38	0.504	1.61	1.18	0.14	1.61	0.62	10.7	1.14	0.21	3.30	0.193	4.13	1.07	2.34	0.072	1.03	0.004	2.85
Sr	51.4	11.4	37.7	18.3	0.799	21.6	13.3	265	28.4	23.4	93.5	12.9	253	245	352	14.58	37.0	3.21	201
Nd	11.0	2.52	8.05	8.79	1.09	10.08	3.60	45.9	5.93	0.71	20.4	3.20	21.5	5.3	14	1.1	5.18	0.255	14.7
Zr	9.99	2.76	28.3	27.0	1.95	29.1	1.4	197	16.6	4.13	155	9.67	61.8	2.8	40.5	0.23	13.4	1.37	48.7
Hf	0.253	0.028	0.650	1.25	0.240	1.30	0.29	3.56	0.346	0.225	5.37	1.37	1.73	1.18	1.67	0.24	0.477	0.16	0.980
Sm	2.64	0.401	2.65	3.58	0.469	3.69	1.13	9.52	1.76	0.06	8.31	1.88	5.95	1.21	4.17	0.40	1.29	0.139	2.95
Eu	1.04	0.200	0.530	1.06	0.338	0.966	0.235	3.30	0.600	0.068	2.13	0.857	1.86	0.74	1.48	0.06	0.459	0.076	1.19
Ti	1953	1611	7001	1858	302	2098	208	2038	2728	593	3452	292	23186	6320	9772	8478	10521	1611	18345
Gd	2.48	1.02	4.17	4.11	0.397	4.23	1.06	15.0	1.91	0.216	9.73	0.572	6.15	1.75	4.57		1.57	0.342	2.91
Tb	0.427	0.141	0.680	0.766	0.052	0.700	0.117	1.86	0.324	0.027	1.49	0.281	0.828	0.288	0.78	0.009	0.254	0.003	0.604
Dy	2.78	0.824	5.13	4.03	0.191	4.03	0.576	15.0	2.11	0.021	9.57	1.03	5.29	1.14	4.41	0.171	1.63	0.173	3.02
Y	15.1	3.98	27.7	18.5	1.67	19.2	1.03	79.6	11.0	0.240	44.4	1.86	24.1	3.40	24.5	0.201	8.83	0.806	16.8
Ho	0.579	0.181	1.01	0.751	0.044	0.795	0.059	2.70	0.443	0.021	1.84	0.362	0.938	0.099	0.989	0.064	0.361	0.065	0.703
Er	1.59	0.328	2.67	1.90	0.080	1.94	0.243	7.81	1.21	0.064	4.10	0.638	2.36	0.060	2.76	0.24	0.917	0.136	1.48
Tm	0.240	0.040	0.466	0.220	0.026	0.246	0.033	0.910	0.170	0.020	0.411	0.235	0.297	0.053	0.367	0.01	0.132	0.049	0.241
Yb	1.61	0.253	2.59	1.36	0.266	1.54	0.127	4.31	1.09	0.089	3.40	0.416	1.92	0.211	2.92	0.299	0.930	0.137	0.940
Lu	0.205	0.065	0.528	0.175	0.056	0.179	0.008	0.950	0.154	0.009	0.378	0.158	0.329	0.238	0.406	0.03	0.128	0.002	0.153

* Composite xenoliths. Due to the uncertainties of modal determinations, composite xenoliths are all attributable to dunites

n: number of averaged analyses; bdl: below detection limit

Du is for Dunite; Hz is for harzburgite; Lh: lherzolite; Opxte: orthopyroxenite

opx: orthopyroxene; cpx: clinopyroxene; amph: amphibole

Table 4: Calculation parameters and *P-T* results of melt modelling

	$^{Fe/Mg}$Kd ol/melt	$^{Fe/Mg}$Kd cpx/melt	^{Ni} Kd ol/melt	T 1	P1	P2
HP121*	0.28	0.20	0.17	1314	0.9	1.0
			0.17			
HP124*	0.29	0.15	0.17	1276		0.8
HP143*	0.32	0.27	0.17	1278	0.9	1.3
HP144	0.27	0.21	0.17	1272	0.8	1.0
HP151	0.31	0.20	0.17	1277	1.0	0.9
HP164	0.36	0.32	0.17	1285	0.9	1.0
HP166	0.28	0.24	0.17	1274	0.8	1.0
HP163	0.34	0.26	0.17	1202	0.5	1.0

* Composite xenoliths. Due to the uncertainties of modal determinations, composite xenoliths are all attributable to dunites

T1: Crystallization Temperature (°C) of olivine from equation [21] of Putirka (2008).

P1 and P2 (GPa): estimated pressure of cumulites emplacements calculated with Putirka (2008) equations [29a] and [30] respectively

Table 5: Theoretical melt compositions

	SiO_2	TiO_2	Al_2O_3	FeOt	MnO	MgO	CaO	Na_2O	K_2O	Ni	Mg#	% of crystallising phases				
												ol	sp	cpx	opx	plg
Melt 1	49.83	0.45	15.77	8.64	0.17	12.20	11.05	1.44	0.38	391	71.56					
Melt 2	50.61-51.24	0.47-0.44	16.1-16.05	8.51-8.40	0.18	10.57-10.26	11.62-11.42	1.52-1.55	0.40-0.41	370-310	68.87- 68.51	5 - 4	1	0 - 3		
Melt 3	52.04-54.71	0.48-0.62	17.21-15.22	8.30-8.89	0.18-0.16	7.13-6.88	12.41-10.73	1.68-1.81	0.47-0.89	348-318	60.49-58.0	5 -1	1	1-4	4- 5	0.5-1

Melt 1 is the theoretical melt able to equilibrate HP121 olivine; Melt 2 and Melt 3 are calculated by modal fractional crystallization equation.

Ol: olivine; sp: spinel; cpx: clinopyroxene; opx: orthopyroxene. plg is for plagioclase, theoretically predicted by fractional crystallization method.

All oxides are reported in wt. %, Ni content is reported in ppm

Figure_S1

Click here to access/download;attachment to manuscript;Fig. 1S_rev.tif

Click here to view linked References

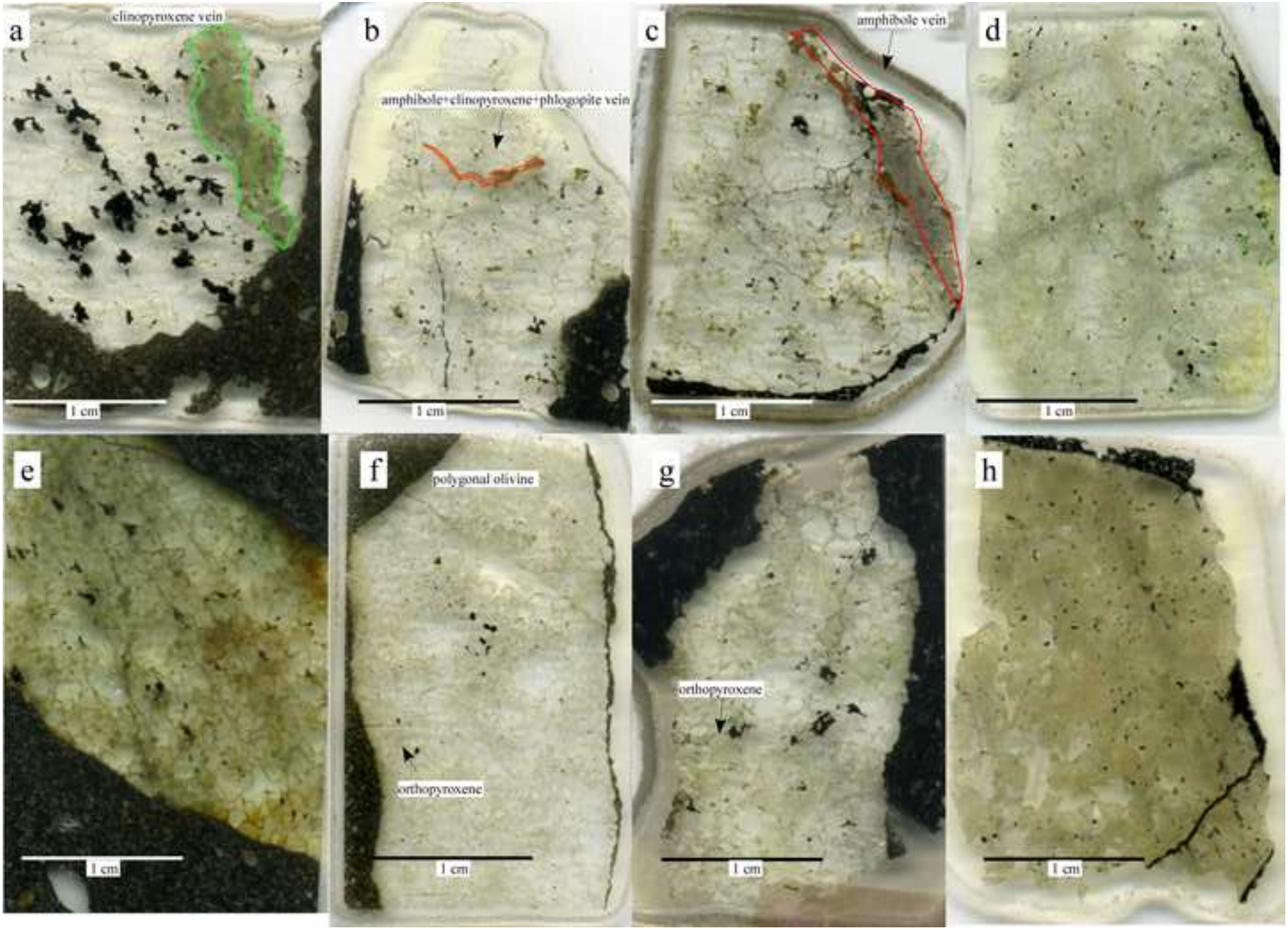

Your MS Excel document "Supplementary Tables.xlsx" cannot be opened and processed. Please see the common list of problems, and suggested resolutions below.

External Data

If you are submitting an Excel file, please make sure that your document does not have links to external data. If it does, break the links, save the document and resend. To break the links please do the following.
-On the Edit menu, click Links.
-In the Source list, click the link you want to break.
-To select multiple linked objects, hold down CTRL and click each linked object. To select all links, press CTRL+A.
-Click Break Link.

Embedded Macros

Your submission should not contain macros. If they do, an alert box may appear when you open your document (this alert box prevents EM from automatically converting your Excel document into the PDF that Editors and Reviewers will use). You must adjust your Excel document to remove these macros.

Excel 2002/Excel XP files

At the present time, EM supports Excel files in Excel 2000 and earlier formats. If you are using a more recent version of MS Excel, try saving your Excel document in a format compatible with Excel 2000, and resubmit to EM.

Other Problems

If you are able to get your Excel document to open with no alert boxes appearing, and you have submitted it in Excel 2000 (or earlier) format, and you still see an error indication in your PDF file (where your Excel document should be appearing). please contact the journal via the 'Contact Us' button on the Navigation Bar.'

You will need to reformat your Excel document, and then re-submit it.

REPLIES TO THE REFEREES AND EDITOR - MS CTMP-D-18-00104

- In the present text, the authors report their replies (with the color code as reported below) to the comments and remarks (in black) of the Referees.
- In the revised manuscript, (Pelorosso et al.2019_rev) any changes or new statements were marked with the same Referees' color code.
- A clean version (black typing) of the revised manuscript (Pelorosso et al.2019_rev1) is also provided.

General comments of the authors.

First of all, we would like to thank the Referees and Editor, whose precious suggestions remarkably enhanced the manuscript.

In the revised version, we modified the tables, both in the text and as supplementary material, adding the analytical information requested by Reviewer #1. We also simplified and clarified the original text. Finally, the abstract was totally rewritten.

We are at your disposal for any further suggestions/ modifications that you believe are needed.

For the authors,

Costanza Bonadiman

Please, find the changes in the manuscript and replies to the reviewers marked by different colors:

Blue, for Reviewer #1 (Rev1)

Red, for Reviewer #3 (Rev3)

COMMENTS FOR THE AUTHOR:

AE's comments: Please pay particular attention to Reviewer #1's comments, in particular reporting errors in the data, and the plotting of all the data vs only some of the data.

Reviewer #1: May 17th, 2018
This paper presents in situ major and trace element data on a suit of xenoliths from Harrow Peaks (northern Victoria Land, Antarctica). Based on major element composition of the olivine, the authors demonstrate the magmatic origin of these xenoliths as well as the secondary origin of the

cpx and amphibole in these xenoliths. They also suggest a cogenetic origin from a single parental melt with high Mg# and close to silica saturation. This paper has geodynamical implications for the initiation and evolution of the Ferrar magmatism, considered as a major magmatic event of West Antarctic Rift system. I think this paper has the ingredients for publications in CMP, but I have a number of comments for the authors to consider for the revision of their paper.

1) Abstract. The abstract does not catch the main conclusions of this paper and could be much shorter (less focused on sample description, more focused on geodynamical implications
Authors' reply: We rewrote the abstract and highlighted the relevance of the results.

2) Tables:

Quality of the data cannot be assessed as errors on analyses are not reported in Tables (the limit of detection is not sufficient). Add the standard variation (or the internal errors when only one analysis or when the internal error is bigger than the standard variation).
Authors' reply: We modified the tables according to this suggestion. Table 2_rev (olivine major composition) reports averaged olivine compositions and the relative standard deviation for each sample.
The entire mineral data set is, in turn, provided as supplementary tables (Tables S1-S5).

Moreover, descriptions of Tables S1 to S5 are unclear. They are way more points plotted in Fig.5 than reported in Tables S1-S5 and I don't understand why.
For instance, I can count at least 10 data points for the sample HP121 only on Fig. 5a while only 3 olivine analyses are reported in table S1 for this samples: 2 core and 1 rim, so they cannot be average compositions (otherwise I would have expect 1 core and 1 rim
Authors' reply: thank you for noticing this! The problem arose because our choice was not properly explained in the table caption notes of the original submission. The tables showed representative analyses for each sample (e.g. max, min and medium of each plotted element pairs) but in the corresponding diagrams all the data set was plotted. The revised Tables S1- S5_rev now include all the analyses plotted in the diagrams; moreover, to facilitate the reader, we inserted in the text Table 2_rev with the averaged values of olivine, for each sample (see also authors reply above).

Line 167, the range of Ni content in olivine from all samples is reported as 0.26 to 0.47. On figure 5a, the 0.47 correspond to HP121, however, this analysis is not in Table S1. …)
So how have the analyses present in Table S1 been selected? Same comments can be done for other minerals…
Authors' reply: Yes, you are right, we modified accordingly. See also the above replies. Now the tables, both in the text and as supplementary material, provide the entire chemical dataset used for supporting the HP genetic model.

Please clarify this. I suggest to do the same than for trace elements (L220-221): add a table in the main manuscript with average composition (with 2SD) and # of analyses per sample for ol, opx,cpx, spinel and hydrous phase and give all the individual analyses in supplementary tables.
Authors' reply: We followed the suggestion: the insertion of a new table in the text and the entire data set in the supplementary material provide the whole analytical frame to support the proposed HP genetic model.

Finally, why glass major element compositions are not reported in a Table?
Authors' reply: Thank you for noticing. Unintentionally, this table disappeared during the original submission process! Table S6 (_rev) is now re-introduced.

3) Parental melt compositions:

First, the authors need to give much more details on the calculation of the melt (for instance, how the P2O5 content has been determined?? - Table 3; why choosing 1wt% water? What would be the effect of more/less water?).

Authors' reply: We agree with this comment: in the original version, the modelling information was too "condensed". In the revised version of the manuscript the paragraph that explains the model and relative parameters is now implemented with additional information (lines 335-337, 345-348).

Regarding P_2O_5 (Table 4 of the original submission): we erroneously included P in the table, since we copied the oxide list of the preset spreadsheet: the output of the calculation is given as wt.% of melt major oxides including P. Since we used olivine to infer the initial melt (melt1), we could not properly determine P contents. The values reported in Table 4 were the content of the real melt used for comparison.

In the revised version, we recalculated all the hypothetical melt compositions based on olivine oxides. In addition, thanks to the Rev1 comments (and suggestions), calculations now include Ni contents. Ni is a clue element to disclose the origin of the HP ultramafic fragments. This is now discussed in the revised text (lines 335-337, 455-467, Table 5_rev)

Second and more importantly, the author suggest that the xenolith suite is cogenetic based mostly on major element compositions of olivine. While I agree with the demonstration showing that they are not melting residue and consequently have a magmatic origin, I am not completely convinced by the cogenitic origin of these cumulats. In fact, (1) the global trend Fo-NiO in Fig.5a seems to be "too straight" to represent a fractional crystallization trend and looks more like what I would expect of a mixing trend… I suggest the author to do the calculations to check this. (2) Even if the trend can be reproduced by fractional crystallization, there is a very large scatter in NiO content for a given Fo content that cannot be explain by fractional crystallization.

Authors' reply: We thank Rev1 for this interesting comment. It is an hypothesis that we initially took into account, but we later discarded, after processing the olivine chemical data set. It was found that within the uncertainty of the data, diffusion rates of Fe-Mg and Ni are very similar to each other at all crystallising conditions, but Ni is more sensitive to the difference between mantle and segregation depth (Petry et al., 2004; Gordeychik et al., 2018).

We present here a plot, showing Fo vs NiO averaged olivine composition of each sample under investigation. This diagram was not inserted in the revised manuscript, because it has the same meaning as Fig.4a, however here it helps the authors to explain their reply to this comment.

Despite the limited number of samples, the positive correlation between Fo and NiO averaged for each sample is clear, with the highest values corresponding to the most primitive (HP121), and the lowest to the most evolved (oxpte HP163) olivines of the hypothetical melts from which they crystallised, as we modelled (melt1-----melt 3). The samples in between, more "scattered", should represent separates of "intermediate" melts of a system that evolves, if our model is correct, from high Mg# (picrites?) to high Mg# melt (basalts).

As stated above, to reinforce our modelling Ni contents were included in the calculations.

The same trend has been observed, and explained as a fractionation trend in i.e. olivine in Deccan trap (Krisnhamarphy et al., 2000 JP) and Haleakela submarine volcano, Hawaii (Ren et al., 2004).

However, it is important to consider that these ultramafic rocks represent cumulates, thus they are affected by variable degrees of subsolidus effect.

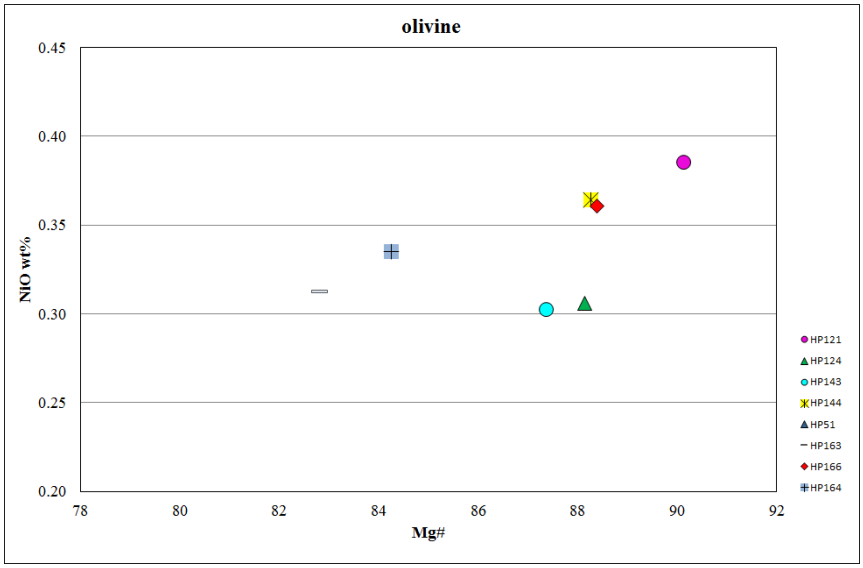

(3) trace elements are not discussed in this statement. If the orthopyroxenite was the result of a more evolved liquid crystallization, I would expect the opx to show more enriched trace element composition. This systematic is not obvious in Fig. 8.

Authors' reply: we agree! However, orthopyroxene that compete with olivine to accomodate REE abundances, partition low to very low REE contents, and the large uncertainties in their measurements-do not allow the identification of a clear fractionation trend from the multi-element diagram, in particular in such a short line of fractionation as we modelled (melts from mg# 72 to mg# 60). If we consider Yb (or Y) and Zr (or Ti), the most robust geochemical fingerprints in orthopyroxene, this relationship emerges.
In the revised manuscript we discussed this statement (lines 412-422).

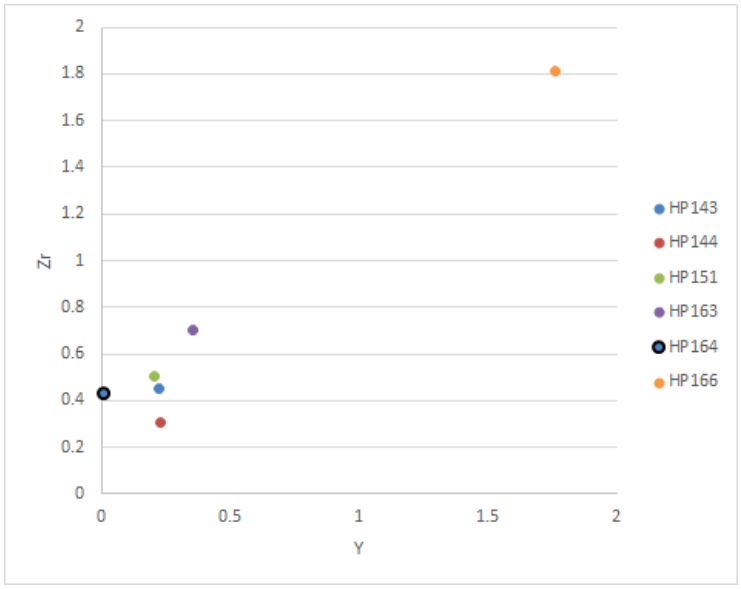

Third, the origin of the high Mg parental melt close to silica saturation is stated as "associated with an anomalous high temperature (excess Tex) melting of the Phanerozoic mantle (picrites) or the Archean cratons (komatiites)." Another potential explanation would be the contribution of a High-Mg pyroxenite. This would also potentially explain the very high Ni content of the olivine (up to

0.47%!). I think that this hypothesis is worth to be discussed (or at least mentioned and maybe dismissed if the authors have good reasons to do so.) see more comments on this below
Authors' reply: Yes, we thank the Rev 1 for these considerations. In the revised version the discussion is now enriched with this suggestion (lines 455-467)

4) Length of the manuscript: Unnecessary long sentences are sometime used in the manuscript. This does not help the reader to assimilate the information. See editorial comments (LOM). The description of the results are also sometime mixed with part of the interpretation (mention of the residual peridotite, mantle array,…) that can confuse the reading.
Yes, we are aware of this, but in some cases the description of the results becomes an interpretation (e.g the Osma diagram). It is difficult to separate the two things. However, in the revised manuscript we avoided this mixing whenever possible.

Comments link to the text:
L 25-26: "and analysed for in situ geochemical purpose." This sentence is weird
Authors' reply: the abstract was re-written (line 159)

L 26: why "<10 cm" here and "2 to 5 cm" on page 5?
Authors' reply: Thank you for noticing. The information was harmonised as "<10 cm "(line 86)

L40 & 322: "potential temperature of crystallization" confusing because of the expression "potential mantle temperature" I suggest to replace "potential" by "estimated" or to simply remove it.
Authors' reply: we agree. In the revised manuscript we simply referred to "temperature", throughout the text.
L.77-79: need references
Authors' reply: done

L 91-92: not clear: in addition to the eight samples? Does it mean that the selected samples do not show evidence for host-basalt contamination?
Authors' reply: You are right. The sentence is confusing and we removed it. Host basalt infiltration is now mentioned *ad hoc* in the mineral chemistry description.

L93: "composite xenoliths": add the definition of a composite xenolith here
Authors' reply: Added (lines 93-94)

L93-94: "Hydrous phases (mainly amphibole) occur in all samples": but amph (or phlogopite) is only reported in 5 samples in Table 1.
Authors' reply: Thank you for noticing! We visually observed traces of amphiboles in all samples, but only in five samples were amphibole crystals large enough to be analysed. In the revised manuscript, we modified Table 1 (Table 1_rev) accordingly.

L104-105: it is not clear on Fig. 3b that what is outlined is a vein. Also, the text on this figure is very small and I don't think it will be visible once placed into the article. Maybe Fig.3 could go in the supplementary material.
Authors' reply: Thank you for the suggestion, we moved this figure to the supplementary material.

L107-108: What is the point of spending so much time doing point-counting (knowing that studies show that above 300-400 points, the statistical difference is small), confirming the results with color analyses to demonstrate that this matrix is a harzburgite if it's to call it dunite based on "textural similarities and high olivine modal contents". Why not continue to call it harzburgite?

Authors' reply: the nomenclature of these samples was a problem since the first petrographic observation. If we named the samples with the proper name derived by the modal classification diagram, as Rev1 suggests, the risk of making the reader confused about the composite samples is high. HP121 and HP124 are formally harzburgite and lherzolite, respectively, but they are far from being harburgite or lherzolite in the proper meaning. Both rocks are dunites with rare orthopyroxenes and clinopyroxenes, crosscut by amphibole or clinopyroxene vein.
In the revised version, we simplified as much as possible the petrographic description, but we think that it is important to address these samples as dunites, for the reasons clarified in the text (lines: 102-104) and reported in Table 1_rev.

L166 & Table S1: add Fo content in Table S1
Authors' reply: done

L167: "from 86.60 to 90.45" this degree of precision is probably unrealistic but because errors (and Fo) are not reported in Table S1, I can't tell. Same comment line 170 and in the abstract
L167: highest value reported in Table S1 for NiO is 0.42% - see comment #2 on supplementary tables
Authors' reply: See replies of the general comment point 2.

Section 4.1: I'm surprised that the author do not comment the fact, that despite a relatively small compositional range for the entire xenolith suite, there is a very limited overlapping between the different samples. This is particularly striking for the spinel on Fig. 5c.
Authors' reply: At magmatic conditions, the spinel mg-number is a function of the melt mg-number and Al2O3, whereas at near- and postmagmatic conditions it is controlled by the rate of cooling and re-equilibration with the silicates. At this stage, the variability of the spinel is reasonable.
Notwithstanding, we agree with Rev1 that mineral chemistry discussion could be improved. In the revised version of the manuscript, we discussed the Fig.4_rev that now includes lines of hypothetical melting trend for olivine (lines 285-294, 455-467)
(Kamenesky et al., 2001 JP; A-Rim An, 2017 Lithos).

L 186-188: Should be in the discussion and requires more information.
Authors' reply: We removed it from this section and inserted it in the initial part of the new "Discussion" section, See also reply above.

L189-190: the "evident" disequilibrium requires more justification and reference to a figure.
Authors' reply: Thank you for the suggestion, we rephrased (lines: 192-193) and clarified these statements adding orthopyroxene-clinopyroxene Fe/Mg equilibrium values

L195: "have TiO2 and Al2O3 contents that reflect a host basalt low-pressure perturbation (Figs.7 a, b)." I do not understand what that means
Authors' reply: Yes, it was not clear, we meant that the high TiO2 and low Al2O3 observed in a few grains in individual samples, is a local effect of low-pressure host basalt infiltration. In line 195 with what we stated above, we modified this section following the Rev1's comments.

L195-197: I don't think this is relevant for the discussion
Authors' reply: we removed this sentence

Table 2: Add the internal error (when only one analysis) or the standard deviation (when multiple analyses and if bigger than the internal error) in the Table
Authors' reply: done. See also replies to general comments point. 2) of Rev1.

L 284-285: I don't see a melting "trend" on Fig. 5a in residual peridotites (green field) but I do see a trend in the samples described here that could be interpreted as a mixing trend (or maybe as a fractional crystallization trend).
Authors' reply: As stated above, Fig. 4_ rev shows theoretical fractional (and melting) trends.
The idea of mixing is intriguing. However, if Rev1 thought of mixing of the sources, it is difficult to identify it (taking into account the cumulitic nature of these rocks).

Authors should try to calculate a fractional crystallization trend and see if it can explain the Fo-NiO variation? (see e.g., Shorttle et al, 2014; Sobolev et al, 2005). If these samples have a magmatic origin as claimed by the author, that could reveal some scatter in the primitive melt composition and also reveal a certain heterogeneity of the source (i.e, variable contribution of a pyroxenite component (Sobolev et al., 2005) or variable pressure of melting (Matzen et al, 2014)).
Authors' reply: see comment above.

L287-290: Not clear and several typos. Change "there is not an observed correlation between spinel and olivine as expected in a potential residual trend, with the sole exception of the composite xenolith HP21, where spinel Fo and Cr# values of the dunitic matrix intercept the mantle array curve," by "the Olivine Fo - Spinel Cr# relationship cannot be reproduced by melting, with the exception of the composite xenolith HP121, where spinel and olivine compositions intercept the mantle array curve".
Authors' reply: thank you for rephrasing.

L300: ΔQFM = - 2.78 seems particularly low!
Authors' reply: in this section we wanted to emphasise that amphibole and dunite matrices are not genetically related. This value, reported by literature, was determined on the "peridotite" assemblage~~,~~ and testifies to the complete disequilibrium of the system.

L331-333: The composition of melt1 reported in table 4 contains a lot of different oxides, including MnO, P2O5, TiO2, etc not present in Putirka' equation (21). Please add details on how these calculations were performed.
Authors' reply: Thank you for noticing this. As mentioned above, we re-calculated the hypothetical melts, removing P2O5 (erroneously reported), but including NiO.
The revised manuscript now includes a detailed explanation of the calculations, supported by the new Table 5 (Table 5_rev)

L 334-335: same comment: please give details of the calculations.
Authors' reply: see above.

L339-340: if the olivines are cogenetic, you should be able to reproduce the Fo-NiO variation by fractional crystallization - see my comment on line 284-285. Note that IF the authors do find a crystallization trend that can broadly reproduce the NiO-Fo variation, fractional crystallization will never explain the scatter of NiO content for a given Fo content. Looking at the sample HP121 only, NiO varies from 0.32 to 0.47 (fig 5a) for a relatively constant Fo content (around 90). This covers almost all the range observed in magmatic olivine of Mauna Loa and has been interpreted as a variable high contribution (50-80%) of a pyroxenitic component to the magma (Sobolev et al., 2005). I think this is worth to be explored or at least slightly discussed in this paper.

L361-363: "parental liquid had high MgO contents (Mg# 72) and was close to silica saturation. Such melts are associated with an anomalous high temperature (excess Tex) melting of the Phanerozoic mantle (picrites) or the Archean cratons (komatiites)." Or with the contribution of a high-Mg pyroxenite! Again Sobolev et al. (2007) generate melts with mg# as high as 77 by melting of a high-mg pyroxenites.
Authors' reply: Part of this interesting discussion is now included in the revised manuscript (lines: 455-467).

Figure 2: 'dunitic" not only, the matrix of HP121 is a harzburgite. Note that the symbols look a bit offset. For instance HP121 seems to plot in the lherzolite field while the middle of the symbol should normally be exactly on the harz-lherz limit (ie, when modal proportions of ol, opx and disseminated cpx are normalized to 100%, cpx mode is 5%). same observation with HP143, the normalized ol mode is 90.1% while the middle of the symbol seems to be below the 90% line.
Authors' reply: the symbol's size is now enlarged

Figure 3. Need to stay big so we can see the details mentioned in the text. So I suggest to put this figure in the supplement
Authors' reply: Done, see also reply to Rev1 general comments, point 4.
Figures 5 &6: remove "Dunitic"
Authors' reply: done

Editorial comment:
Name of the samples are not the same in the entire manuscript: e.g, HP121 vs HP21. Make sure to check and uniform this, including in the Supplementary Tables

L109: LOM suggestion: "Regardless of the lithology, most of the samples are tabular to equigranular"
Authors' reply: done. We re-phrased accordingly line 104.

L113-114: " small irregular spinel is scattered within the olivine grains." I guess they are plural
Authors' reply: yes plural. Correct. We always use the singular form for minerals, also in the plural meaning (i.e. the case mentioned here)

L117: "small irregular spinels within the olivine grains": "within" (ie, inclusion) or "between"?
Authors' reply: corrected: Inclusion (line 112)

L120-121: it's either: "it's absent in most of the..." or "it's completely absent in other xenolith suits"
Authors' reply: corrected

L158-160 : LOM suggestion : Change it for: "Major element data on olivine, pyroxenes, spinel and amphibole are provided in the Supplementary material (Tables S1 to S5). and place this sentence below the title 4.1 Note that the Table numbers are wrong.
Authors' reply: correction accepted (158-160)

Amphibole is in Table S5, not S4.
Authors' reply: corrected

L173-174: "showing an apparent equilibrium with the coexisting olivine in all the investigated samples, and remarkable differences from those of the residual peridotites." At this point in the manuscript, I don't know on what is based this affirmation and I have no idea where the term "residual peridotites" comes from in this article and which samples the authors are talking about
Authors' reply: we modified the text and removed this sentence.

Figure 9 - L 754: typo
Authors' reply: Ok

Table2:
- n. is number of average analyses: I do not understand, do you mean: n. is number of analyses?
Authors' reply: yes it is. In Table 2_rev, we added an explicative note

- Remove the footnote Ol:olivine as there is no analyses of olivine in this table Tables S1 to S5: The row "phase" can be removed.
Authors' reply: corrected.

References cited in this review
A.K. Matzen, M.B. Baker, J.R. Beckett, E.M. Stolper. The temperature and pressure dependence of nickel partitioning between olivine and silicate melt J. Petrol., 54 (2013), pp. 2521-2545
Sobolev AV, Hofmann AW, Kuzmin DV, Yaxley GM, Arndt NT, Chung, SL, Danyushevsky LV, Elliott T, Frey FA, Garcia MO, Gurenko AA, Kamenetsky VS, Kerr AC, Krivolutskaya NA, Matvienkov VV, Nikogosian IK, Rocholl A, Sigurdsson IA, Sushchevskaya NM, Teklay M (2007) The amount of recycled crust in sources of mantle-derived melts. Science 316:412-417. doi:10.5800/gt-2012-3-1-0059
Sobolev, A.V., Hofmann, A.W., Sobolev, S.V., Nikogosian, I.K., 2005. An olivine-free mantle source of Hawaiian shield basalts. Nature 434, 590-597
Shorttle, O., Maclennan, J., Lambart, S. (2014) Quantifying lithological variability in the mantle. Earth and Planetary Science Letters 39

Reviewer #3: This is an interesting study on mantle xenoliths from Harrow Peaks in Antarctica. I think the data are convincing and are of high quality, and the interpretation and conclusions consistent. My major comment about the manuscript is that it suffers from significant problems in grammar. I started making notes in the pdf, but stopped about half way through. The authors need to make sure that they revise the writing significantly before submitting a final version for publication. Other than that, the authors should be congratulated on a study well done.

Authors' reply: we would thank for the appreciation of our work. The revised manuscript has been checked by mother tongue- reviewer for English language.